TALEN-MEDIATED HOMOLOGY DIRECTED INSERTION OF ANTI-VIRAL SEQUENCES TO INHIBIT HEPATITIS B VIRAL GENE EXPRESSION AND REPLICATION

Timothy James Dreyer

A dissertation submitted to the Faculty of Health Science, University of the Witwatersrand, Johannesburg, in fulfilment of the requirements for the degree of

Master of Science in Medicine.

Johannesburg, 2014.

DECLARATION

I, Timothy James Dreyer, declare that this dissertation is my own, unaided work. It is being submitted for the degree of Master of Science in Medicine at the University of the Witwatersrand, Johannesburg. It has not been submitted before for any degree or examination at any other University.

_____

Timothy James Dreyer

_____day of_____2015

PUBLICATIONS AND PRESENTATIONS

Publications

1. A manuscript is currently in preparation

Conference proceedings

1. DREYER, T., NICHOLSON, S., BLOOM, K., ELY, A., CATHOMEN, T., MUSSOLINO, C. AND ARBUTHNOT, P. (2013). Homology directed insertion of anti-viral sequences to inhibit hepatitis B viral gene expression and replication. *South African Society for Microbiology - 18th Biennial Congress. Forever Resorts Warmbaths, Bela-Bela, South Africa*

2. DREYER, T., NICHOLSON, S., BLOOM, K., ELY, A., CATHOMEN, T., MUSSOLINO, C. AND ARBUTHNOT, P. (2014). TALEN mediated homology directed insertion of anti-viral sequences to inhibit hepatitis B viral gene expression and replication. *24th Biennial Congress of the South African Society of Biochemistry and Molecular Biology (SASBMB). Goudini Spa Resort, Worcester, South Africa.*

3. DREYER, T., NICHOLSON, S., BLOOM, K., ELY, A., CATHOMEN, T., MUSSOLINO, C. AND ARBUTHNOT, P. (2014). Designer TALEN mediated homology directed insertion of anti-viral sequences into the HBV genome to inhibit viral gene expression and replication. *Biennial Research Day & Postgraduate Expo. University of the Witwatersrand, Faculty of Health Sciences.*

4. DREYER, T., NICHOLSON, S., BLOOM, K., ELY, A., CATHOMEN, T., MUSSOLINO, C. AND ARBUTHNOT, P. (2014). Designer TALEN mediated homology directed insertion of anti-viral sequences into the HBV genome to inhibit viral gene expression and replication. *6th Cross-Faculty Graduate Symposium. University of the Witwatersrand, Graduate Support Division.*

ABSTRACT

More than 350 million people are chronic hepatitis B virus (HBV) carriers. Viral covalently closed circular DNA (cccDNA) persists as a replication intermediate and can remain dormant. Current HBV therapeutics do not eradicate viral cccDNA reservoirs. Transcription activator-like effector nucleases (TALENs) target and cleave specific DNA sequences, and have shown promise as antiviral agents. Here we propose TALEN-mediated homology directed disruption and silencing of the cccDNA. The designer TALENs introduce double stranded breaks (DSBs) at the HBV cccDNA *core* and *surface* ORFs, which activate the non-homologous end joining (NHEJ) and homology directed repair (HDR) cellular repair pathways. We utilise the HDR process to introduce specific mutations at the TALEN cleavage sites. Here we facilitate integration of a HBV-targeting artificial primary micro RNA (pri-miR) mimic into the HBV genome by co-introducing TALENs and donor template strands that contain a pri-miR cassette flanked by sequences that are homologous to the TALEN target sites. Integration of the donor sequences was evaluated by PCR and disruption of HBV replication was evaluated using ELISA. HBsAg knockdown when targeting the *surface* and *core* targets was 94% and 63% respectively, a significant improvement on use of TALENs alone. PCR analysis and sequencing confirmed successful integration of donor sequences into the HBV *core* and *surface* target sites, verifying that HBsAg knockdown is as a result of sequence insertion and possible pri-miR-mediated silencing of *HBx*. In conclusion, integration of an artificial DNA sequence at specific HBV target sites was demonstrated and the synergistic activity of TALENs and donor template strands shows promising anti-HBV abilities. Results of this study provide the means to improve targeted disruption of HBV DNA by TALEN constructs. Moreover, the potential for combining different anti-HBV gene therapies to result in better viral suppression is demonstrated.

DEDICATION

To my King and my parents and brother, Cobus, Deirdre and David Dreyer

ACKNOWLEDGEMENTS

1. I would like to thank my supervisors, Prof. Patrick Arbuthnot and Dr Samantha Nicholson, for their endless support, encouragement, patience and assistance over the past two years.

2. I would like to thank Dr Betty Maepa for her continuous assistance on challenging practical aspects of my project.

3. I would like to thank all the members of the Antiviral Gene Therapy Research Unit (AGTRU) for their company, advice and continuous assistance throughout the past two years.

4. I wish to extend my heartfelt gratitude to my family for their limitless and unwavering support.

5. Finally, I would like to thank the various funding organisations for their financial assistance during my degree:
   - The University of the Witwatersrand (Merit Award)
   - The National Research Foundation (NRF)
   - The Poliomyelitis Research Foundation (PRF)

TABLE OF CONTENTS

LIST OF FIGURES

LIST OF TABLES

LIST OF ABBREVIATIONS

1.	5mC	-	5-methylated cytosine
2.	BIR	-	Break induced replication
3.	Bp	-	Base pair
4.	Cas9	-	CRISPR associated protein 9
5.	cccDNA	-	covalently closed circular DNA
6.	CMV	-	Cytomegalovirus
7.	CTL	-	Cytotoxic T lymphocyte
8.	CRISPR	-	Clustered regular interspaced short palindromic repeats
9.	crRNA	-	CRISPR RNA
10.	DMEM	-	Dulbeco's modified eagles medium
11.	DNA	-	Deoxyribonucleic Acid
12.	DR1	-	Direct repeat 1
13.	DR2	-	Direct repeat 2
14.	DSB	-	Double stranded break
15.	dsDNA	-	double stranded DNA
16.	*E. coli*	-	*Escherichia coli*
17.	ELISA	-	Enzyme-linked immunosorbant assay
18.	FBS	-	Fetal bovine serum
19.	g	-	gram
20.	HBV	-	Hepatitis B virus
21.	HBcAg	-	Hepatitis B core antigen
22.	HBeAg	-	Hepatitis B e antigen
23.	HBsAg	-	Hepatitis B surface antigen
24.	HBx	-	Hepatitis B virus X protein
25.	HCC	-	Hepatocellular carcinoma

26.	HDR	-	Homology directed repair
27.	HLA	-	Human leukocyte antigen
28.	HIV	-	Human immunodeficiency virus
29.	HJ	-	Holliday junctions
30.	IFN	-	Interferon
31.	kb	-	kilobase
32.	µg	-	microgram
33.	µl	-	microliter
34.	µM	-	micromole
35.	M	-	Molar
36.	Mg	-	milligram
37.	Mmol	-	millimoles
38.	mRNA	-	messenger RNA
39.	miRNA	-	microRNA
40.	ng	-	nanogram
41.	NHEJ	-	Non-homologous end joining
42.	NK	-	Natural killer
43.	NPC	-	Nuclear pore complexes
44.	NTCP	-	Sodium taurocholate cotransporting polypeptide
45.	ORF	-	Open reading frame
46.	PAM	-	Protospacer adjacent motif
47.	PBS	-	Phosphate buffered saline
48.	PCR	-	Polymerase chain reaction
49.	pgRNA	-	pre-genomic RNA
50.	pre-miR	-	precursor microRNA
51.	pri-miR	-	primary microRNA
52.	rcDNA	-	relaxed circular DNA

53.	RGEN	-	RNA-guided endonucleases
54.	RISC	-	RNA-induced silencing complex
55.	RNA	-	Ribonucleic acid
56.	RNAi	-	RNA interference
57.	RVD	-	Repeat variable diresidue
58.	SDSA	-	Synthesis-dependent strand annealing
59.	sgRNA	-	subgenomic mRNA
60.	SNV	-	Single-nucleotide variants
61.	SSA	-	Single strand annealing
62.	SSB	-	Single strand break
63.	ssDNA	-	single strand DNA
64.	TALE	-	Transcription activator like effector
65.	TALEN	-	Transcription activator-like effector nuclease
66.	TNF	-	Tumour necrosis factor
67.	tracrRNA	-	trans-activating crRNA
68.	T*m*	-	Melting temperature
69.	YMDD	-	tyrosine-methionine-aspartate-aspartate
70.	ZF	-	Zinc finger
71.	ZFN	-	Zinc finger nuclease

LIST OF SYMBOLS

1. α - Alpha
2. β - Beta
3. γ - Gamma
4. μ - Micro

1. Introduction

1.1 Hepatitis B virus epidemiology and pathogenesis

More than 350 million people are chronic hepatitis B virus (HBV) carriers (1, 2). This presents a major public health challenge, as exposure to HBV can result in either acute or chronic liver infection. In adults HBV is predominantly transmitted through blood and sexual contact (horizontal transmission), while children can become infected through peri- or neonatal exposure and horizontal transmission, the predominant mode of infection in African infants and young children (3-5). Peri- and neonatal transmitted HBV is rarely cleared and up to 90% of neonatal infected children become chronically infected (2, 6). In contrast, the virus is usually cleared by the adult immune system and less than 5% of infected adults develop persistent infections (7). HBV infection may result in acute and chronic liver disease, cirrhosis and hepatocellular carcinoma (HCC) (1, 2). These diseases have a high risk of developing in chronically infected patients and claim approximately 500 000 to 1.2 million lives per annum, therefore, developing a cure is a top priority (1). Effective vaccines against HBV infection have been developed and have reduced the incidence of chronic HBV infections and HCC in areas where HBV immunisation has been introduced (2, 8). However, the vaccines do not cure existing chronic HBV infections and are difficult to access in far removed and secluded areas where HBV infection is unchecked (2, 8-12). Current HBV therapeutics manage HBV infections, but as a result of persistent HBV covalently closed circular DNA (cccDNA) are unable to clear the virus (13). The HBV cccDNA acts as an essential transcriptional template for viral replication, persists as a replication intermediate and needs to be addressed to facilitate viral clearance (14). DNA sequence specific nucleases such as transcription activator-like effector nucleases (TALENs) have recently shown promise as antiviral agents that can target, modify and disrupt the viral cccDNA (15). These TALENs introduce

double stranded breaks (DSBs), which are repaired by the non-homologous end joining (NHEJ) DNA repair pathway. These DSBs can also be repaired by the homology directed repair (HDR) pathway if homologous donor template strands are present (16). It should therefore be possible to exploit the HDR pathway by introducing an artificial donor template strand that contains an anti-viral sequence. HDR should integrate the artificial sequence into the HBV cccDNA and result in disruption of the viral genome and subsequent replication.

1.2 HBV life cycle

The current knowledge of HBV structure and life cycle is perused to identify potential target genome sites for TALEN cleavage and HDR-mediated integration of an anti-viral sequence.

HBV is a non-cytopathic virus that belongs to the *Hepadnaviridae* family of the *Orthohepadnavirus* genus. It has two DNA arrangements: partially double-stranded relaxed circular DNA (rcDNA) in the virions and cccDNA, which only exists inside the host. The virus has a limited host range and an affinity for hepatocytes (2, 17). The viral core, containing the rcDNA and viral polymerase, is encapsulated by an outer lipid envelope that consists of viral surface antigens and host-derived lipids (2) (Figure 1.1). The envelope proteins are essential for cell binding and entry into the susceptible hepatocytes (18, 19). During infection the virion binds to low-affinity receptors (heparan sulphate proteoglycans). This is followed by viral entry through endocytosis mediated by specific interaction between HBV and sodium taurocholate co-transporting polypeptide (NTCP), a recently described functional receptor for HBV (2, 20-22). The lipid envelope is dissolved and the nucleocapsid particles are

transported to the nuclear membrane by chaperone proteins, where they are disassembled by host nuclear pore complexes (NPC) (Figure 1.1). After disassembly of the nucleocapsid particles the rcDNA is released into the cell nucleus and undergoes DNA repair by host factors to form cccDNA (2, 17, 23). This cccDNA acts as an essential transcriptional template for viral replication and does not have to be integrated into the host genome (14, 24). The pool of transcriptional templates within the hepatocyte is amplified by transcriptional regulation of cccDNA. These cccDNA templates encode pre-genomic RNA (pgRNA) and four viral subgenomic mRNAs (sgRNAs) required for virion assembly, and are transcribed by the host RNA polymerase II (17, 25). Viral mRNAs are translated and progeny virion particles are produced. HBV core antigens (HBcAg) self-assemble and form nucleocapsid particles within the host cytoplasm. During virion assembly the pgRNA and viral polymerase are packaged in the core capsid (Figure 1.1). The viral polymerase reverse transcribes the pgRNA, a replication intermediate, to form rcDNA within the nucleocapsid. Once reverse transcription is complete, the virion acquires an outer envelope that is completed by the Golgi apparatus and mature virions with complete envelopes are then secreted from the cell. The nucleocapsid enclosing the rcDNA can also be redirected to the cell nucleus to increase the cccDNA pool of the host cell. The cccDNA in this pool can persist as HBV replication intermediates in the hepatocyte during disease progression (2). The epigenetic regulation of cccDNA through the acetylation status of coupled histones in DNA allows it to remain dormant in the hepatocyte nucleus for months or years (26, 27). This allows the virus to evade the host immune response and reactivate viral replication, resulting in latent or occult viral infection (reviewed by (27-30)).

1.3 HBV genome structure and viral proteins

The HBV genome expresses viral proteins that are important for viral replication and virion assembly. Therefore, knowledge of the genome structure, the viral proteins, and their roles in HBV replication is essential for development of effective anti-HBV therapies that target these latent HBV cccDNA reservoirs.

The HBV partially double-stranded DNA genome has a length of approximately 3.2 kilobases (kb) and is repaired upon entry into the cell nucleus to form cccDNA. The cccDNA consists of four open reading frames (ORFs) that transcribe the pgRNA and three sgRNAs (reviewed by (25, 31, 32)) (Figure 1.2). The pgRNA is 3.5 kb long and contains the ORFs for translation of the viral polymerase and precore/core proteins. The Golgi apparatus processes the precore protein to form hepatitis e antigen (HBeAg), which is an important regulator of the innate and adaptive immune responses and down regulates interferon (IFN)-γ expression by natural killer (NK) cells (33, 34). HBeAg and the precore protein are not required for HBV replication, but are important for establishment of persistent viral infection (35, 36). Hepatitis B core antigens (HBcAgs) are the translational products of the second initiation codon of the *precore/core* ORF and are essential for the formation of the viral nucleocapsid. HBV polymerase initiates reverse transcription of pgRNA to produce rcDNA, which contains an incomplete positive DNA strand that is capped by a short RNA oligomer at the 5’ end (37, 38). The negative rcDNA strand contains a gap region that is flanked by Direct Repeat 1 and 2 (DR1 and 2) (Figure 1.2). DR1 and 2 are repetitive sequences on both the positive and negative DNA strands that function as recognition sites during viral replication (37, 39, 40). The *surface* ORF encodes the major surface proteins and contains two upstream reading frames, *pre-S1* and *pre-S2*, which encode the large and middle surface proteins respectively. The major, large and middle surface proteins are essential for the formation of the new viral envelope and are immunologically

identified as hepatitis B surface antigens (HBsAgs), which are indicators of HBV infection. Transactivator hepatitis B X protein (HBx) is encoded by the *HBx* ORF. Its complete role in regulation of HBV replication remains elusive, but recent studies indicate that HBx has an important role in stimulating HBV transcription and replication in the host cell by regulating transcription of cellular genes (41-44).

However, there are currently 10 different HBV genotypes (A-J). The genome structure and HBV protein expression vary for each genotype, making development of anti-HBV treatments challenging (45-49). Current treatments are not effective for all HBV genotypes, necessitating development of novel treatments that target all HBV genotypes.

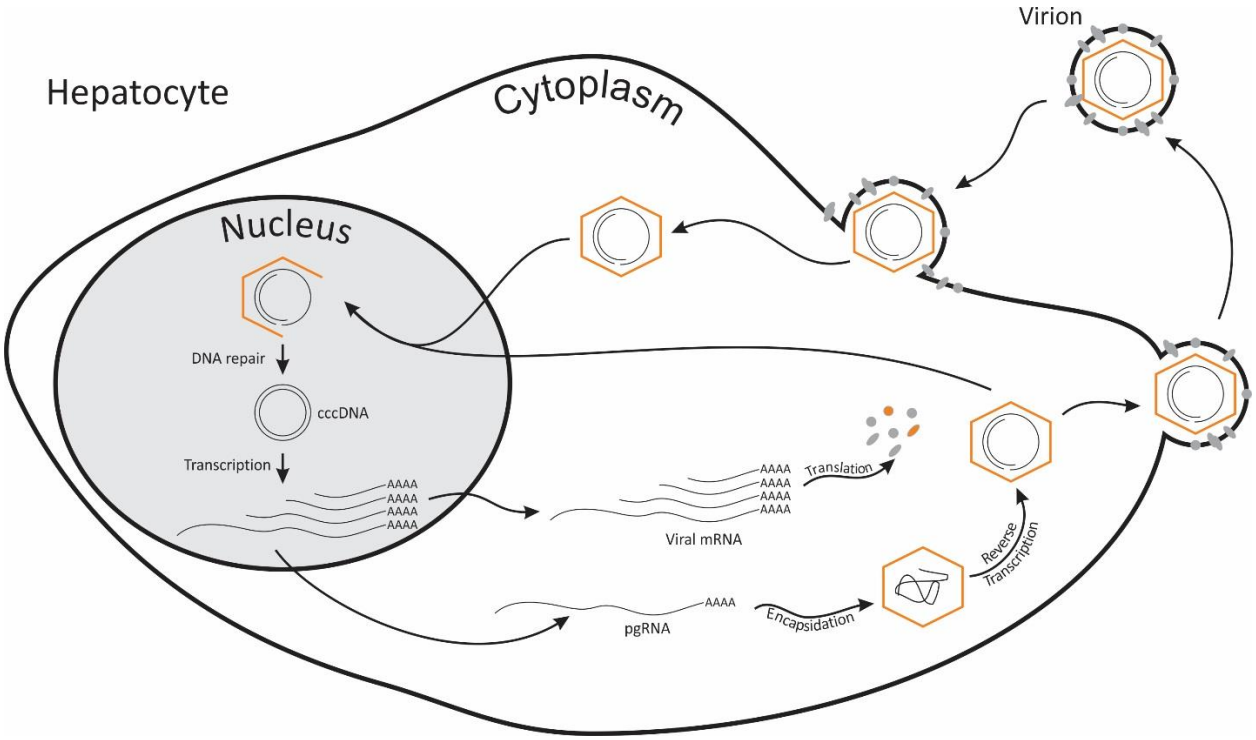

Figure 1.1: Hepatitis B virus life cycle. The virus enters the host cell through endocytosis mediated by specific interaction between HBV and sodium taurocholate co-transporting polypeptide (NTCP). The partially double stranded DNA genome of the virus is released from the viral capsid upon entry into the host cell. The genome is translocated to the cell nucleus and repaired to form cccDNA. pgRNA and various subgenomic mRNAs are transcribed from the cccDNA. Proteins required for new virion assembly are translated from the mRNAs and the pgRNA is translated into polymerase. The pgRNA is reverse transcribed to form rcDNA within the new viral capsid and the viral genome is either surrounded by surface proteins and buds from the cell or it can re-enter the cell nucleus to produce more viral cccDNA. (Diagram used with permission from Dr A. Ely, Antiviral Gene Therapy Research Unit (AGTRU), University of the Witwatersrand, South Africa)

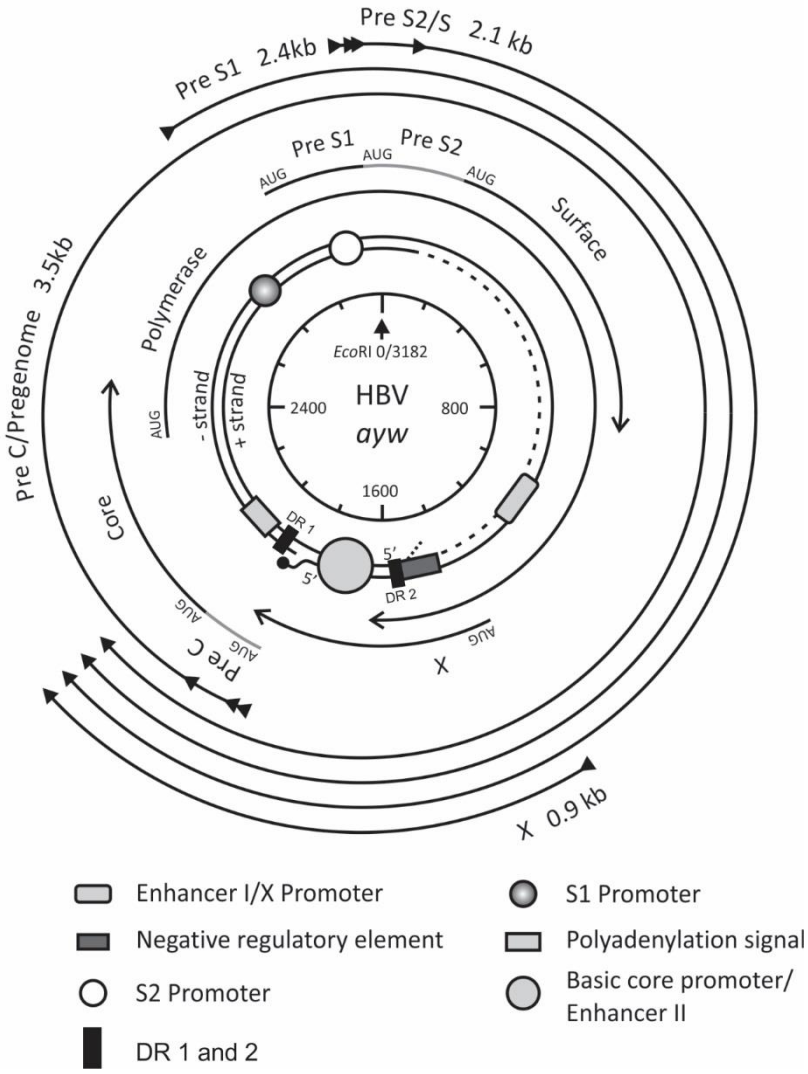

Figure 1.2: Hepatitis B Virus genome organization. The centre of the circular genome map is a schematic representation of the HBV rcDNA. The viral genome consists of *precore/core*, *pre-S1*, *pre-S2/S* and *HBx* ORFs (shown by arrows immediately surrounding the HBV genome at the centre of the circular genome map). Viral transcripts are represented by the four outer arrows and transcription initiation sites are represented by various objects. HBV polymerase initiates reverse transcription of pgRNA to produce rcDNA with a positive strand that is only partially synthesized. DR1 and DR2 flank the gap region in the negative strand and function as recognition sites during viral replication (31).

1.4 Host immune response

The adult immune response effectively clears most acute HBV infections (7). As a result, multiple anti-HBV treatments that induce, amplify or mimic the immune response have been developed (13, 50-54). However, these treatments are unable to clear the virus and further investigation of the immune response could lead to novel HBV treatments.

Liver disease and viral clearance after HBV infection occur as a result of the host immune response to viral agents (55). The immune response involves CD4+ T-helper cells and cytotoxic CD8+ T-cells, production of type 1 interferon α/β (IFN-α/β), and activation of natural killer (NK) cells. The NK cells are activated during the innate immune response and are able to eliminate infected cells by direct cytolysis and production of inflammatory cytokines, such as IFN-γ and tumour necrosis factor α (TNF-α). These cytokines are important in the cytotoxic CD8+ T-cell response and containment of the virus during the early phase of infection (33, 34). The innate immune system responds to HBV infection by eliciting strong human leukocyte antigen (HLA) class I and II restricted T cell responses. The antigens stimulate increased production of T-helper cells, which in turn stimulate the antibody-producing B-cells to produce antibodies to HBV antigens (56). A polyclonal cytotoxic T lymphocyte (CTL) response to the multiple HBV encoded antigens is observed in patients with acute viral infection who successfully clear the virus. The T-cell response is weak or absent in patients that do not clear the virus and become chronically infected, confirming the importance of the CTL for viral clearance (3, 57, 58). The IFN-γ produced by the NK and cytotoxic CD8+ cells lyses infected hepatocytes and is the primary cause of HBV associated liver injury (59). The degree of liver injury and the outcome of acute HBV infection are determined by the magnitude of the immune response to the HBV related antigens (60). However, IFN-γ can also suppress viral replication without damaging hepatocytes (61, 62). This ability to suppress viral replication without damaging

the liver cells and the efficiency of the host immune response to clear the virus resulted in development of multiple HBV treatments that exploit these attributes.

1.5 Managing HBV infections

1.5.1 Current HBV treatments

Current HBV vaccines cause the host immune response to produce antibodies against an inactive form of the virus (9-12). These vaccines are very effective in preventing HBV infection, but do not cure existing HBV infections (25). Therefore, developing novel treatment strategies to manage chronic HBV remains an important medical objective. Current therapeutics for HBV include immunomodulators and nucleotide/nucleoside analogues (13, 63, 64). The ability of IFN to induce the host immune response against HBV encouraged researchers to develop immunomodulators that boost the host response. Current immunomodulators include IFN-α-2b and pegylated interferon (pegIFN) α-2a. These immunomodulators function as anti-viral agents and aid in clearing the virus by boosting the host T-cell response (52, 53). HBeAg, an important regulator of the innate and adaptive immune responses, inhibits IFN-γ expression. Therefore, changes in HBeAg levels may predict HBV response to IFN treatment (35, 36). IFN-α has been used as treatment for both HBeAg positive and negative chronic hepatitis B and has been successful in reducing HBV replication. However, IFN treatment is only effective in ±35% of HBeAg positive patients and approximately 60% of patients did not respond to repeat treatment (65). IFN induced development of antibodies against HBeAg in 85-90% of patients, while delayed antibody formation occurred after 1-2 years in

10-15% of patients (66, 67). IFN therapy was successful in 60-90% of treated HBeAg negative patients. However, more than half of these patients relapsed post-therapy, resulting in a low sustained response. Retreatment resulted in a 20-40% response rate (68, 69). PegIFN has a higher combined response and resulted in antibody development in approximately 31% of patients (70). This data indicates that chronic HBV can be treated successfully with IFN therapy, but the effectiveness of the treatment is low and successful alternatives are required (25, 50). Lamivudine, Entecavir, Adefovir dipivoxil, Telbivudine and Tenofovir are nucleotide/nucleoside analogues that show anti-HBV efficacy (13, 50, 51, 54). These analogues are chemically synthesised and can be incorporated into HBV DNA during DNA polymerisation, facilitated by their structural similarity to the nucleosides (56). The analogues disrupt viral replication by inhibiting viral reverse transcriptase and polymerase. Lamivudine is equally effective in HBeAg-positive and HBeAg-negative carriers. It inhibits establishment of new cccDNA, reduces HBV DNA levels, and reverses liver damage (71, 72). However, a major drawback of Lamivudine usage is the emergence of drug-resistant strains of HBV after treatment. Mutations within the tyrosine-methionine-aspartate-aspartate (YMDD) motifs in the catalytic site of the HBV polymerase have been shown to confer Lamivudine resistance and reactivation of HBV (73). Adefovir dipivoxil and Entecavir have achieved increased efficacy against HBV and both agents inhibit the emergence of mutant viral strains (50, 63, 74). Telbivudine and Tenofivir have been available since 2006 and 2008 respectively. These agents exhibit activity against both HBV and the human immunodeficiency virus (HIV) and are used to treat HBV/HIV co-infection (75).

However, these existing therapeutics are unable to eradicate the established HBV cccDNA reservoirs and continuous treatment is required to prevent future viral reactivation and emergence of mutated viral strains. Therefore, HBV

cccDNA remains a major hurdle for chronic HBV treatment and novel methods are required to eliminate these cccDNA reservoirs.

1.6 Engineered site-specific endonucleases

Manipulation of DNA and RNA shows promise as antiviral agents against HBV, allowing targeting of both pre- and post-transcriptional events in the viral life cycle (63, 76-78). As a result, various technologies, such as antisense compounds, aptamers, RNA interference (RNAi) effectors, ribozymes and designer endonucleases, have been developed for this purpose. These technologies manipulate HBV DNA and RNA and have shown promise for the treatment of various persistent infectious diseases (76, 79-84).

Precise, predictable alteration of a target DNA sequence is required for genome manipulation (77, 78, 85). Advances in engineering targeted nucleases that contain programmable, site-specific DNA binding domains have facilitated significant progress in development of technologies that can be used to target specific sequences and further development of these technologies remains top priority (86). Meganucleases, RNA-guided endonucleases (RGENs), zinc finger nucleases (ZFNs) and transcription activator-like effector nucleases (TALENs) are four different designer nucleases currently used specifically for DNA engineering (87).

Meganucleases and RNA-guided endonucleases (RGENs) both have natural endonuclease activity. Meganucleases were first identified in mobile genetic elements of yeast and are engineered versions of naturally occurring DNA targeting restriction enzymes with extended DNA recognition sequences that bind a specific 12-40 bp DNA target sequence (87). The enzymes cleave the DNA target, creating a double stranded break (DSB) which triggers

homologous recombination events (88, 89). Artificially designed meganucleases have been successful in targeting specific target DNA sequences (90-92). However, the DNA recognition and cleavage function of meganucleases are intertwined in a single domain, making the engineering of these enzymes a challenge for most researchers (93).

RGEN is an alternative method that has recently shown promise for genome engineering applications. RGENs are based on a bacterial clustered regular interspaced short palindromic repeats (CRISPR) defence system which uses RNA-guided endonuclease activity to disable invading DNA. In this system CRISPR RNA (crRNA), which contains protospacers, hybridises with transactivating crRNA (tracrRNA) and forms a complex with CRISPR associated protein 9 (Cas9). The protospacer-encoded region of the crRNA then directs Cas9 to a complimentary DNA target sequence adjacent to a protospacer adjacent motif (PAM), allowing Cas9 to facilitate DNA cleavage (87, 94, 95). CRISPR is an important new approach for generating RNA-guided nucleases with customizable specificities. CRISPR technology has potential for RGEN-mediated site-directed cleavage and has recently been successful in multiple genome engineering projects (79, 87, 96-98). However, these designer nucleases have only recently been described and further analysis of the CRISPR-Cas9 system activity and genome-wide specificities is required (87, 99).

Zinc finger nucleases (ZFNs) are a more established genome engineering technology. Zinc finger (ZF) domains are capable of recognising nucleotide triplets and have been studied in-depth (85, 100). The modular structure of the ZF motif permits several domains to be joined in series. These arrays are capable of targeting various DNA sequences upstream of genes and can be fused with transcriptional activation or repressor proteins to form gene regulators (101). ZF arrays have also been fused to a non-specific *Fok*I catalytic domain to generate ZF nucleases (ZFNs) (85, 100). A ZFN monomer

usually consists of 3-6 ZF motifs and targets DNA sequences that are 9-18 bp long. The *Fok*I domains of two ZFN monomers dimerise to form a functional endonuclease that results in cleavage of both the positive and negative DNA strands (100). Designer ZFNs have been used in multiple genome engineering projects that involved targeted DNA mutations and specific editing of complex genomes in a variety of cells and organisms (78, 79, 85, 100-109). However, robust construction of ZFNs has proven difficult. Neighbouring ZFs in ZFNs affect the specificity of the ZFN and therefore a specific context dependent subunit arrangement is required to effectively bind DNA (85, 110-114). This warrants investigation into technologies, such as TALENs, that require less or no context specificity.

Transcription activator like effectors (TALEs) also recognise specific DNA sequences (115, 116). TALEs were first discovered in *Xanthomonas*, a pathogenic plant bacteria. The bacterial type III secretion system injects the TALEs into plant cells. The injected TALEs are then transported to the cell nucleus, where they bind to the target DNA sequence and activate downstream gene expression (110, 117, 118). TALEs consist of individual monomers, which consist of 33-35 amino acid repeat domains that recognise a single DNA base pair (Figure 1.3) (115, 116). Most TALEs consist of 13 to 28 repeats and the last repeat is truncated at 20 amino acids (110, 119). Polymorphisms are formed by the hypervariable amino acid residues 12 and 13, which are known as the repeat variable diresidues (RVDs). These RVDs show specific preferences for different DNA nucleotides. The NG, HD, NI and NN RVD domains show affinity for thymidine (T), cytosine (C), adenine (A) and guanine (G) respectively (115, 116, 120). These repeats can be added in tandem to target a specific DNA sequence. However, it has recently been reported that engineered TALE DNA binding domains are affected by the 5-methylated cytosine (5mC), an epigenetic modification, in their target DNA sequence (121, 122). 5mC is very common in different cell types and genomic kingdoms. The

negative impact that 5mC has on dTALE activity is potentially a major drawback to the use of TALE-based technologies considering how ubiquitous this modification is. However, Valton *et al*. demonstrated that substituting the sensitive-to-cytosine-methylation HD domain with a methylation insensitive N* domain efficiently accommodates 5mC in the target sequence and negates the negative impact on TALE activity (122). There are other known RVD domains that also associate more specifically with certain DNA bases and more than one type of nucleotide, but TALEs with these alternative RVD domains tend to exhibit decreased activity (116, 123). The number and composition of TALE DNA-binding domains determine the DNA sequence that the TALE array will bind. User defined DNA sequences can be targeted by designer TALEs that are assembled by joining the TALE repeats in a specific order (15, 86, 124, 125).

The designer TALEs can be fused to different effector domains to create nucleases, repressors and transcriptional activators. TALE nucleases (TALENs) are TALEs fused with a *Fok*I catalytic domain (Figure 1.3). These TALENs are designed in pairs (a left and right TALEN pair) that target complimentary DNA targets separated by a 14-15 bp spacer region (110, 126). TALEN specificity is of utmost importance to prevent off-target effects, and may be affected by various factors. The composition and number of repeats in TALENs affect TALEN specificity, as RVDs differ in their stringency for specific nucleotide preferences (110, 127). The length of the spacer region between two TALENs also affects TALEN specificity (85, 124, 127). However, in contrast to ZFNs, TALEN specificity is not affected by the context of the TALE repeats (116).

TALENs are effective and have successfully been used in multiple genome engineering projects (79, 99, 124, 127-131). Recently Reyon *et al*. demonstrated that TALENs have good efficacy against a wide variety of targets within the human genome and by applying careful design rules it is possible to

develop TALENs which target essentially any DNA sequence in the human genome (132). These results were supported by findings from Mussolino *et al*., who showed that TALENs are able to discriminate between highly similar sequences (CCR5 and CCR3) (85). Early studies indicate that TALENs result in little or no off-target mutagenesis (85, 127, 133, 134). However, these studies are limited in scope as they only analyse predicted off-target sites (135, 136). As a result, recent studies sequenced the complete genome of human induced pluripotent stem cells (hiPSCs). These studies demonstrated that gene correction by TALENs in single cell clones exhibits a low level of sequence variation and few off-target effects. The observed single-nucleotide variants (SNVs) were not within the potential off-target regions. Results suggest that TALENs induce rare SNVs in a non-random manner, or that the mutations were not direct results of off-target TALEN activities, but were randomly accumulated during regular cell expansion (135-137). Therefore, TALENs provide highly specific and efficient genome-editing tools and the incidence of off-target effects is not a significant concern for disease modelling and genome-editing applications (135, 137).

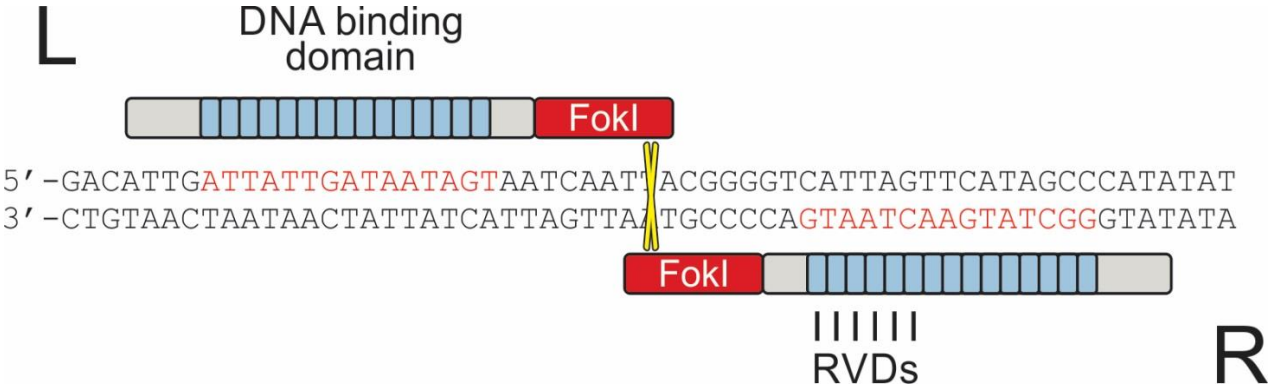

Figure 1.3: TALEN pairs that introduce DNA double stranded breaks. Each TALEN consists of a number of RVD-containing TALE repeats and a *Fok*I catalytic domain which is separated from the TALE repeats by a spacer region. *Fok*I acts as a dimer, thus requiring two *Fok*I catalytic domains (left and right TALENs) to cleave the DNA strand.

1.7 DNA repair pathways

Dimerisation of the TALEN *Fok*I domains introduces site specific DNA double stranded breaks (DSBs) (16). These DSBs result in DNA transcription, replication, and segregation complications and can lead to a rise in chromosomal instability if they are not correctly processed and repaired. DSBs induce the DNA repair response, which has two primary components in eukaryotic cells: (1) non-homologous end joining (NHEJ) and (2) homology directed repair (HDR) (110, 138-140). Both NHEJ and HDR may be manipulated to change the underlying DNA sequence by either inclusion or deletion of specific base pairs. Both repair pathways have been successfully exploited to introduce targeted genome alterations in multiple organisms and cell types, and present a novel mechanism by which to influence or edit an organism's genome (78, 111, 141).

1.7.1 Non-homologous end joining

NHEJ is the predominant repair mechanism in mammalian cells and operates at all stages of the mammalian cell cycle (Figure 1.4) (138, 142). The repair mechanism uses micro homologies to stabilise the NHEJ complex, but does not require sequence homologies or an intact homologous DNA template to ligate DNA ends and as a result produces junctions that can vary in sequence composition (138, 143-146). NHEJ may be error prone and can introduce deletions or short insertions of foreign DNA that can result in harmful frameshift mutations and gene knockouts (110, 111, 140, 147, 148). However, NHEJ is efficient in restoring the phosphodiester backbone and structural integrity of the DNA strand (140). Bloom *et al.* demonstrated that NHEJ can be exploited to introduce specific HBV genome alterations that are harmful to the virus (15).

1.7.2 Homology-directed repair

Homology directed repair (HDR) is an accurate DNA repair mechanism used by cells to repair DSBs (16, 143, 149-151). The mechanism is crucial for accurate genome duplication and preservation of the genome. HDR is induced if a double-stranded homologous DNA donor template is present at a DSB site. This undamaged homologous DNA sequence is used as a template for new DNA synthesis, allowing accurate repair of the DSB (139). There are four main HDR models: 1) Single strand annealing (SSA), 2) Break induced replication (BIR), 3) Double-strand break repair (DSBR) and 4) Synthesis-dependent strand annealing (SDSA). The SSA model states that a DSB flanked by homologous direct repeats is repaired by a deletion process. SSA is independent of strand invasion and does not require homologous donor template strands for DNA repair. However, DNA repair results in deletion of the sequences between the direct repeats and one of the flanking direct repeats (152, 153). BIR is a single ended invasion process that occurs if a single resected DSB end is present (154, 155). The single-strand tail invades a homologous DNA template and information is copied from the invaded sequence by DNA synthesis. BIR restores the integrity of the chromosome, but can also result in loss of heterozygosity of genetic information distal to the DSB (156).

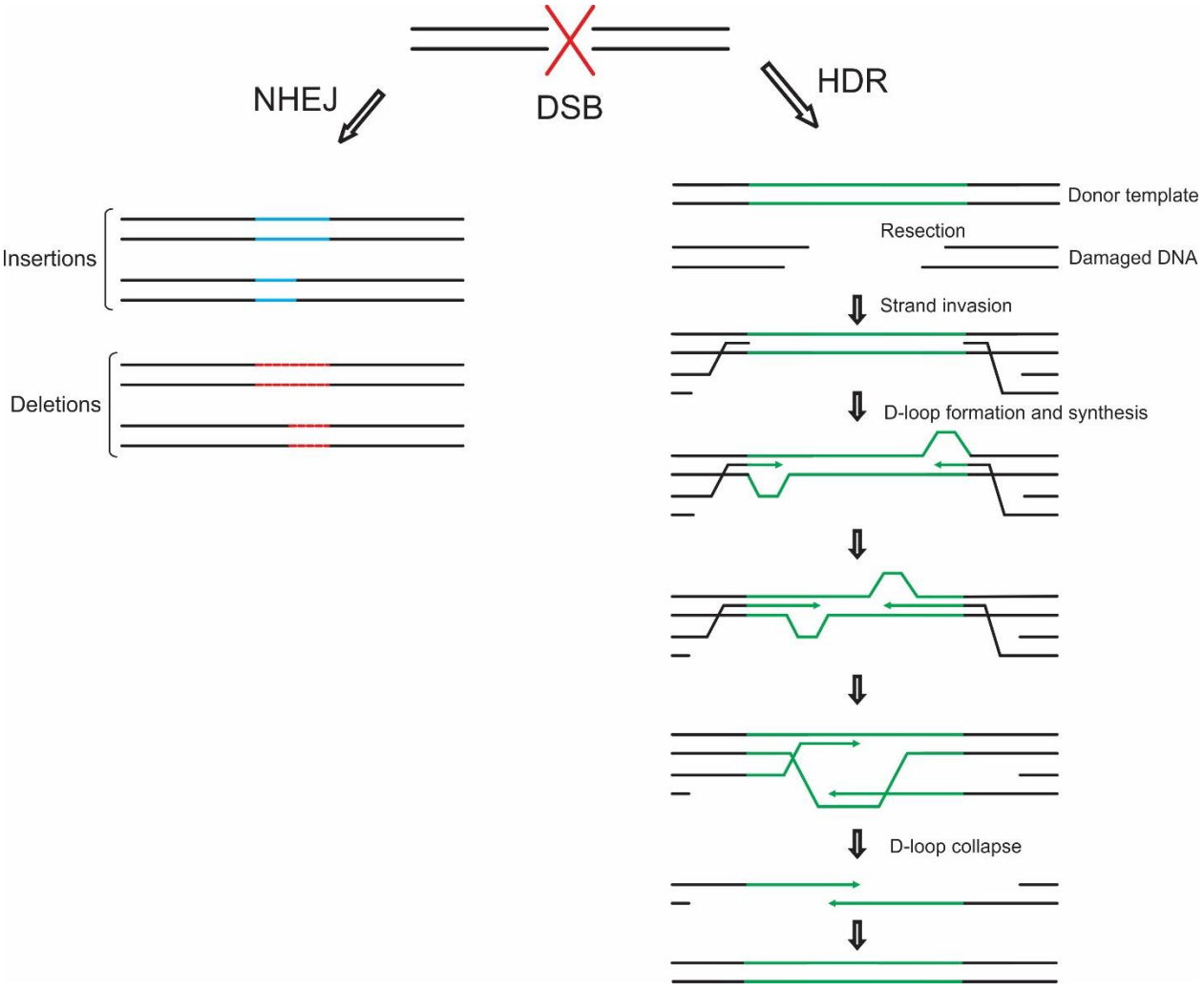

Figure 1.4: Double stranded break repair pathways. The imprecise NHEJ repair pathway can produce indels (insertions and/or deletions) of various lengths. The SDSA model of HDR uses a donor strand (from a sister chromatid or artificial sequence) as a template. The single-stranded chromosome end invades the homologous sequences of the donor. A D-loop is formed and is trailed by the newly synthesised single-stranded DNA. The two newly synthesised stretches of DNA can leave the D-loops once they overlap. The D-loops collapse once the new synthesised strands leave and the two overlapping strands anneal to each other and use each other as templates in order to restore the DNA integrity. The repaired DNA now contains the donor-specified transgene/artificial sequence.

During DSBR and SDSA the DSB undergoes nucleolytic processing, resulting in single strand DSB tails with 3'-OH ends. The single strand DNA (ssDNA) ends become the substrates for HDR protein machinery to execute invasion of the donor strand. Recombinases bind to the ssDNA end and form a helical filament that searches for homology through random collisions between the nucleoprotein filament and DNA sequences (16, 157, 158). Homologous sequence strand invasion occurs after a successful homology search and results in formation of a nascent D-loop intermediate, during which the 3' end of the invading strand is extended by DNA polymerase. During DSBR the second DSB end is annealed to the extended D-loop, thereby capturing it and resulting in formation of two crossed strands (Holliday junctions (HJs)). The HJs are resolved by a specialised endonuclease to produce crossover or non-crossover products. Most mitotic DSB repairs are not associated with crossovers (16, 159).

SDSA is the predominant pathway in mitotic repair if a second DSB end is present (Figure 1.4) (reviewed by Shinohara and Ogawa (160)). With SDSA the migration D-loop does not capture the second DSB end as in DSBR. The D-loop unwinds and the invading strand is displaced after initial DSB-end resection, strand invasion, and DNA repair synthesis. The displaced strand then anneals to the complementary ssDNA strand that is associated with the opposite resected DSB end (144, 161). Gap-filling DNA synthesis and strand annealing occur and finish the replication process. No crossover products are formed as HJ formation is blocked by HDR proteins *in vitro*, thus reducing potential genomic rearrangements during the repair process (162). This results in bias towards the SDSA mechanism, which can be exploited to introduce specific genomic alterations.

HDR can be co-opted to facilitate the integration of specific sequences at targeted genomic loci. This is achieved by developing donor sequences with high sequence homology, either flanking a portion of non-homologous DNA, or

with a single base pair change that can facilitate gene disruption or augmentation. Use of HDR as a genome engineering tool is becoming more frequent. Research groups recently demonstrated that ZFN-based nicking enzymes can be used to insert DNA sequences at predetermined sites in selected genomes (163, 164). Wang *et al*. utilised engineered ZFNs (ZFNickases) that introduce site-specific DNA single-strand breaks (SSBs) or nicks in the endogenous *CCR5* locus in both transformed and primary human cell lines (164). Researchers stimulated gene addition and correction by introducing a homologous donor template and succeeded in inserting an artificial DNA sequence at the *AAVSI* locus. Ramirez *et al*. also demonstrated that ZFNickases efficiently generate DNA SSBs *in vitro*. The SSBs and addition of donor templates stimulated HDR, and they were able to successfully repair a chromosomal enhanced green fluorescent protein (EGFP) sequence in U2OS-based reporter cells by inserting artificial DNA sequences at the nicking site (163). Both groups reported reduced levels of NHEJ-mediated mutagenesis. Bedell *et al*. demonstrated that their designer TALENs efficiently induce locus-specific DSBs in zebrafish somatic and germline tissue. The researchers stimulated HDR in zebrafish by introducing TALEN-mediated DSBs and single stranded donor template strands, and were able to precisely modify sequences at selected locations in the zebrafish genome. They also inserted a custom *Eco*RV site and a modified *loxP* sequence into zebrafish somatic tissue *in vivo* (165). Osborn *et al*. used HDR to repair the type VII collagen gene defects in cells with recessive dystrophic epidermolysis bullosa (166). The research group generated TALEN-induced site-specific DSBs which stimulated HDR from an exogenous donor template and resulted in gene mutation correction (*COL7A1*) in primary fibroblasts. Wang *et al*. were able to edit the mouse Y chromosome in mouse embryonic stem cells. They created TALEN-induced DSBs at the *Sry* and *Uty* loci and introduced a donor template that contained a puromycin selection marker and a promoterless GFP flanked by 700 bp 5’ and 385 bp 3’ homologous regions. Introduction of the donor

template stimulated HDR and subsequent analysis confirmed that the donor constructs were successfully inserted at the target sites (167). The collective results from these research groups indicate that targeting the HBV genome with designer TALENs and introducing homologous donor templates to induce HDR is a promising prospect for developing anti-HBV therapy. It follows that possible anti-HBV sequences, such as RNA interference effecters, can be incorporated into these homologous donor templates and needs to be investigated.

1.8 RNA interference pathway

Alternative gene therapies, such as RNA interference, have been shown to have significant potential. Therefore, it should be possible to disrupt viral activity by targeting selected viral genome targets with both RNA interference effecters and designer endonucleases.

The RNA interference pathway (RNAi) forms part of the post-transcriptional mechanism of HBV replication and studies demonstrated that RNAi effecters have potential for antiviral gene therapies that target chronic HBV (168, 169). RNAi induces posttranscriptional gene silencing by degradation or translational suppression of a target messenger RNA (mRNA) (170). RNA polymerase II transcripts express primary microRNAs (pri-miRs) which are cleaved to produce precursor microRNAs (pre-miR) (Figure 1.5) (171). Pre-miR is exported to the cytoplasm and cleaved to form a miR/anti-miR duplex (172). This duplex is loaded onto the RNA-induced silencing complex (RISC) which guides the miR to the target mRNA(168). The miR/RISC complex then either inhibits mRNA translation or cleaves the mRNA (168, 173). Polymerase II expression cassettes achieve tissue-specific and inducible expression of RNAi

effecters (168, 174, 175). Ely *et al*. demonstrated that modular cassettes expressed from Poll II promoters should be advantageous for simultaneous silencing of multiple different genome sites (169). The researchers targeted three different HBV viral genome sites with primary pri-miR-31-derived shuttles encoded by modular trimeric anti-HBV Pol II cassettes. They then demonstrated that their transcribed pri-miR trimers generated the intended guide strands and effectively silenced the selected targets. HBV replication was inhibited both in cell culture and *in vivo*, without disrupting the endogenous miR function or inducing an IFN response. We propose that this pri-miR cassette can be incorporated into the homologous donor template strands utilised by HDR. HDR should integrate the pri-miR cassette into a selected target sequence to facilitate pri-miR expression and subsequent inhibition of HBV replication.

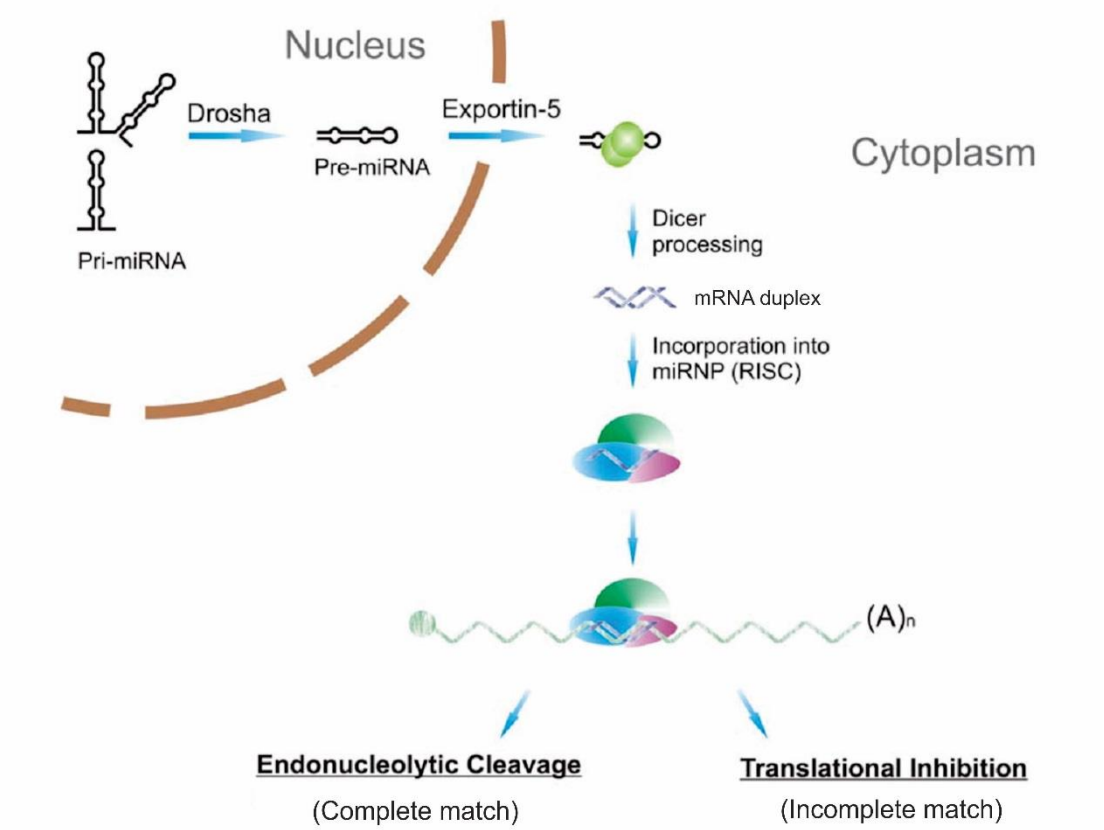

Figure 1.5: MicroRNA biogenesis in the RNAi pathway. Pri-miRNA is transcribed in the cell nucleus and is processed by Drosha into pre-miRNA. An Exportin-5 mediated pathway exports the pre-miRNA to the cytoplasm, where it is processed by Dicer into a miRNA duplex. The miRNA duplex unwinds when it associates with RISC and guides the complex to the target mRNA for translational repression or endonucleolytic cleavage (Diagram adapted with permission from Dr A. Ely, Antiviral Gene Therapy Research Unit (AGTRU), University of the Witwatersrand, South Africa).

1.9 Designer endonucleases targeting HBV cccDNA

As discussed in 1.4.2, current therapeutics rely on post-transcriptional mechanisms to inhibit HBV replication and do not target HBV cccDNA. HBV cccDNA drives HBV transcription and progeny virus production and is, therefore, a promising target for genome engineering applications and alternative HBV therapies. Zimmerman *et al*. reduced viral RNA levels by targeting the enhancer region of HBV cccDNA with ZFNs in a duck hepatitis B virus (DHBV) model. They transfected longhorn male hepatoma cells with DHBV replicating plasmids and ZFNs. Transfection with the ZFNs resulted in significant reduction in viral RNA levels, HBV protein concentration and intracellular viral particles, and a subsequent decrease in viral product production and progeny virus genomes (176). Another research group used designer TALENs to target conserved regions of viral genomic DNA in different HBV genotypes (177). Transfection of Huh7 cells with monomeric full length HBV DNA and TALENs resulted in significant reduction of HBcAg, HBeAg, HBsAg and pgRNA. The TALENs also resulted in misrepaired cccDNAs and a decrease in cccDNA levels, while no apparent cytotoxic effects were noted. In addition, Chen *et al*. demonstrated anti-HBV activity via TALENs in a hydrodynamic, injection-based mouse model. They also tested a TALEN and IFN-α combination treatment, which successfully restored the suppressed IFN-stimulated response against HBV (177). In another study, Bloom *et al*. successfully designed four TALENs that target four different HBV specific sites within the viral genome (15). TALENs targeting the HBV *surface* and *core* ORFs (S and C TALENs) resulted in sequence disruption at the target sites and a decrease in viral replication markers (HBsAg). Transfecting HepG2.2.15 cells thrice with S TALENs resulted in mutation of approximately 35% of the cccDNA. The researchers also demonstrated TALEN-mediated reduction of HBV replication markers in a murine hydrodynamic injection model of HBV replication. In this model the *surface* and *core* ORF target sites were mutated

and no *in vivo* cytotoxic effects were reported. The results from these research groups confirm that designer endonucleases can be used to successfully target HBV cccDNA and induce site-directed mutagenesis, thereby permanently disabling viral replication (15, 176, 177). The TALEN-mediated DSBs in cccDNA can also stimulate HDR if a homologous donor template is introduced. It follows that HDR could then integrate an artificial donor sequence at the cccDNA target site.

1.10 Experimental design and rationale

We propose that homology directed disruption of the HBV cccDNA using designer TALENs and donor template strands with pri-miR cassettes will result in improved HBV inactivation in an HBV replication model in cultured cells. Designer TALENs can be utilised to induce DNA DSBs at specific HBV cccDNA genome targets, resulting in both NHEJ and HDR. NHEJ has been shown to introduce indels at specific target sites and resulted in significant inactivation of HBV replication by disrupting viral transcription processes (15). HDR can be exploited to insert a pri-miR cassette at the target sites, as pri-miR expression has been shown to disrupt HBV replication without affecting the rest of the HBV genome (Figure 1.6) (78, 163, 165, 178). Ely *et al*. demonstrated pri-miR-31/5/8/9 cassettes that result in efficient disruption of HBV replication(169). Therefore, combining TALENs and pri-miR-31/5/8/9 should result in improved HBV disruption, as disruption will be caused by pri-miR expression as well as DSB-mediated NHEJ and HDR. Double stranded DNA strands are effective donor templates for HDR-mediated genome editing (124, 128). Therefore, an exogenous pri-miR sequence can be integrated into artificial dsDNA strands that are homologous to the TALEN target sites. These custom DNA sequences then act as donor templates for HDR of the TALEN-induced DSBs. In our

project designer TALENs were used to create DSBs at HBV *core* and *surface* target sites, which result in site-directed mutagenesis of HBV DNA (15). These TALEN-mediated DSBs should also result in HDR-mediated disruption of HBV DNA if a donor template is introduced. Donor templates with longer flanking homologous sequence lengths (400-800 bp) result in increased target efficiency and HDR frequency (167). However, it has been suggested that shorter homologous sequence lengths may also result in optimal HDR in some cell types, therefore, the optimum homologous sequence length has to be determined (127, 179). Our first objective was to construct linear donor template strands which contain a promoter-less pri-miR-31/5/8/9 cassette flanked by sequences that vary in length and are homologous to HBV *core* and *surface* target sites (169). The second objective was to analyse and optimise the integration of the donor sequence at the TALEN-mediated DSBs. The linear artificial donor template strands and designer TALENs are co-introduced to the cell cytoplasm and the viral *core* and *surface* target sites should be disrupted by TALEN-mediated NHEJ and HDR. HDR should incorporate the pri-miR-31/5/8/9 cassette at the target sites where an HBV promoter will drive pri-miR expression (Figure 1.6). Pri-miR will then be processed into mRNA, which forms a complex with RISC. This complex silences *HBx* and should result in significant disruption of HBV replication. Therefore, our proposed method targets HBV cccDNA and viral replication in a synergistic manner and should result in decreased viral replication and possible elimination of the viral cccDNA reservoirs.

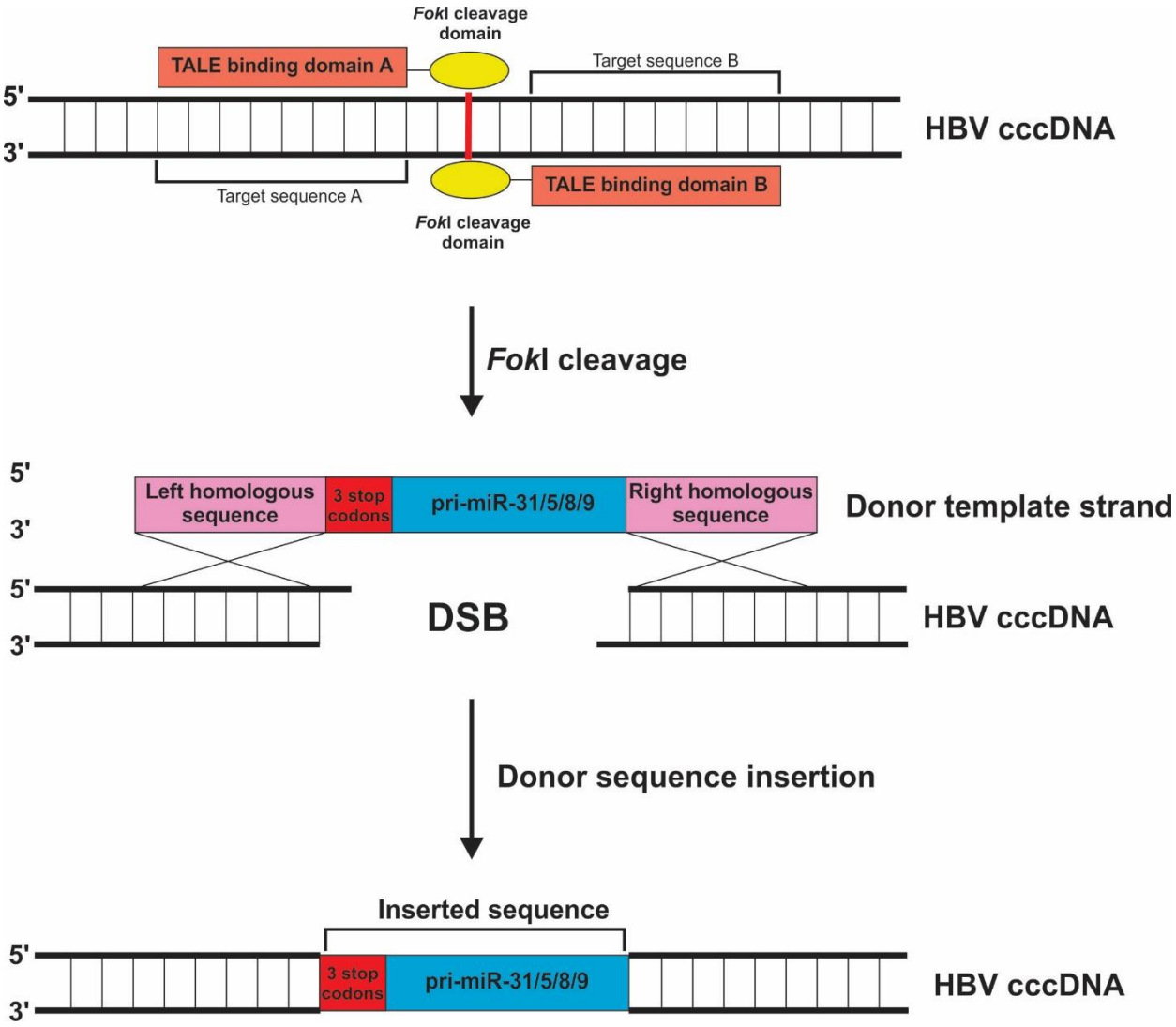

Figure 1.6: Insertion of the donor sequence at the *core* and *surface* cccDNA target sites. Two TALENs bind to their respective target sites, allowing the *Fok*I catalytic sites to dimerise and cleave the double stranded DNA, thus introducing a DSB and activating the DNA repair pathways. Donor template strands containing three stop codons and a pri-miR-31/5/8/9 cassette flanked by sequences that are homologous to the TALEN target sites are introduced. The HDR pathway uses the donor strands as repair templates and integrates the artificial sequence into the cccDNA. Successful integration should then result in target site disruption and HBV promoter driven pri-miR expression, which should disrupt HBV replication and decrease HBsAg expression.

2. Materials and methods

2.1 Plasmids

2.1.1 pCH-9/3091

pCH-9/3091 is a longer than genome length HBV equivalent developed by Nassal *et al*. to simulate HBV replication in cell culture (180). This plasmid is capable of replicating *in vitro* and encodes the wild-type HBV subtype D genome, using a cytomegalovirus (CMV) immediate early promoter to drive viral protein expression. The circular structure of the HBV genome is mimicked by including two terminal repeats. RNA produced from the pCH-9/3091 template is greater than genome length, as would occur in conventional HBV replication. HBV cccDNA is produced by reverse transcribing the HBV pre-genomic transcript, which can be recapitulated using this HBV genome equivalent.

2.1.2 pCMV-GFP

pCMV-GFP is a mammalian expression vector that encodes an enhanced green fluorescent fusion protein (EGFP) that expresses green fluorescence protein (GFP) (181). It can be used as a reporter plasmid to determine transfection efficiency, where higher GFP expression indicates greater transfection efficiency.

Table 2.1: Descriptions of transfection plasmids

Plasmid name	Plasmid description	Reference
pCH9/3091	HBV equivalent that simulate HBV infection in cell culture	[180]
pCMV-GFP	A reporter plasmid expressing GFP, used to determine transfection efficiency	[181]
pUC118	Standard cloning vector used to ensure consistent DNA quantities for transfections	[182]
C TALEN L	Left TALEN subunit targeting the HBV *core* ORF	[15]
C TALEN R	Right TALEN subunit targeting the HBV *core* ORF	[15]
S TALEN L	Left TALEN subunit targeting the HBV *surface* ORF	[15]
S TALEN R	Right TALEN subunit targeting the HBV *surface* ORF	[15]
Inactive TALEN	Left TALEN subunti with an inactive *Fok* I domain	This study
pCI-pri-miR-31/5/8/9	pCI-neo that encode a pri-miR-31/5/8/9 cassette	[169]
pri-miR-31/5/8/9	Linear DNA sequence encoding pri-miR-31/5/8/9	[169]
pTZ-C300	pTZ57 plasmid with a three stop codons and restriction enzyme recognition sites (*Sac* I, *Cla* I and *Nhe* I), flanked by 300 bp sequences that are homologous to the C TALEN recognition site	K. Bloom
pTZ-S300	pTZ57 plasmid with a three stop codons and restriction enzyme recognition sites (*Sac* I, *Cla* I and *Nhe* I), flanked by 300 bp sequences that are homologous to the S TALEN recognition sites	K. Bloom
pTZ-C300(pri-miR)	pTZ57 plasmid with a pri-miR cassette, three stop codons and restriction enzyme recognition sites (*Sac* I, *Cla* I and *Nhe* I), flanked by 300 bp sequences that are homologous to the C TALEN recognition sites	This study
pTZ-S300(pri-miR)	pTZ57 plasmid with a pri-miR cassette, three stop codons and restriction enzyme recognition sites (*Sac* I, *Cla* I and *Nhe* I), flanked by 50 bp sequences that are homologous to the S TALEN recognition sites	This study
pTZ-C50(pri-miR)	pTZ57 plasmid with a pri-miR cassette, three stop codons and restriction enzyme recognition sites (*Sac* I, *Cla* I and *Nhe* I), flanked by 50 bp sequences that are homologous to the C TALEN recognition sites	This study
pTZ-S100(pri-miR)	pTZ57 plasmid with a pri-miR cassette, three stop codons and restriction enzyme recognition sites (*Sac* I, *Cla* I and *Nhe* I), flanked by 100 bp sequences that are homologous to the S TALEN recognition sites	This study
pTZ-pri-miR	pTZ57 plasmid with a pri-miR-31/5/8/9 cassette	This study

2.1.3 pUC118

pUC118 is a standard cloning vector that does not encode a transgene. The plasmid was used in these experiments to ensure that all of the DNA quantities for the transfections was consistent (182).

2.1.4 TALENs

TALENs were designed to the *core* and *surface* ORF of HBV and are encoded on a pVAX TALEN backbone (15). The TALENs were transfected into cells in pairs (sense and antisense recognition) to allow for the obligate dimerization of the *Fok*I domains to facilitate DNA cleavage.

2.1 Donor template construction

2.1.1 Cloning pri-miR-31/5/8/9 into pTZ-C300 and pTZ-S300 vector plasmids

The plasmids used to construct the donor templates were obtained from K. Bloom. Previously K. Bloom constructed the pTZ-C300 and pTZ-S300 plasmids which contained 300 bp flanking sequences that are homologous to the HBV *core* and *surface* ORFs respectively (Figure 2.1 and 2.3 A; Table 2.1). These regions contained the TALEN recognition sequence as well as a central cassette with three stop codons and several restriction enzyme recognition sites (*Sac*I, *Cla*I and *Nhe*I).

The pTZ-C300 and pTZ-S300 plasmids were modified to act as vector backbones by cleaving the plasmids at the *Nhe*I site between the flanking

homologous regions. Each plasmid was digested with *Nhe*I (Thermo Scientific, Waltham, MA, USA) in Tango™ 1X buffer (33 mM Tris-acetate (pH 7.9); 10 mM Mg-acetate; 66 mM K-acetate; 0.1 mg/ml Bovine Serum Albumin (BSA)) (Thermo Scientific, Waltham, MA, USA) for 60 minutes at 37°C. The samples were incubated for an additional 30 minutes after addition of Fast AP (Thermo Scientific, Waltham, MA, USA) to prevent self-annealing of the digested plasmids (Figure 2.1).

Modular trimeric Pol II expression cassettes that encode primary microRNA (pri-miR-31/5/8/9) shuttles showed efficient silencing of HBV gene expression(169). The pCI-pri-miR-31/5/8/9 plasmid (described by Ely *et al*.(169)) was digested with *Nhe*I and *Xba*I in Tango™ 1X buffer (Thermo Scientific, Waltham, MA, USA) for 60 minutes at 37°C to excise the pri-miR-31/5/8/9 sequence.

The excised pri-miR-31/5/8/9 (21 ng for pTZ-C300 and 31.6 ng for pTZ-S300) with *Xba*I and *Nhe*I overhangs was ligated into the pTZ-C300 (37 ng) and pTZ-S300 (55 ng) vector backbones by T4 DNA ligase (Thermo Scientific, Waltham, MA, USA) (Figure 2.1). The ligation mix consisted of the vector backbones, the excised pri-miR sequence, 10x Ligase buffer and T4 DNA ligase, made up to 20 µl and was incubated for 2 hours at 22°C.

2.1.2 Chemically competent cells and transformation

XL1 Blue *Escherichia coli* (*E. coli*) were used to develop competent cells. Cells were grown for 16 hours at 37°C in Luria-Bertani (LB) culture medium, diluted 1:50 in fresh LB and incubated at 37°C until mid-log was reached (OD = 0.4). These cells were collected by centrifugation (15 min at 1000 x g and 4°C). The pellet was then resuspended in 20 ml transformation buffer (100 mM CaCl; 10 mM piperazine-N,N′-bis(2-ethanesulfonic acid) (PIPES) (pH 7.0); 15% glycerol;

pH 7.0; made up to 100 ml with dH_2O) and incubated at 4°C for 30 min. After incubation cells were collected, resuspended in 1.5 ml transformation buffer, aliquoted and stored at -70°C. The ligation mix (5 µl) containing the ligated vector backbones and pri-miR-31/5/8/9 cassette was added to 20 µl chemically competent cells and mixed gently. The reaction mixture was incubated at 4°C for 25 minutes, followed by heat shocking at 42°C for 90 seconds and incubation for 2 min at 4°C. The transformed competent cells were plated on ampicillin-containing (100 µg/ml) LB agar plates and were incubated at 37°C for 16 hours. Picked colonies were cultured in LB medium containing ampicillin (100 µg/ml) for 16 hours at 37° in a shaking incubator (Labcon, Gauteng, South Africa).

2.1.3 Screening for insertion and orientation of pri-miR-31/5/8/9

Plasmid extraction

Successful transformants potentially contain the desired plasmid construct and to verify plasmid identity it was necessary to extract and screen the relevant plasmids. Plasmids were extracted from the cultured transformants with a QIAamp DNA Mini Kit (Qiagen, Venlo, Limburg, Netherlands). Cells were collected by centrifugation (30 min at 2800 x g and 4°C). The cell mass was then resuspended in PBS (phosphate-buffered saline) and 20 µl Proteinase K (24 mg/ml) and 200 µl Buffer AL were added to lyse cells. The cell suspension was thoroughly mixed and then incubated at 56°C for 10 min to ensure cell lysis. This lysed suspension was inverted and an equivalent volume of 100% ethanol was added. The whole mixture was then applied to a QIAmp spin column and centrifuged for 1 min at 5900 x g. The plasmid DNA is adsorbed onto the QIAamp silica membrane during the centrifugation step. AW1 wash buffer was added to the spin column and the centrifugation step was repeated

to remove residual contaminants. This was followed by addition of AW2 wash buffer to the column and centrifugation for 1 min at 16300 x g to improve the purity of the eluted DNA. Distilled H_2O was added to the centre of the columns and the plasmids were collected by centrifugation (1 min at 5900 x g). The purified plasmids were analysed on a 1% agarose gel (gels were run with a PowerPac™ Basic power supply(BioRad, Hercules, CA, USA)), and quantified using a Nanodrop ND-1000 Spectrophotometer (Thermo Scientific, Waltham, MA, USA). Aliquoted samples were then stored at -20°C.

*Bam*HI/*Eco*RI and *Nhe*I/*Pci*I restriction digest

The purified plasmids (200 ng) were treated with *Bam*HI and *Eco*RI (Buffer: 10 mM Tris-HCl (pH 8.0), 5 mM MgCl2, 100 mM KCl, 0.02% Triton X-100, 0.1 mg/ml BSA) as these restriction sites flank the pri-miR-31/5/8/9 insert and do not appear in the vector backbone. Digestion with these enzymes would thus indicate successful ligation. Plasmids were screened for inserts that are in the same orientation as the cassette in pCI-pri-miR-31/5/8/9 (forward orientation). Insert orientation was established using a *Nhe*I and *Pci*I double restriction digest (Tango™ 1X buffer) and was only performed on those plasmids which had been shown to have the necessary insertion. The digested pTZ-C300 and pTZ-S300 backbones have two *Nhe*I overhangs, whereas the pri-miR shuttle has a *Nhe*I and *Xba*I overhang. Therefore, ligation of the backbones and pri-miR shuttles will result in a single *Nhe*I site that will vary in position, depending on the orientation of the inserted pri-miR sequence. *Pci*I is a unique restriction site in the pTZ-C300 and pTZ-S300 plasmids and does not appear in the pri-miR insert. Therefore, double enzyme digestion with *Pci*I and *Nhe*I will result in DNA strands with different lengths as a result of the varying position of the *Nhe*I restriction site (Figure 2.2). The digested samples were analysed on a 1% agarose gel and the samples containing a forward orientated insert were

selected for maxiprep. The pTZ-C300 and pTZ-S300 backbones containing the forward orientated insert are hereafter referred to as pTZ-C300(pri-miR) and pTZ-S300(pri-miR).

pTZ-C300(pri-miR) and pTZ-S300(pri-miR) plasmid extraction

Chemically competent cells were transformed with pTZ-C300(pri-miR) and pTZ-S300(pri-miR) and were cultured in LB for 16 hrs at 37°C. To generate plasmid stocks for multiple PCR reactions, a QIAGEN Plasmid Maxi Kit (Qiagen, Venlo, Limburg, Netherlands) was used to maxiprep the cultured transformants. The cultured cells were collected by centrifugation (15 min at 1000 x g and 4°C) and were resuspended in P1 suspension buffer (50 mM Tris-HCl (pH 8.0); 10 mM EDTA; 100 µg/ml RNase A). P2 lysis buffer (200 mM NaOH; 1% SDS) was added and the cell suspension was inverted and incubated at 21°C for 5 min to ensure lysis. After addition of P3 neutralisation buffer (3 M potassium acetate (pH 5.5)) to the suspension, the suspension was mixed thoroughly, incubated at 4°C for 20 min and centrifuged twice (2x 45 min at 2800 x g and 4°C). The supernatant was transferred to a filter column (QIAGEN-tip 500) (Qiagen, Venlo, Limburg, Netherlands) that was equilibrated with QBT equilibration buffer (750 mM NaCl; 50 mM MOPS (pH 7.0); 15% isopropanol; 0.15% triton X-100). Plasmid DNA binds to the column resin (under low salt conditions) when the column empties via gravity flow. The column was washed twice with medium-salt QC wash buffer (1 M NaCl; 50 mM MOPS (pH 7.0); 15% isopropanol) to remove proteins, dyes, RNA and impurities, followed by DNA elution with a high-salt QF elution buffer (1.25 M NaCl; 50 mM Tris-HCl (pH 8.5); 15% isopropanol). The collected DNA was mixed with isopropanol and stored at -20°C for 16 hours to desalt the plasmid DNA by isopropanol precipitation.

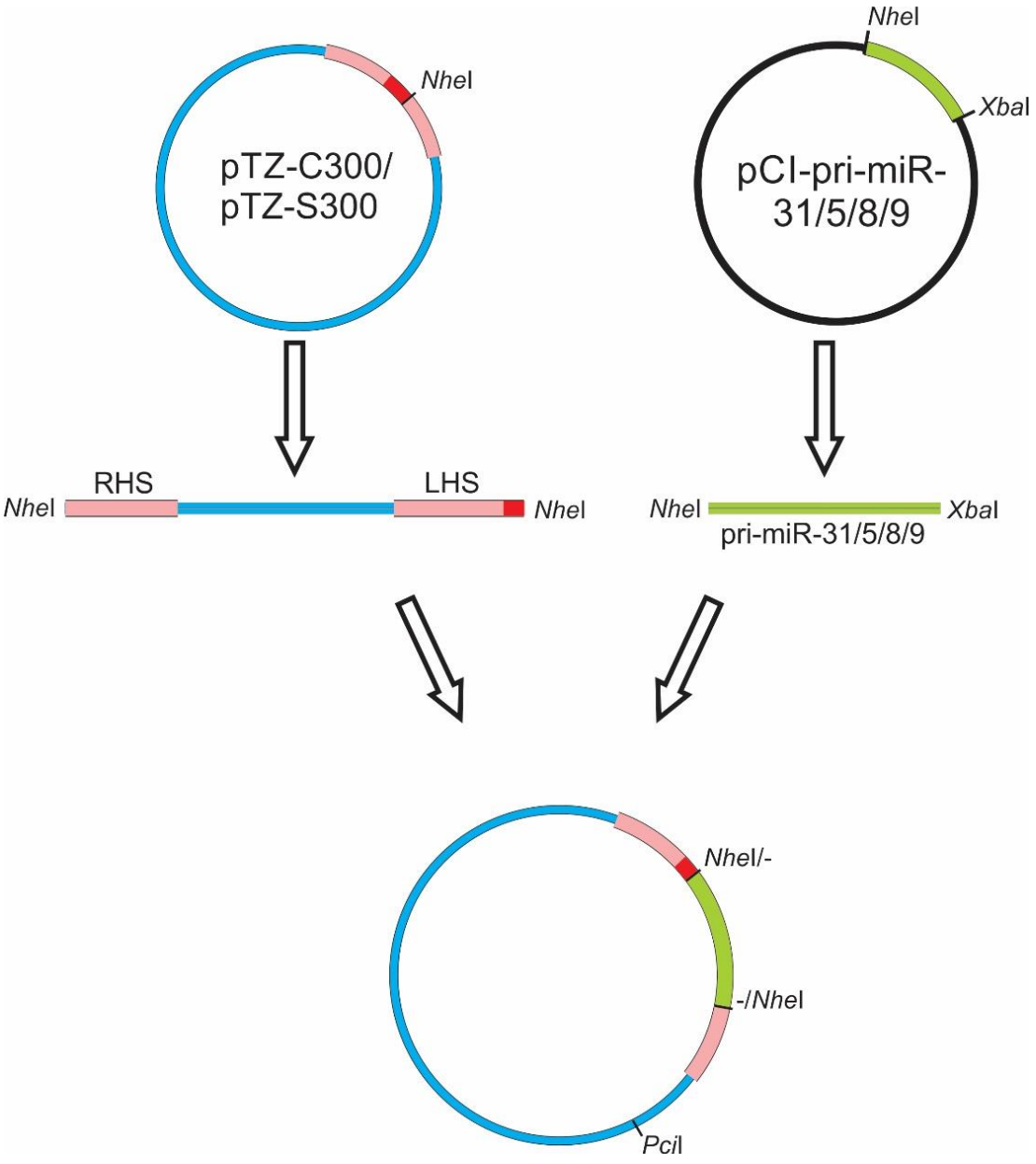

Figure 2.1: Donor template construction. The pTZ-C300 and pTZ-S300 plasmids contain a *Nhe*I site between the left and right homologous sequences (LHS and RHS) and were linearised with a *Nhe*I restriction digest. The pri-miR-31/5/8/9 sequence was excised from the pCI-pri-miR-31589 plasmid with a *Nhe*I/*Xba*I double restriction digest and then ligated into the linear pTZ-C300 and pTZ-S300 vector backbones.

The stored DNA was then centrifuged and the DNA pellets were washed with 70% ethanol. Centrifugation was repeated for 30 min and the DNA pellets were left to air dry. The air dried pellets were resuspended in 250 µl distilled H_2O, quantified by Nanodrop ND-1000 Spectrophotometer, and stored at -20°C.

2.1.4 Linear, double stranded Core and Surface donor template strands

Conventional PCR can be used to produce adequate quantities of double stranded, linear donor template strands for transfection experiments. pTZ-C300(pri-miR) and pTZ-S300(pri-miR) were used as templates to generate Core and Surface donor template strands that contain the pri-miR-31/5/8/9 cassette. The required donor template strands have flanking regions that vary in length and are homologous to HBV *core* and *surface* target sites (50 bp, 100 bp, 150 bp and 300 bp respectively), thus, multiple sets of primers were required (Figure 2.3). Donor template strands without the pri-miR insert were generated with the same primer pairs, using pTZ-C300 and pTZ-S300 (see 2.2.1) as templates (Figure 2.3). These non-insert donor template strands were used as controls to determine if insertion of the pri-miR shuttle into pCH-9/3091 and the resultant pri-miR expression result in improved HBsAg reduction when compared to pCH-9/3091 lacking the pri-miR insert.

Primer design for amplification of the *core* and *surface* donor template strands

Multiple primer sets were designed to flank the pri-miR insert and its two flanking homologous regions. The primers were compared to the pCH9/3091 plasmid and the pri-miR-31/5/8/9 sequence to ensure lack of similarity to these sequences. Primers were analysed and validated with NetPrimer analysis software (PREMIER Biosoft International) and were synthesised by Inqaba

Biotech (Pretoria, Gauteng, South Africa) using standard phosphoramidite technology. A 630 bp region containing 50 bp flanking homologous regions and the pri-miR-31/5/8/9 insert (Figure 2.3 B) was amplified from pTZ-C300(pri-miR) and pTZ-S300(pri-miR) using the following two primer sets: C50-F (928) - 5' ATA GAC CAC CAA ATG CCC CTA TC 3' (forward), C50-R (1552) - 5' CTG CGA GGC GAG GGA GTT 3' (reverse) and S50-F (928) - 5' GGC GTT TTA TCA TCT TCC TC- 3' (forward), S50-R (1550) - 5' GGA ATT AGA GGA CAA ACG GG 3' (reverse) (Table 2.2). The following primer sets were used to amplify regions of pTZ-C300(pri-miR) and pTZ-S300(pri-miR) that contain the prim-miR insert and 100 bp, 150 bp, and 300 bp flanking homologous regions respectively: C100-F (878) - 5' TAT AGA GTA TTT GGT GTC TT 3' (forward), C100-R (1603) - 5' GAG ATT CCC GAG ATT GA 3' (reverse), C150-F (828) - 5' CAA CTC TTG TGG TTT CAC AT 3' (forward), C150-R (1650) - 5' TAA AGC CCA GTA AAG TTC CC 3' (reverse), C300-F (678) - 5' TCA CCT CAC CAT ACT GC 3' (forward), C300-R (1802) - 5' GCA GGC ATA ATC AAT TGC 3' (reverse), S100-F (878) - 5' ACC AAC CTC TTG TCC TCC AA 3' (forward), S100-R (1601) - 5' CAG TAG TCA TGC AGG TCC G 3' (reverse), S150-F (828) - 5' ACT ACC GTG TGT CTT GGC C 3' (forward), S150-R (1650) - 5' GTC CGA AGG TTT GGT ACA GC 3' (reverse), S300-F (678) - 5' GGG GAC CCT GCG CTG AAC 3' (forward) and S300-R (1798) - 5' AAC TGA AAG CCA AAC AGT GGG G 3'(reverse) (Table 2.2). The primer sets generated Core and Surface donor template strands (amplicons) that were 630 bp (C50(pri-miR); S50(pri-miR)), 730 bp (C100(pri-miR); S100(pri-miR)), 830 bp (C150(pri-miR); S150(pri-miR)) and 1130 bp (C300(pri-miR); S300(pri-miR)) in length (Table 2.3). The same primer sets were used to amplify 121 bp (C50; S50), 221 bp (C100; S100), 321 bp (C150; S150) and 621 bp (C300; S300) regions within the pTZ-C300 and pTZ-S300 plasmids (see 2.2.1) (Table 2.2). These regions contain the donor template strands with homologous regions but lack the pri-miR insert (Figure 2.3 A).

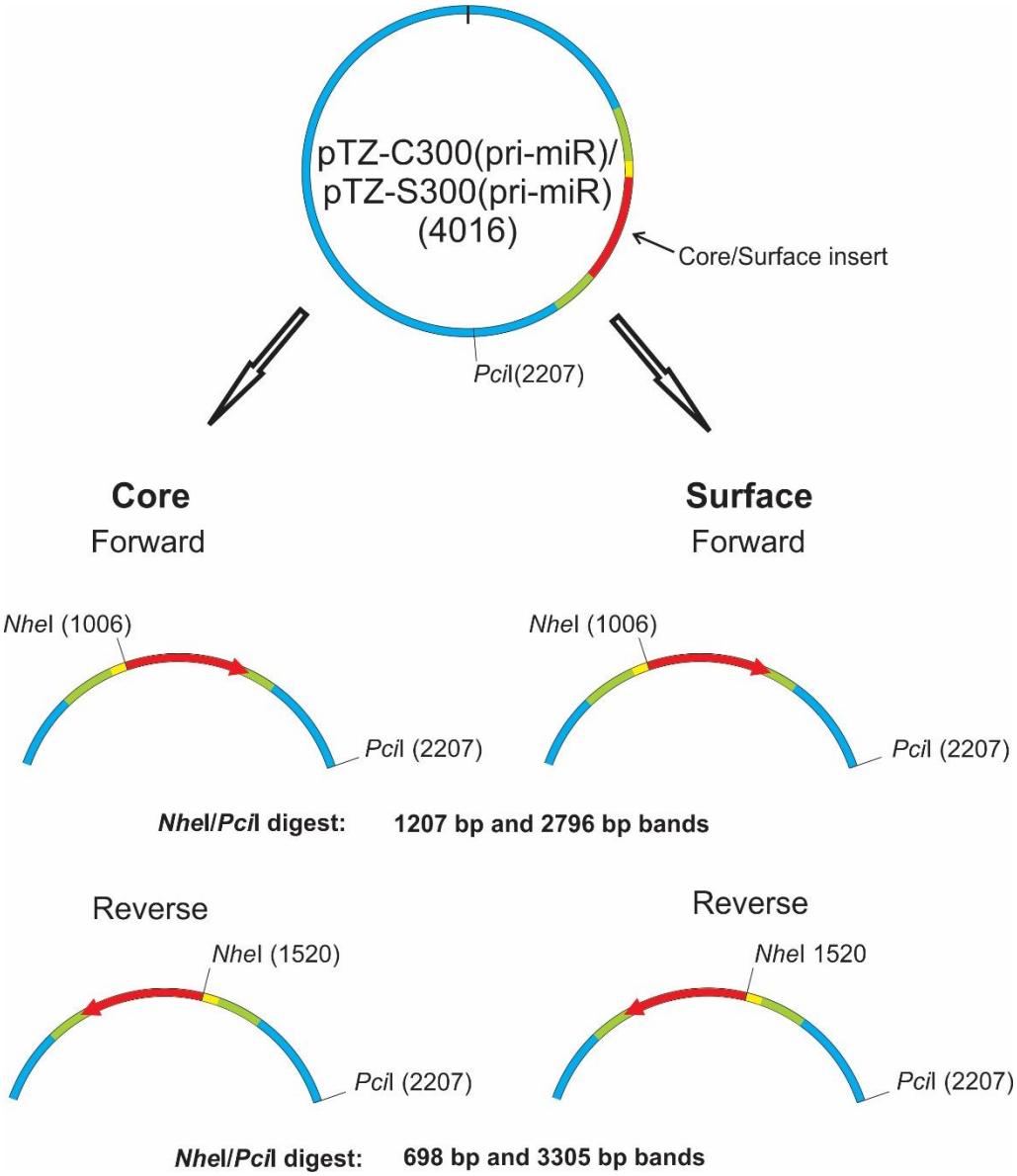

Figure 2.2: Orientation of the integrated pri-miR-31/5/8/9 sequence. The pTZ-C300 and pTZ-S300 plasmids containing the pri-miR-31/5/8/9 insert were digested with *Pci*I and *Nhe*I. The *Pci*I restriction site is a unique site. The location of the *Nhe*I site after ligation depends on the orientation of the inserted pri-miR-31/5/8/9 sequence. The *Nhe*I site is closer to the plasmid origin (the 0 position on the plasmid) if the inserted sequence is in a forward orientation and a *Nhe*I/*Pci*I double digest should result in a 1207 bp and 2796 bp band. The *Nhe*I site is further from the plasmid origin if the insert is reverse orientated and should result in a 698 bp and 3306 bp band when double digested with *Nhe*I and *Pci*I.

PCR amplification of the donor template strands

pTZ-C300(pri-miR), pTZ-S300(pri-miR), pTZ-C300 and pTZ-S300 (see 2.2.1) were used as amplification templates. The PCR system for all Core donor template strand amplifications included 2x KAPA Taq RM (Kapa Biosystems, Wilmington, Massachusetts, USA), 10 µM Cxx-F forward primer, 10 µM Cxx-R reverse primer, and 100-150 ng pTZ-C300(pri-miR) and pTZ-C300, made up to a final volume of 50 µl with distilled H_2O (dH_2O) in a 0.2 ml PCR grade microcentrifuge tube (Axygen Scientific, Union City, CA, USA). The PCR components used for Surface donor template strand amplifications were: 2x KAPA Taq RM, 10 µM Sxx-F forward primer, 10 µM Sxx-R reverse primer, and 100-150 ng pTZ-300(pri-miR) and pTZ-S300, made up to 50 µl with dH_2O. The PCRs were performed in a Bio Rad T100™ Thermal cycler (BioRad, Hercules, CA, USA) under the following conditions: initial denaturation at 95°C for 2 min; 30 cycles of: denaturation at 95°C for 30s, annealing at x°C for 30s (depending on which primer set is used) and extension at 72°C for 1 min; final elongation at 72°C for 2 min, followed by cooling at 4°C (Table 2.3). The annealing temperature for each primer set was calculated by subtracting 5°C from the primer melting temperatures (T*m*) listed in Table 2.2. The PCR products were analysed on 1% agarose gels and quantified with a Nanodrop ND-1000 Spectrophotometer.

A Gene JET PCR Purification Kit (Thermo Scientific, Waltham, MA, USA) was used to remove primers, dNTPs, unincorporated labelled nucleotides, enzymes and salts from PCR mixtures to use the donor template strands for transfection experiments (Table 2.4). An equal volume of Binding buffer was added to the completed PCR mixtures and transferred to a GeneJET purification column. The proteins in the solution are denatured by a chaotropic agent in the binding buffer, which also promotes DNA binding to the proprietary silica-based membrane. The suspension was centrifuged (60 seconds at 16300 x g),

followed by addition of Wash buffer to remove impurities. Residual wash buffer was removed by repeating the previous centrifugation step twice, followed by addition of Elution buffer (10 mM Tris-HCl (pH 8.5)) to collect the donor template strands. The purified donor template strands were analysed with a 1% agarose gel, quantified with a Nanodrop ND-1000 Spectrophotometer and stored at -20°C.

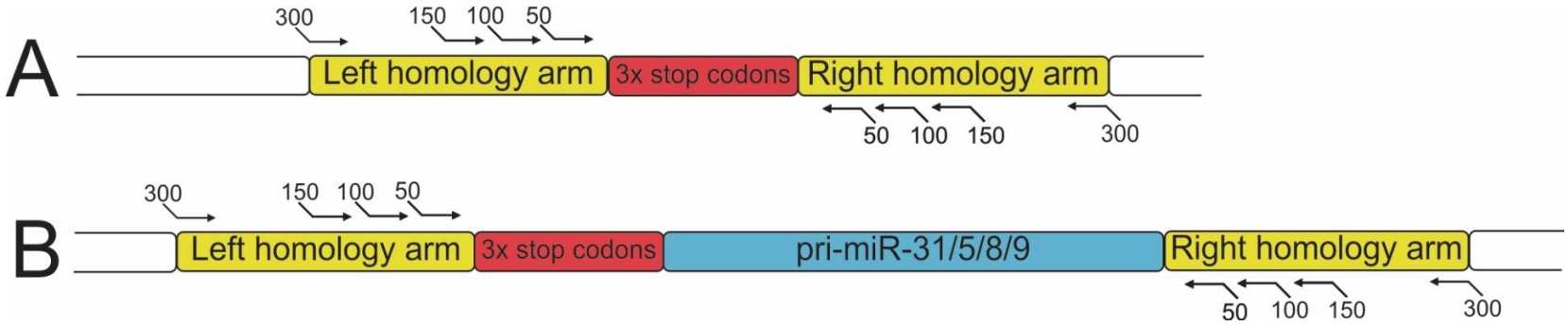

Figure 2.3: Core and Surface donor template strands. Donor template strands with flanking sequences that are homologous to the C and S TALEN target sites were generated by PCR. The length of the flanking homology arms were varied (50, 100, 150 and 300 bp respectively) to analyse their effect on HDR efficiency. A: Donor template strands without the pri-miR-31/5/8/9 insert were constructed as controls. B: Donor template strands containing the pri-miR-31/5/8/9 sequence that will be incorporated at the pCH-9/3091 target site. The primers are listed in Table 2.2.

Table 2.2: Forward and reverse primers used to generate the donor template strands

Name	Sequence	T*m* (°C)
50 bp Core (forward)	5' ATAGACCACCAAATGCCCCTATC 3'	62.77
50 bp Core (reverse)	5' CTGCGAGGCGAGGGAGTT 3'	64.46
100 bp Core (forward)	5' TATAGAGTATTTGGTGTCTT 3'	52.2
100 bp Core (reverse)	5' GAGATTCCCGAGATTGA 3'	54.78
150 bp Core (forward)	5' CAACTCTTGTGGTTTCACAT 3'	56.3
150 bp Core (reverse)	5' TAAAGCCCAGTAAAGTTCCC 3'	58.35
300 bp Core (forward)	5' TCACCTCACCATACTGC 3'	57.19
300 bp Core (reverse)	5' GCAGGCATAATCAATTGC 3'	55.34
50 bp Surface (forward)	5' GGCGTTTTATCATCTTCCTC 3'	58.35
50 bp Surface (reverse)	5' GGAATTAGAGGACAAACGGG 3'	60.4
100 bp Surface (forward)	5' ACCAACCTCTTGTCCTCCAA 3'	60.4
100 bp Surface (reverse)	5' CAGTAGTCATGCAGGTCCG 3'	62.32
150 bp Surface (forward)	5' ACTACCGTGTGTCTTGGCC 3'	62.32
150 bp Surface (reverse)	5' GTCCGAAGGTTTGGTACAGC 3'	62.45
300 bp Surface (forward)	5' GGGGACCCTGCGCTGAAC 3'	66.73
300 bp Surface (reverse)	5' AACTGAAAGCCAAACAGTGGGG 3'	62.67

Table 2.3: Temperature and time for each PCR cycle

	Temperature (°C)	Time (min)
Initial denaturation	95°C	2
Denaturation	95°C	0.5
Annealing	T*m*	0.5
Extension	72°C	1
Final extension	72°C	2

Table 2.4: Descriptions of donor template strands

Donor template strand name	Donor template strand description	Reference
C50	Core donor template strand with three stop codons and restriction enzyme recognition sites flanked by 50 bp homologous sequences	This study
C100	Core donor template strand with three stop codons and restriction enzyme recognition sites flanked by 100 bp homologous sequences	This study
C150	Core donor template strand with three stop codons and restriction enzyme recognition sites flanked by 150 bp homologous sequences	This study
C300	Core donor template strand with three stop codons and restriction enzyme recognition sites flanked by 300 bp homologous sequences	This study
C50(pri-miR)	Core donor template strand with pri-miR-31/5/8/9 flanked by 50 bp homologous sequences	This study
C100(pri-miR)	Core donor template strand with pri-miR-31/5/8/9 flanked by 100 bp homologous sequences	This study
C150(pri-miR)	Core donor template strand with pri-miR-31/5/8/9 flanked by 150 bp homologous sequences	This study
C300(pri-miR)	Core donor template strand with pri-miR-31/5/8/9 flanked by 300 bp homologous sequences	This study
S50	Surface donor template strand with three stop codons and restriction enzyme recognition sites flanked by 50 bp homologous sequences	This study
S100	Surface donor template strand with three stop codons and restriction enzyme recognition sites flanked by 100 bp homologous sequences	This study
S150	Surface donor template strand with three stop codons and restriction enzyme recognition sites flanked by 150 bp homologous sequences	This study
S300	Surface donor template strand with three stop codons and restriction enzyme recognition sites flanked by 300 bp homologous sequences	This study
S50(pri-miR)	Surface donor template strand with pri-miR-31/5/8/9 flanked by 50 bp homologous sequences	This study
S100(pri-miR)	Surface donor template strand with pri-miR-31/5/8/9 flanked by 100 bp homologous sequences	This study
S150(pri-miR)	Surface donor template strand with pri-miR-31/5/8/9 flanked by 150 bp homologous sequences	This study
S300(pri-miR)	Surface donor template strand with pri-miR-31/5/8/9 flanked by 300 bp homologous sequences	This study

2.2 Transfection of cultured Huh7 cells with TALENs and donor template strands

2.2.1 Huh7 cell culture

Huh7 cells, a liver derived human hepatoma cell line that supports viral replication when transfected with HBV DNA, were used to quantify the total HBsAg generated in a cell culture model system (183, 184). The cells were cultured in Cellstar® 75 cm^3 cell culture flasks (Greiner Bio-One GmbH, Frickenhausen, Germany) using Dulbeco's Modified Eagles Medium (DMEM) (Gibco, Invitrogen, USA) supplemented with 10% foetal bovine serum (FBS) (Biochrom GmbH, Berlin, Germany). The cultured cells were maintained at 37°C and 5% CO_2 in a humidified incubator until the cells covered 90-100% of the flask base (90-100% confluent). Cell confluency was analysed with a Olympus CKX31 light microscope (Olympus, Shinjuku, Tokyo, Japan) at 10x magnification.

The cell culture supernatant was removed and the adherent cells were washed with PBS. Washed cells were removed by trypsinisation (TrypLE™, Carlsbad, CA, United States of America) followed by resuspension in fresh DMEM growth medium. The cell suspension (4.8-5.3 x 10^5 cells/ml) was distributed in a 24 well Cellstar® Cell Culture Plate (Greiner Bio-One GmbH, Frickenhausen, Germany) (500 µl per well) and maintained in a humidified incubator at 37°C and 5% CO_2 until the cells were 80-90% confluent. Fresh DMEM growth medium was added to the confluent cultured cells just prior to transfection.

2.2.2 Transfecting cultured Huh7 cells

Each transfection sample consisted of a total 2 µg DNA (Table 2.5). The Core transfection samples consisted of the following (plasmids and donor template strands listed in Table 2.1 and 2.4): 200 ng pCH-9/3091; 100 ng pCMV-GFP; pUC118; 350 ng left C TALEN subunit (CPL); 350 ng right C TALEN subunit (CPR); 1 µg donor template strands (C50(pri-miR), C100(pri-miR), C150(pri-miR) and C300(pri-miR)) (Table 2.5), made to a final volume of 25 µl. The components in the Surface transfection samples were the same as those of the Core transfection samples, except CPL and CPR were substituted with SPL and SPR and the Core donor template strands were substituted with the Surface donor template strands (S50(pri-miR), S100(pri-miR), S150(pri-miR) and S300(pri-miR)) (Table 2.5). A third and fourth set of Core and Surface transfection samples substituted the insert-containing donor template strands with donor template strands that have three stop codons and no pri-miR-31/5/8/9 insert (C50, C100, C150, C300, S50, S100, S150 and S300) (Table 2.5). A mock (containing 200 ng pCH-9/3091, 100 ng pCMV-GFP, and 1.7 µg pUC118) as well as negative controls (containing an inactive left surface TALEN constructed by S. Nicholson (Table 2.1)) were also included (Table 2.5). Each transfection was done in triplicate.

Cells were transfected with polyethylenimine (PEI) (185, 186). Equal volumes of PEI (mg/ml) were added to each sample. The samples were thoroughly mixed and incubated at 21°C for 10 min. The incubated samples were then added drop wise to the cultured cells. The transfected cells were maintained in a humidified incubator at 37°C and 5% CO_2 for 24 hours, followed by addition of fresh DMEM growth medium and incubation for 48 hours.

Table 2.5: DNA amounts for Huh7 transfection in 24 well plates

Mock	**ng**	**C TALENs**	**ng**	**Core donor template strands with pri-miR**	**ng**	**Donor template strands without pri-miR**	**ng**
pCMV-GFP	100	pCMV-GFP	100	pCMV-GFP	100	pCMV-GFP	100
pCH-9/3091	200	pCH-9/3091	200	pCH-9/3091	200	pCH-9/3091	200
pUC-118	1700	pUC-118	1000	pUC-118	0	pUC-118	0
		CPR	350	CPR	350	CPR	350
		CPL	350	CPL	350	CPL	350
				Core donor template strands with pri-miR	1000	Donor template strands without pri-miR	1000
Total	**2000**	**Total**	**2000**	**Total**	**2000**	**Total**	**2000**

S TALENs	**ng**	**S donor template strands with pri-miR**	**ng**	**S donor template strands without pri-miR**	**ng**	**Inactive TALEN**	**ng**	**Inactive TALEN + C donor template strands with pri-miR**	**ng**
pCMV-GFP	100	pCMV-GFP	100	pCMV-GFP	100	pCMV-GFP	100	pCMV-GFP	100
pCH-9/3091	200	pCH-9/3091	200	pCH-9/3091	200	pCH-9/3091	200	pCH-9/3091	200
pUC-118	1000	pUC-118	0	pUC-118	0	pUC-118	1000	pUC-118	0
SPR	350	SPR	350	SPR	350	inactive TALEN	700	inactive TALEN	700
SPL	350	SPL	350	SPL	350			Inactive TALEN + C donor template strands with pri-miR	1000
		S donor template strands with pri-miR	1000	S donor template strands without pri-miR	1000				
Total	**2000**	**Total**	**2000**	**Total**	**2000**	**Total**	**2000**	**Total**	**2000**

2.3 Analysis

2.4.1 GFP

GFP expression by the transfected Huh7 cells was analysed with 488 nm and 509 nm excitation and emission wavelengths respectively using a Zeiss Axiovert 100 M fluorescence microscope (Carl-Zeiss, Oberkochen, Germany).

2.4.2 HBsAg ELISA

Huh7 cells transfected with pCH-9/3091, an HBV equivalent, produces HBsAg, thus simulating natural HBV replication. The effect of TALENs and donor template strands on HBV activity can be analysed by measuring the HBsAg concentration of the transfected cells, where a decrease in HBsAg concentration indicates reduced viral activity. The HBsAg levels were measured using an HBsAg enzyme-linked immunosorbent assay (ELISA), which is a one-step enzyme immune assay technique for the detection of HBV surface antigen.

HBsAg concentrations were measured with a Monolisa HBsAg Ultra kit (BioRad, Hercules, CA, USA). The supernatants (100 µl) of transfected cells were collected and distributed in a microplate with mouse monoclonal anti-HBsAg antibody coated wells. Conjugate working solution (mouse monoclonal anti-HBsAg antibodies and goat polyclonal anti-HBsAg antibodies which binds to the peroxidase) was added and aspirated with a pipette. The microplate was then covered with adhesive film and incubated at 37°C for 1 hour and 30 minutes. The unbound conjugate was removed by washing the microplate wells 5 times with washing buffer (Tris-NaCl (pH 7.4); 0.04% ProClin™ 300 (preservative)), using an Immuno Wash™ 1575 Microplate Washer (BioRad,

Hercules, CA, USA). Development solution (Citric acid and Sodium acetate solution (pH 4); 0.015% H_2O_2; 4% Dimethyl sulfoxide (DMSO)) was added to the wells, followed by incubation in the dark at 21°C for 30 minutes, after which the reaction was terminated by addition of stopping solution (1N sulphuric acid solution). After 5 minutes the optical densities of the samples were read at 450-620/700 nm using a Model 680 Microplate Reader (BioRad, Hercules, CA, USA). The results were printed for analysis.

2.4.3 PCR analysis of pri-miR-31/5/8/9 integration sites

DNA extraction from transfected Huh7 cells

The transfected Huh7 cells were loosened with a rubber cell scraper and the pCH-9/3091 plasmids from the collected cells were extracted with a QIAamp DNA Mini Kit (Qiagen, Venlo, Limburg, Netherlands) for PCR analysis.

PCR amplification of the pCH-9/3091 *core* and *surface* insertion sites

Primers were designed to amplify the *core* and *surface* target sites to confirm successful insertion of the pri-miR-31/5/8/9 cassette. A forward primer was designed to bind to the inserted pri-miR sequence and two reverse primers were designed to bind regions downstream of the insert and the right flanking homologous sequence of the *core* and *surface* target sites respectively (Figure 2.4). This design ensures that the insert site is amplified if the pri-miR-31/5/8/9 sequence was successfully integrated at the *core* or *surface* target sites. The primers were compared with the pCH9/3091 plasmid and the pri-miR-31/5/8/9 sequence to ensure lack of similarity to these sequences. Oligonucleotide primers were analysed and validated with NetPrimer analysis software

(PREMIER Biosoft International) and were synthesised by Inqaba Biotech (Pretoria, Gauteng, South Africa). The *core* insert site was amplified from pCH-9/3091 using the following primer set: Insert-F (459) - 5' CTG ATC ATC GAT AGC TAG CC 3' (forward) and InsertC-R (1067) - 5' GAG ATT CCC GAG ATT GAG AT 3' (reverse) (Table 2.6). The same forward primer (1733) and InsertS-R (2914) - 5' AAG TTG GCG AGA AAG TGA A 3' (reverse) were used to amplify the *surface* insert site from pCH-9/3091. The PCR system for *core* site amplification included 2x KAPA Taq RM (Kapa Biosystems, Wilmington, Massachusetts, USA), 10 µM Insert-F forward primer, 10 µM InsertC-R reverse primer, and 100-150 ng purified plasmid, made up to a final volume of 25 µl with dH_2O in a 0.2 ml PCR grade microcentrifuge tube (Axygen Scientific, Union City, CA, USA). The components for *surface* site amplification are the same as for the *core* site amplification except for the substitution of InsertC-R reverse primer with InsertS-R reverse primer. The PCRs were performed in a BioRad T100™ Thermal cycler (BioRad, Hercules, CA, USA) under the following conditions: initial denaturation at 95°C for 2 min; 30 cycles of: denaturation at 95°C for 30s, annealing at xx°C for 30s (depending on which primer set is used) and extension at 72°C for 1 min; final elongation at 72°C for 2 min, followed by cooling at 4°C (Table 2.3). The annealing temperature for each primer set was calculated by subtracting 5°C from the primer melting temperatures (T*m*) listed in Table 2.6. The PCR products were analysed on a 1% agarose gel and stored at -20°C.

Table 2.6: PCR primers for analysis of pri-miR-31/5/8/9 integration into pCH-9/3091

Name	Sequence	T*m* (°C)
Insert-F (forward)	5' -CTGATCATCGATAGCTAGCC- 3'	60.4
InsertC-R (reverse)	5' -GAGATTCCCGAGATTGAGAT- 3'	58.35
InsertS-R (reverse)	5' -AAGTTGGCGAGAAAGTGAA- 3'	55.85

Figure 2.4: PCR analysis confirming integration of the pri-miR-31/5/8/9 cassette and three stop codons into pCH-9/3091. A forward primer binds a target sequence within the region containing the 3 stop codons and a reverse primer binds a target sequence within the pCH-9/3091 plasmid. The primer pair should not amplify the donor template and should only yield products if the insert (3 stop codons and the pri-miR-31/5/8/9 cassette) is present within the pCH-9/3091 plasmid.

2.4.4 Sequencing of the PCR products

The PCR products from the PCR integration analysis have to be sequenced to confirm successful insertion of the pri-miR-31/5/8/9 cassette at the *core* and *surface* target sites. Extraction of the PCR products from the 1% agarose gels was carried out using a QIAquick Gel Extraction Kit (Qiagen, Venlo, Limburg, Netherlands). DNA bands were excised using a clean, sharp scalpel and were suspended in 3 volumes of QG buffer (5.5 M guanidine thiocyanate; 20 mM Tris-HCl (pH 6.6)). The suspended gel fragments were incubated at 50°C for 10 min to dissolve the gel, followed by addition of one gel volume of isopropanol. The mixture was applied to a QIAquick spin column and centrifuged for 1 minute at 16300 x g. This was followed by addition of QG buffer and centrifugation (1 minute at 16300 x g). The column was then washed with Buffer PE (10 mM Tris-HCl (pH 7.5); 80% ethanol) and incubated for 3 min at 21°C, followed by centrifugation at 16300 x g for 1 minute. Centrifugation was repeated to remove residual wash buffer. Distilled H_2O was added to the centre of the column and the plasmids were collected by centrifugation (1 min at 5900 x g).

The collected DNA was purified using the Gene JET PCR Purification Kit (see 2.2.4), quantified using a Nanodrop ND-1000 Spectrophotometer, and sequenced by Inqaba Biotech (Gauteng, Pretoria, RSA).

To determine whether the pri-miR insert was successfully incorporated into pCH-9/3091, multiple sequence alignments were performed between the target *core* and *surface* sites, and the Inqaba Biotech sequencing results. These sequences were aligned and evaluated with BLASTN (187, 188).

2.4.5 pri-miRNA expression analysis

Cloning donor template strands into pTZ57 plasmids

The donor template strands were cloned into pTZ57 R/T plasmids for production of large plasmid quantities required for transfection of cells in 10 cm plates.

The plasmids containing the required C300(pri-miR) and S300(pri-miR) donor template strands were previously constructed in 2.1.1 (see Table 2.1: pTZ-C300(pri-miR) and pTZ-S300(pri-miR)). C50(pri-miR) and S100(pri-miR) donor template strands were respectively cloned into pTZ57 R/T plasmids with an InsTAclone™ PCR Cloning Kit (Thermo Scientific, Waltham, MA, USA). The ligation reaction was set up as follows: 4 µl of 5x ligation buffer, 0.165 µg of pTZ57 R/T, 7.5 U of T4 DNA ligase and 0.1 µg of either C50(pri-miR) or S100(pri-miR), made up to a final volume of 20 µl in a 1.5 ml microcentrifuge tube. The reaction mixture was then incubated at 21°C for 2 hours and added to chemically competent cells. These chemically competent cells were transformed and cultured as in 2.1.2.

The plasmids (pTZ-C50(pri-miR) and pTZ-S100(pri-miR)) (Table 2.1) were purified using a QIAamp DNA Mini Kit (Qiagen, Venlo, Limburg, Netherlands), as described in 2.1.3. Once successfully extracted, transformants were screened for insertion of C50(pri-miR) and S100(pri-miR). This was established using *Pvu*II restriction digest. The purified plasmids (200 ng) were treated with *Pvu*II as this restriction site flanks the insert and does not appear in the vector backbone, indicating successful ligation.

The artificial pri-miR-31/5/8/9 cassette was also cloned and purified, following the same cloning, purification and enzyme digestion protocols as with C50(pri-miR) and S100(pri-miR), except for the substitution of C50(pri-miR) and S100(pri-miR) with the pri-miR-31/5/8/9 sequence. The pTZ57 R/T plasmids

containing the C50(pri-miR), S100(pri-miR) and pri-miR-31/5/8/9 insert will hereafter be referred to as C50(pri-miR), S100(pri-miR) and pTZ-pri-miR respectively (Table 2.1).

Large quantities of C50(pri-miR), S100(pri-miR and pTZ-pri-miR are required for transfecting large cell volumes. Therefore, chemically competent cells were transformed with C50(pri-miR), S100(pri-miR and pTZ-pri-miR respectively and were cultured in LB medium for 16 hrs at 37°C. A QIAGEN Plasmid Maxi Kit (Qiagen, Venlo, Limburg, Netherlands) was used to maxiprep the cultured transformants, as described in 2.1.3.

Cell culturing and transfection

Huh7 cells were cultured in Cellstar® 175 cm^2 cell culture flasks (Greiner Bio-One GmbH, Frickenhausen, Germany) using DMEM growth medium supplemented with 10% FBS. The cultured cells were maintained at 37°C and 5% CO_2 in a humidified incubator until confluent.

The cell culture supernatant was removed and the adherent cells were washed with PBS. Washed cells were removed by trypsinisation, followed by resuspension in fresh DMEM growth medium. No wash step was required as TrypLE™ is used to dissociate cells, not porcine trypsin. The cell suspension was then distributed in 10 cm plates (Greiner Bio-One GmbH, Frickenhausen, Germany) and maintained in a humidified incubator at 37°C and 5% CO_2 until the cells reached 80-90% confluency. Fresh DMEM growth medium was added to the confluent cultured cells just prior to transfection.

Each transfection sample consisted of a total 25 µg DNA. The core transfection samples consisted of the following (Table 2.7): 3 µg pCH-9/3091; 2 µg pCMV-GFP; pUC118; 4 µg left C TALEN subunit (CPL); 4 µg right C TALEN subunit (CPR); 12 µg donor template (pTZ-C50(pri-miR) and pTZ-C300(pri-miR)); 250

mM NaCl, made up to a final volume of 500 µl with dH_2O (see Table 2.1 for plasmid descriptions). The components in the surface transfection samples were the same as those of the core transfection samples, except for the substitution of the left and right C TALENs with the left and right S TALENs (SPL and SPR) as well as substitution of the Core donor template strands with the Surface donor template strands (pTZ-S100(pri-miR) and pTZ-S300(pri-miR)). In two of the surface samples the Surface donor template strands were exchanged with pTZ-pri-miR to analyse the effect of the pri-miR-31/5/8/9 cassette without the flanking homologous regions. A positive control (containing 3 µg pCH-9/3091, 2 µg pCMV-GFP, and 20 µg pCI-pri-miR-31589, a plasmid that expresses pri-miRNA when transfected(169)) was also included.

Equal volumes of PEI were added to each transfection sample, bringing each sample to a final volume of 1 ml. The samples were thoroughly mixed and incubated at 21°C for 10 min. The incubated samples were then added drop wise to the cultured cells. The transfected cells were maintained in a humidified incubator at 37°C and 5% CO_2 for 24 hours, followed by addition of fresh DMEM growth medium and incubation for an additional 48 hours.

Table 2.7: Huh7 transfection DNA amounts for 10 cm plates

Pri-miR control	µg	Donor template strands	µg	Linear pri-miR	µg	Linear pri-miR with S TALENs	µg
pCMV-GFP	2	pCMV-GFP	2	pCMV-GFP	2	pCMV-GFP	2
pUC-118	0	pUC-118	0	pUC-118	8	pUC-118	0
pCH-9/3091	3	pCH-9/3091	3	pCH-9/3091	3	pCH-9/3091	3
pCI-pri-miR-31589	20	CPL	4	pTZ-pri-miR	12	SPL	4
		CPR	4			SPR	4
		Donor template strands with pri-miR	12			pTZ-pri-miR	12
Total	**25**	**Total**	**25**	**Total**	**25**	**Total**	**25**

RNA isolation

Transfected cells were collected with a cell scraper, centrifuged (5 min at 50 x g), and resuspended in Tri-reagent (contains guanidine thiocyanate and phenol in a monophase solution) (Sigma-Aldrich, St. Louis, MO, USA). The resuspended cells were thoroughly mixed and incubated at room temperature for 5 minutes to ensure lysis. This was followed by addition of chloroform and incubation for 10 min at 21°C. Samples were then centrifuged for 10 minutes at 13300 x g and 4°C. The top aqueous phase was transferred to a 2 ml microcentrifuge tube and isopropanol was added. The samples were inverted and incubated at 21°C for 10 min, followed by centrifugation at 13300 x g and 4°C for 10 min. The pellets were washed with 75% ethanol in diethylpyrocarbonate (DEPC) water (Ambion®, Austin, Texas, USA). The washed pellets were vortexed briefly and centrifuged at 13300 x g and 4°C for 5 min. Finally, the pellets were air dried for 10 minutes and resuspended in 100 µl RNase free water. The isolated RNA was viewed on a 1% agarose gel and quantified using a Nanodrop ND-1000 Spectrophotometer. Samples were aliquoted (30 µg/15 µl) and stored at -70°C.

Radiolabeled RNA molecular weight markers

All work involving radioactive material was done behind a shield to protect the body from damaging radiation and all solid and liquid radioactive waste was discarded in allocated radioactive waste drums. A series 900 mini-monitor (Saint-Gobain, Courbevoie, France) was used to monitor radiation levels at all times.

Radiolabeled RNA molecular weight markers were generated with an Ambion®Decade™ Markers System (Ambion®, Austin, Texas, USA). The radiolabelled molecular markers included 100 ng RNA, nuclease free H_2O, 10x

kinase reaction buffer A, [γ-^{32}P]ATP (≥ 3000 Ci/mmol) and T4 polynucleotide kinase that were mixed and incubated at 37°C for 1 hour. Both nuclease free H_2O and 10x cleavage reagent were added after the 1 hour incubation, followed by incubation at 21°C for 5 min. The molecular weight marker solution was then mixed with gel loading buffer II and stored at 4°C.

Acrylamide gel

A 15% acrylamide gel was set on the day before loading the RNA samples and molecular weight markers. The gel solution consisted of the following: bis-acrylamide and acrylamide at a 1:19 ratio, 8 M urea, and 10x Tris-borate-EDTA (TBE) (1 M boric acid, 0.2 M Ethylenediaminetetraacetic acid (EDTA) and 1 M Tris-Cl, pH 8), made up to 60 ml with dH_2O and heated to dissolve the contents. Newly made 1% ammonium persulphate (APS) (250 µl) and tetramethylethylenediamine (TEMED) (25 µl) (Sigma-Aldrich, St. Louis, MO, USA) were added to the gel mixture to catalyse the polymerization of acrylamide and bis-acrylamide. The gel was poured in a SE400 Vertical Slab Gel Electrophoresis Unit (GE Healthcare Life Sciences, Piscataway, NJ, USA).

Once the gel was set, the comb was removed and the gel apparatus buffer tanks were filled with 0.5x TBE buffer. The gel ran at 150 V for 30 minutes and then the wells were flushed with a Hamilton syringe to remove residual buffer at the bottom of the wells. The 15 µl aliquoted RNA samples were mixed with 15 µl gel loading buffer II, followed by 5 min denaturation of the RNA samples and the RNA molecular weight markers at 80°C and 95°C respectively. The denatured samples were incubated at 4°C for 5 min and then loaded onto the gel. The samples ran on the gel for 5 hours (150V and 4°C), after which the gel was removed and stained with 0.01% ethidium bromide (EtBr) in 0.5x TBE buffer for 5 min.

The samples were transferred to a hybond positively charged nylon membrane (GE Healthcare Life Sciences, Piscataway, NJ, USA) for treatment with the radioactive probe. The gel was placed on the nylon membrane and sandwiched between six 3 mm filter paper sheets (3 underneath and 3 on top) that were soaked in 0.5x TBE buffer. Excess buffer was removed and the samples were transferred for 45 min using a Sigma Aldrich SV20-SDB gel transfer system (Sigma-Aldrich, St. Louis, MO, USA) at 0.76 A and 4°C. The membrane was then transferred to new dry blotting paper and placed in a UV cross linker (120 milliJoules/cm^2 for 20 seconds) to immobilise the RNA on the membrane. After UV cross linking RNA solubilising H_2O was removed from the membrane by incubating the membrane for 1 hour at 80°C.

The Decade™ Marker ladder was cut from the membrane and stored in a Bass cassette II case for 24 hours, with an imaging plate placed over the ladder. The imaging plate was then placed in a Fujifilm FLA7000 image reader to view the Decade™ ladder. On completion, the imaging plate was erased in an IPEraser 3 and the membrane was discarded in a radioactive waste bin.

Radioactive labelling of the probe

The radiolabelled probe included the following: Polynucleotide kinase (PNK) buffer A, 10 µM miR-31/5 guide probe oligonucleotide(169), and [γ-^{32}P]ATP (≥ 3000 Ci/mmol) radioactive labels, made up to a final volume of 20 µl with dH_2O. The probe-radiolabel mixture was then incubated at 37°C for 30 minutes and stored at 4°C.

Half a millilitre compacted filter floss was placed at the bottom of a 1 ml disposable syringe (Neomedic Ltd, Rickmansworth, Hertfordshire, United Kingdom) to prepare the Sephadex column required to purify the radiolabelled probe. Sephadex G-25 was added to the syringe, which was centrifuged inside

a 15 ml falcon tube at 700 x g for 2 minutes. This process was repeated until the Sephadex column volume was approximately 0.8 ml (approximately 0.4 g Sephadex). The final volume of the radiolabelled probe was made up to 50 µl with dH_2O, after which the probe was applied to the Sephadex column. The purified probe was then collected in the 15 ml falcon tube by centrifugation (700 x g for 2 min) and stored at 4°C.

Hybridisation

The membrane was placed in a hybridisation bottle with hybridisation buffer (Sigma-Aldrich, St. Louis, MO, USA) that was heated to 42°C. This was followed by incubation of the membrane and buffer at 42°C for 20 minutes. The labelled probe was denatured at 95°C for 5 min and added to the membrane. The membrane was then hybridised in a hybridisation oven at 42°C for 16 hours.

Stringency washes and exposure

The hybridisation buffer was discarded and the membrane was washed with 5x SSC (20x SSC: 3M NaCl, 0.3M $Na_3C_6H_5O_7.2H_2O$, distilled H_2O, pH 7) and 0.1% sodium dodecyl sulphate (SDS) for 20 min at 21°C. This was followed by two 1x SSC and 0.1 % SDS washes at 42°C for 15 minutes per wash. The membrane was then placed in a plastic sleeve and stored with an imaging plate in a Bass cassette II for 7 days at 21°C. After 7 days the membrane was analysed in a Fujifilm FLA7000. The imaging plate was erased and the membrane was discarded in the solid radioactive waste bin.

2.5 Statistical analysis

All HBsAg quantifications were carried out in triplicate for each sample type and condition, unless otherwise stated. GraphPad Prism version 5.00 (GraphPad software, San Diego, CA, USA) was used to perform two-tailed paired and unpaired Student's *t* tests. *P* values of < 0.05 were regarded as statistically significant and data is represented as the mean ± the standard error of the mean (SEM).

3. Results

3.1 Donor template strand construction

HDR uses a homologous template to repair DSBs and can be exploited to insert an artificial DNA sequence at the DNA break (163, 165-167). To that end we designed a donor template strand that contains an anti-HBV pri-miR-31/5/8/9 cassette without a promoter (Figure 3.1). The rational was that HDR, stimulated by TALEN-mediated DSBs, would recognise the flanking homologous sequences of the donor DNA strands and utilise it as donor templates to repair the DSB. HDR would then incorporate the pri-miR cassette at the *core* and *surface* target sites within the HBV cccDNA, which should result in viral-promoter driven pri-miR expression. The pri-miRs are then processed to form mRNA, which forms a complex with RISC and silences *HBx*. The combined silencing of *HBx* and disruption of the cccDNA target sites should result in synergistic disruption of viral replication and subsequent HBsAg expression.

3.1.1 Cloning the pri-miR-31/5/8/9 cassette into pTZ-C300 and pTZ-S300 backbones

Construction of the donor template strands with the pri-miR-31/5/8/9 cassette for each of the TALEN targets was undertaken using standard restriction enzyme digest and ligation methods as discussed in the previous chapter.

Core and Surface donor template strands were constructed by cloning a pri-miR-31/5/8/9 cassette into pTZ-C300 and pTZ-S300 plasmids (Table 2.1) that contain three stop codons flanked by regions that are homologous to the C and S TALEN target sites (received from K. Bloom) (Figure 3.1). Clones were screened for insertion of the pri-miR cassette and positive clones were

identified using a *BamH*I/*EcoR*I double digest (Chapter 2). The *BamH*I and *EcoR*I restriction sites flank the insertion site (Figure 3.2), therefore the double restriction digest yielded a positive result for the Core donor template strand when a 1.2 kb band was identified on a 1% agarose gel, while a positive clone for the Surface donor template strand was identified when the digest yielded a 917 bp and a 283 bp band (Figure 3.3). These two bands were a result of two *BamH*I and one *EcoR*I restriction sites (Figure 3.2). Using these criteria, lanes 3, 5, 6 and 10 were identified as positive clones for the C TALEN target and lanes 15, 17, 18, 19 and 20 were identified as positive clones for the S TALEN target (Figure 3.3).

3.1.2 Orientation of the inserted pri-miR-31/5/8/9 cassette

The pri-miR-31/5/8/9 cassette could be inserted in a forward orientation (same orientation as pri-miR-31/5/8/9 in pCI-pri-miR-31/5/8/9) or a reverse orientation. Pri-miR-31/5/8/9 in reverse orientation may affect pri-miR expression, thus determination of the insert's orientation within the positive C and S TALEN target clones is necessary to ensure that the pri-miR would function correctly once inserted at the *core* and *surface* target sites. To ascertain orientation the use of a second restriction digest with *Nhe*I and *Pci*I was warranted. The *Nhe*I site varies for each orientation of the insert and *Pci*I is a unique restriction site in the pTZ-C300 and pTZ-S300 plasmids (Figure 3.4). The *Nhe*I/*Pci*I double restriction digest of the positive clones resulted in two pairs of bands for the forward and reverse orientation respectively. The 4500 bp bands at the top consist of plasmids that were not fully digested (sample concentrations were too high). The plasmids were completely digested where this third band is absent (lane 3). A positive result for the Core and Surface donor template strands with a pri-miR-31/5/8/9 cassette in the forward orientation yielded a ≈1300 bp and 2796 bp band on a 1% agarose gel (Figure 3.5). Using this

criterion, lanes 2, 4, 5, 10, 14, 15 and 16 were identified as negative clones for the C and S TALEN targets and lanes 3, 11, 12, 13 and 19 were identified as positive clones for both the C and S TALEN targets. These positive clones can be used as templates to construct linear double stranded donor template strands. Core clone D (lane 5) and Surface clone C (lane 15) were sequenced and selected for PCR amplification of the donor template strands.

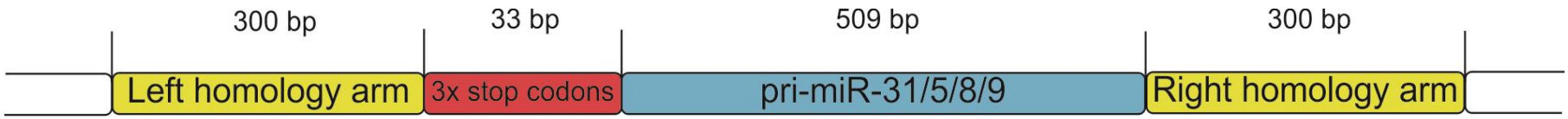

Figure 3.1: Donor template strand with pri-miR-31/5/8/9 cassette. A pri-miR-31/5/8/9 cassette was cloned into pTZ-C300 and pTZ-S300 plasmids (received from K. Bloom). The final donor template strand consisted of three stop codons, a pri-miR-31/5/8/9 cassette and two 300 bp flanking sequences (homology arms) that are homologous to the C and S TALEN target sites.

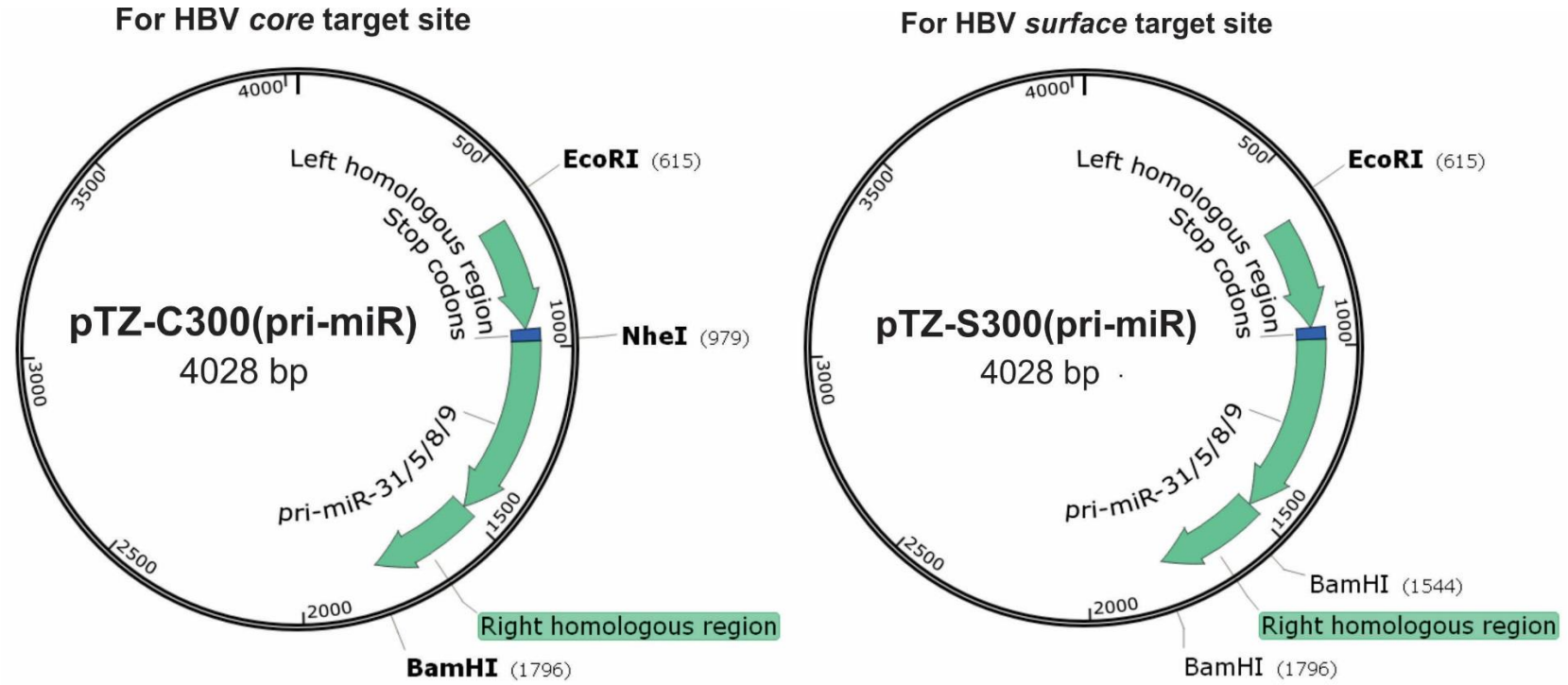

Figure 3.2: Plasmid maps of pTZ-C300(pri-miR) and pTZ-S300(pri-miR). *Eco*RI and *Bam*HI restriction sites flank the pri-miR-31/5/8/9 insertion site. Successful insertion of the pri-miR-31/5/8/9 cassette into the pTZ-C300 (homologous to *core* target site) and pTZ-S300 (homologous to *surface* target site) was confirmed by *Eco*RI/*Bam*HI double restriction digest. An *Eco*RI/*Bam*HI digest of pTZ-C300 with a pri-miR-31/5/8/9 cassette should result in a 1.2 kb DNA band, while pTZ-S300 should yield a 917 bp and 283 bp band as it contains two *Bam*HI restriction sites downstream from the insert. See Table 2.1 for plasmid descriptions.

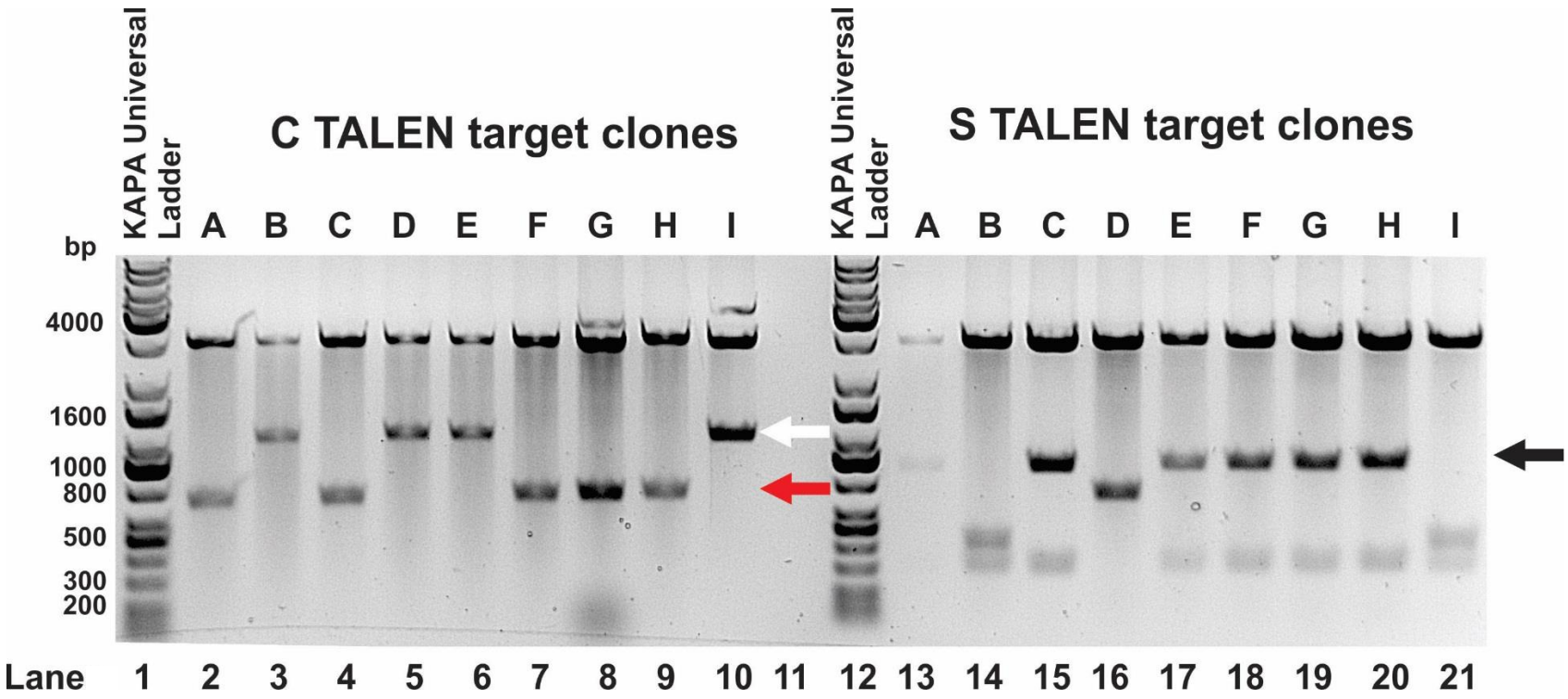

Figure 3.3: pri-miR-31/5/8/9 sequence insertion. Nine C TALEN target clones and nine S TALEN target clones were screened for successfully transformed clones by *Bam*HI/*Eco*RI double digest. Successfully transformed Core clones yielded a 1.2 kb band (white arrow) on a 1% agarose gel (lanes 3, 5, 6 and 10), while successfully transformed Surface clones resulted in a 917 bp and 283 bp band (lanes 15, 17, 18, 19 and 20) (black arrow). Core and Surface clones that were not transformed yielded 700 bp bands (lanes 2, 4, 7, 8, 9 and 16) (red arrow).

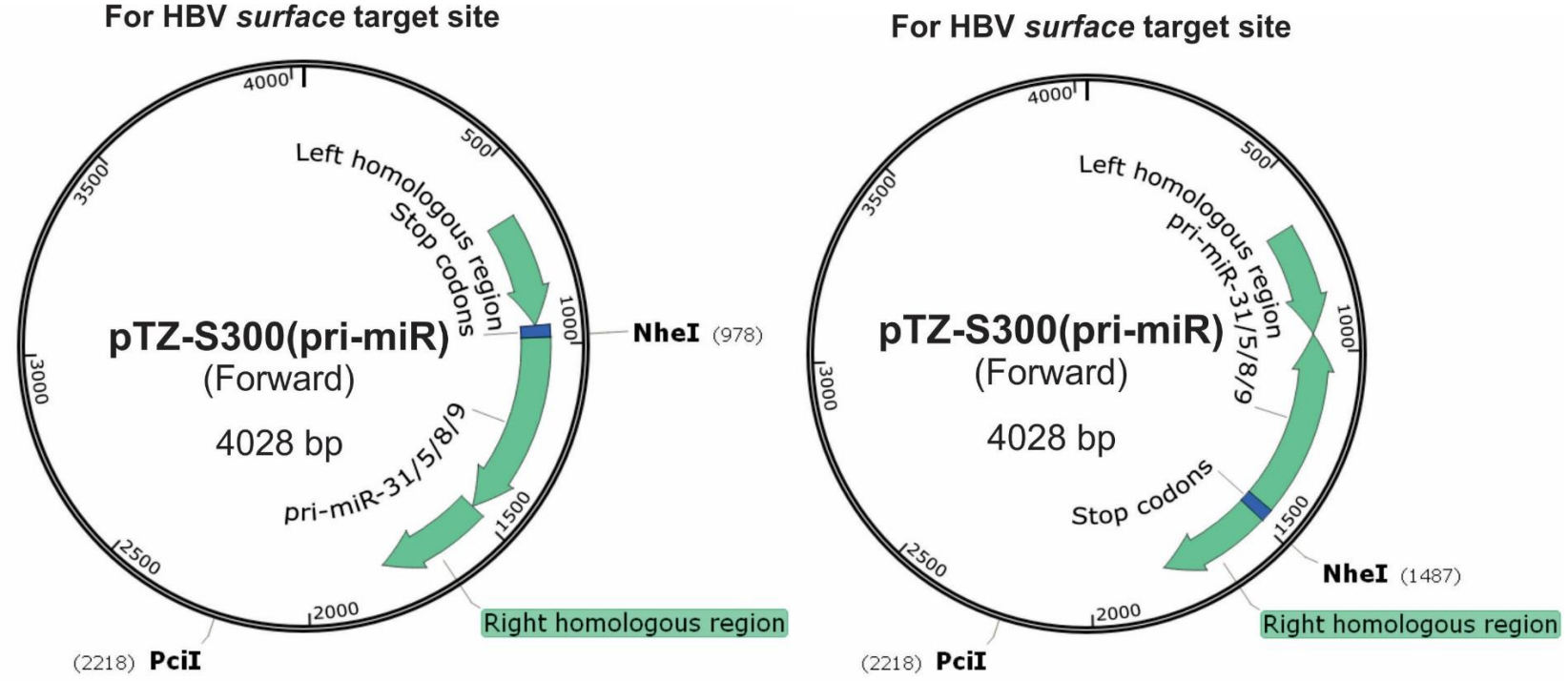

Figure 3.4: pri-miR-31/5/8/9 forward and reverse orientations. The plasmid maps for pTZ-S300(pri-miR) (homologous to the *surface* target site) contain a pri-miR-31/5/8/9 insert in a forward or reverse orientation. The location of *Pci*I is the same for both orientations, while the position of the *Nhe*I restriction site changes depending on the insert orientation (positions 978 and 1458 for the forward and reverse orientation respectively). As a result, *Nhe*I/*Pci*I double digest should yield a 1207 bp and 2796 bp band for a forward orientated insert, while an insert in reverse orientation should result in a 3305 bp and a 698 bp band.

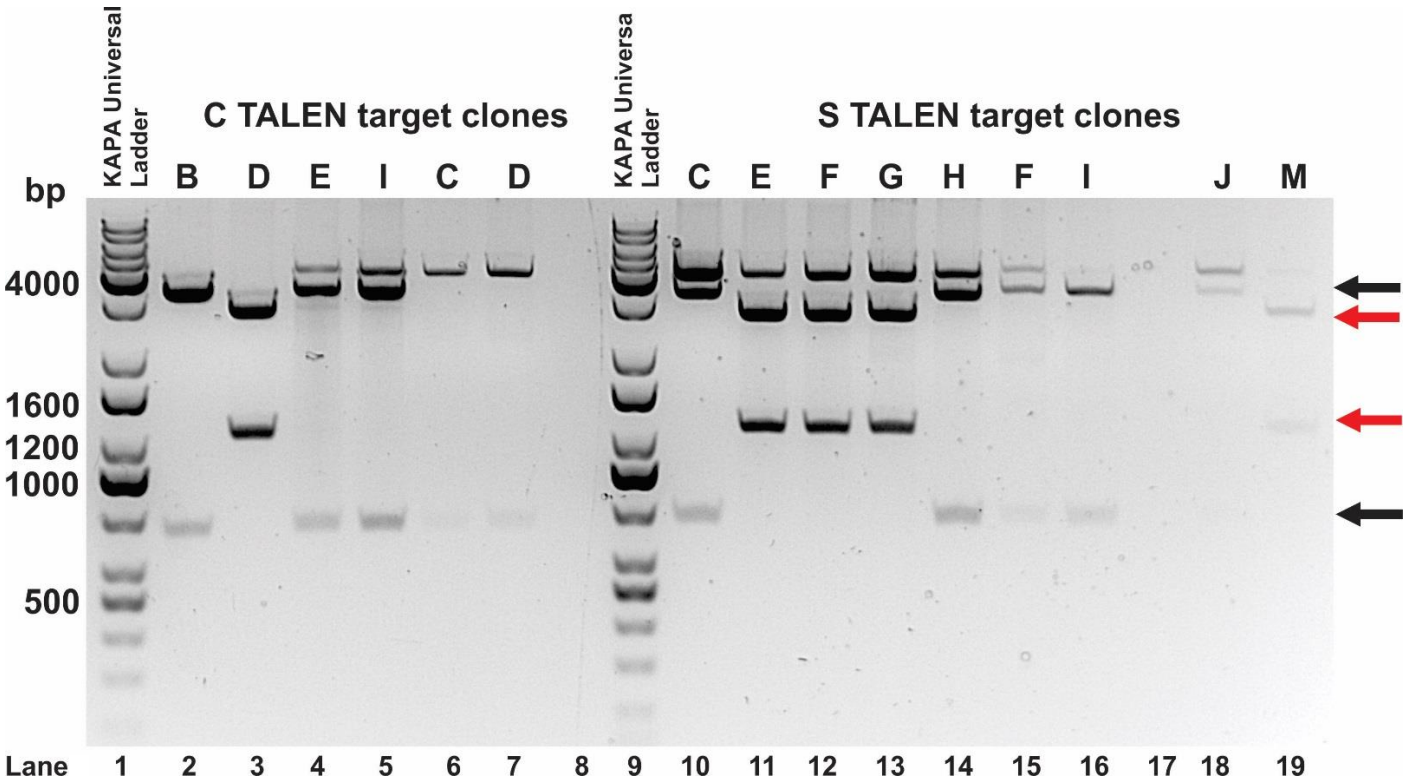

Figure 3.5: Orientation of the pri-miR-31/5/8/9 insert. Six positive C TALEN target clones and nine S TALEN target clones were screened for pri-miR-31/5/8/9 insert orientation by *Nhe*I/*Pci*I double digest. Samples were analysed on a 1% agarose gel. Core and Surface clones positive for *Nhe*I/*Pci*I restriction digest resulted in approximately 1300 bp and 2796 bp bands (lanes 3, 11, 12, 13 and 19) (red arrows). The remaining clones were negative for *Nhe*I/*Pci*I restriction digest and yielded a 3305 bp and a 698 bp band (lanes 2, 4, 5, 10, 14, 15 and 16) (black arrows). The 4500 bp bands at the top consist of plasmids that were not fully digested. The plasmids were completely digested where this band is absent (lane 3).

3.1.3 Donor template strands

The length of a donor template strand's homologous regions affect HDR efficiency and literature suggests that linear dsDNA donor template strands for HDR are better recognised and incorporated at the DNA break than plasmid templates (124, 127, 128, 165-167, 179). Therefore, to develop these linear donor template strands, the pTZ-C300 and pTZ-S300 donor template plasmids with the forward orientated pri-miR-31/5/8/9 cassette were subjected to conventional PCR. Primer pairs were designed for the HBV *core* and *surface* target sites respectively and were used to generate linear Core and Surface donor template strands with flanking homologous sequences that vary in length (Figure 3.6). The varying lengths allowed us to determine the optimum homologous sequence length for HDR.

Pri-miR-containing Core and Surface donor template strands with 50 bp flanking homologous regions yielded a 630 bp band on a 1% agarose gel (lanes 2 and 6), while donor template strands with 100 bp flanking homologous regions yielded a 730 bp band (lanes 3 and 7) and donor template strands with 150 bp flanking homologous regions a 830 bp band (lanes 4 and 8) (Figure 3.7). Finally, the Core and Surface donor template strands with 300 bp flanking homologous regions resulted in an 1130 bp band (lanes 5 and 9). The same primer pairs were also used to produce linear donor template strands without the pri-miR-31/5/8/9 insert, which were used as pri-miR negative controls (Figure 3.6). Core and Surface donor template strands with 50 bp flanking homologous regions yielded a 130 bp band (lanes 2 and 6), while donor template strands with 100 bp flanking homologous regions yielded a 230 bp band (lanes 3 and 7) (Figure 3.8). Donor template strands with 150 bp flanking homologous regions yielded a 330 bp band (lanes 4 and 8) and the donor template strands with 300 bp flanking homologous regions resulted in an approximately 630 bp band (lanes 5 and 9). The band in lane 5 is slightly higher

than the 700 bp molecular weight marker, possibly as a result of the high concentration of the sample. All these bands correlated with the predicted amplicon sizes for each template and the developed linear donor template strands were used in subsequent transfection experiments.

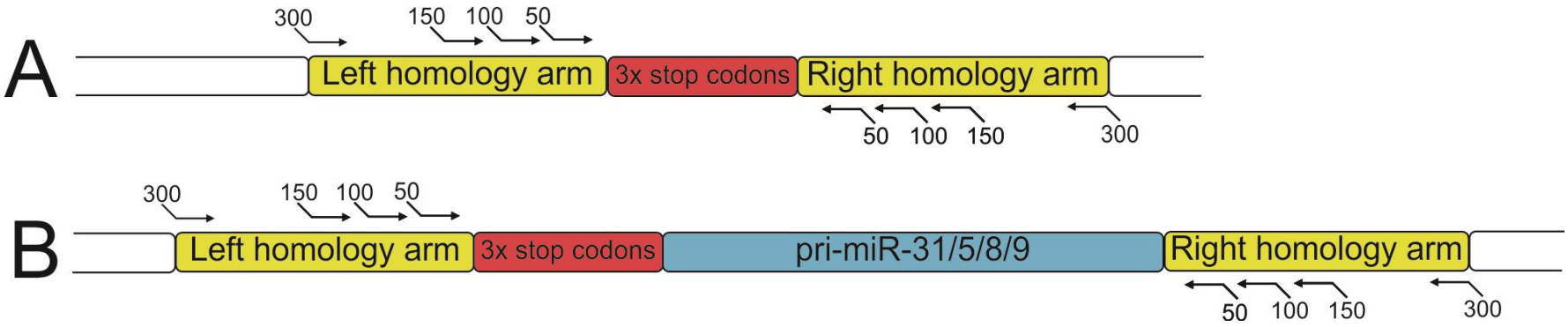

Figure 3.6: Core and Surface donor template strands. Donor template strands with flanking sequences that are homologous to the C and S TALEN target sites were generated by PCR. The length of the flanking homology arms were varied (50, 100, 150 and 300 bp respectively) to analyse their effect on HDR efficiency. A: Donor template strands without the pri-miR-31/5/8/9 insert were constructed as controls. B: Donor template strands containing the pri-miR-31/5/8/9 sequence that will be inserted at the pCH-9/3091 *core* and *surface* target sites. The primers are listed in Table 2.2.

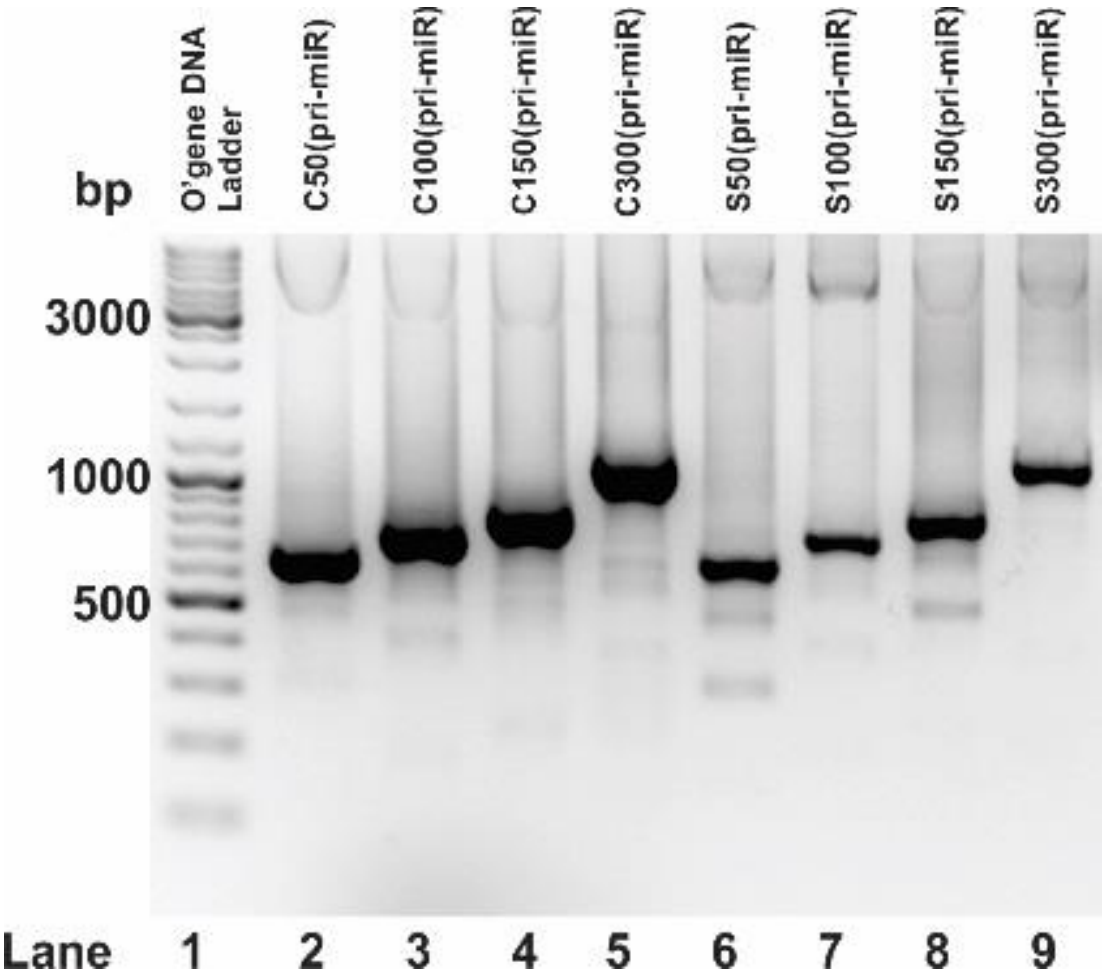

Figure 3.7: Core and Surface donor template strands containing the pri-miR-31/5/8/9 insert. The donor template strands were generated by conventional PCR and primer pairs were designed for the pTZ-C300(pri-miR) and pTZ-S300(pri-miR) plasmids. Samples were analysed on a 1% agarose gel. Core and surface donor template strands with 50 bp and 100 bp homologous flanking regions yielded 630 bp (lanes 2 and 6) and 730 bp (lanes 3 and 7) bands respectively, whereas donor template strands with 150 bp and 300 bp homologous flanking regions resulted in 830 bp (lanes 4 and 8) and 1130 bp (lanes 5 and 9) bands respectively. The donor template strands are described in Table 2.4.

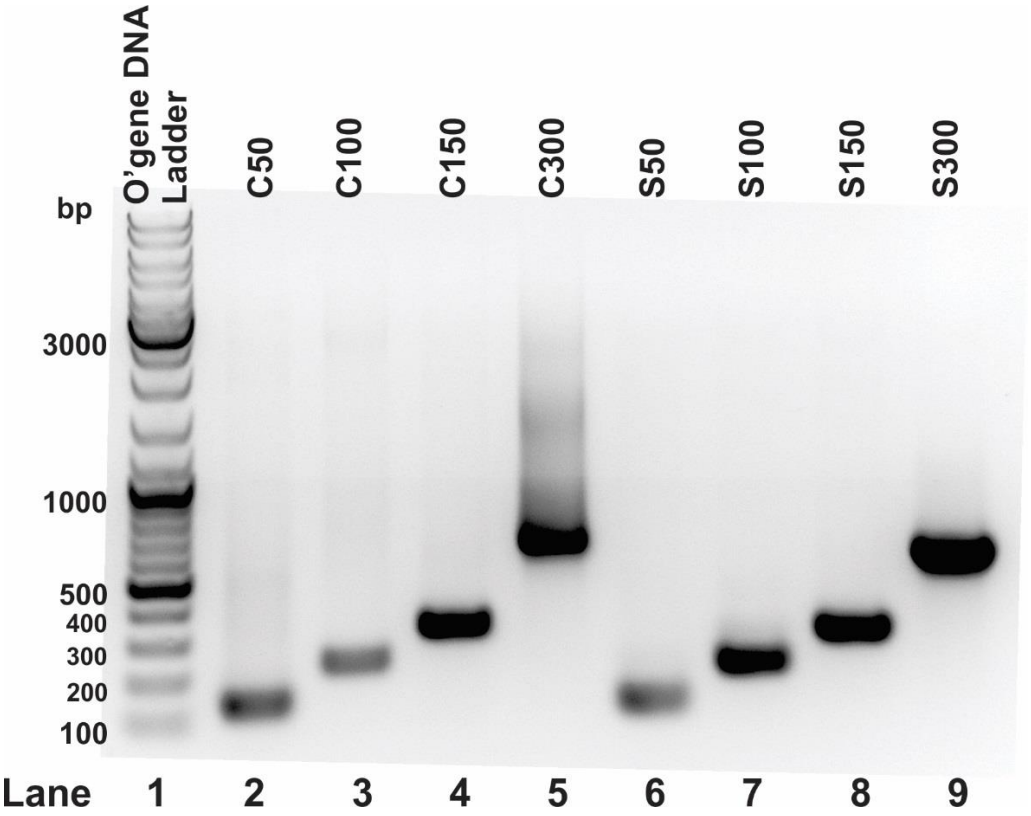

Figure 3.8: Core and Surface donor template strands with no pri-miR-31/5/8/9 insert. The donor template strands were generated by conventional PCR, using the pTZ-C300 and pTZ-S300 plasmids as templates. Samples were analysed on a 1% agarose gel. Core and surface donor template strands with 50 bp homologous flanking regions yielded a 130 bp band (lanes 2 and 6), while donor template strands with a 100 bp homologous flanking region resulted in a 230 bp band (lanes 3 and 7). Donor template strands with 150 bp and 300 bp homologous flanking sequences resulted in 330 bp (lanes 4 and 8) and 700 bp (lanes 5 and 9) bands respectively. Donor template strands are described in Table 2.4.

3.2 Effect of transfected donor template strands and TALEN pairs on HBsAg concentration

The effect of the donor template strands and previously described anti-HBV activity of the C and S TALEN pairs was assessed using a Huh7 cell model that supports viral replication when transfected with HBV DNA. In this model pCH9-3091, an HBV replication competent plasmid that actively expresses the viral pgRNA and sgRNAs required for HBV replication, is transiently co-transfected with the TALEN pairs and donor template strands into Huh7 cells. Successful transfection was established by GFP expression in control wells and anti-HBV activity was evaluated using HBsAg ELISA. HBsAg, HBV surface proteins that are essential for formation of the viral envelope, is an immunological marker of HBV infection and can be measured with HBsAg ELISA. It follows that a reduction in HBsAg concentration indicates a decrease in HBV replication, therefore, HBsAg concentration can be used to assess the efficiency of TALEN- and HDR-mediated disruption of HBV replication.

3.2.1 C and S TALENs reduce HBsAg expression

C and S TALENs create DSBs at the pCH-9/3091 *core* and *surface* target sites. These DSBs are repaired by error-prone NHEJ when donor templates are absent and result in gene disruption. Our HBsAg knockdown efficiency by these C and S TALENs were consistent with the results reported by Bloom *et al*. (15). Transfecting Huh7 cells with the C TALENs resulted in no significant HBsAg knockdown ($p=0.1857$), as the C TALENs target the viral *core* ORF and not the viral *surface* ORF (Figure 3.9). In contrast to C TALENs, transfection with S TALENs resulted in approximately 80% reduction in HBsAg expression (Figure 3.10). S TALENs are more effective in reducing HBsAg expression, as they target the viral *surface* ORF that encodes HBsAg. A left S TALEN with an

inactive *Fok*I domain was used to assess the effect of transfection on HBsAg concentrations and did not result in significant decreased HBsAg expression (p=0.5358), confirming that a decrease in HBsAg concentration is a result of TALEN activity.

3.2.2 Transfection with the Core and Surface donor template strands reduce HBsAg expression

We did not expect significant HBsAg knockdown when transfecting cells with the donor template strands and no TALENs. The donor template strands are not able to express pri-miR, as they do not contain a promoter sequence. Any reduction in HBsAg expression should thus be a result of pri-miR-31/5/8/9 integration into pCH-9/3091.

Little or no HBsAg knockdown was observed when transfecting with either the Core or Surface donor template strands without the pri-miR insert (Figure 3.9 and 3.10). The Core donor template strands without the pri-miR insert resulted in 0-24% decrease in HBsAg expression, while the Surface donor template strands without the pri-miR insert reduced HBsAg expression by 15-25%. This decrease in expression when introducing the donor template strands without the TALENs should be expected and may likely be a result of dsDNA or ssDNA damage repair and spontaneous recombination. Low frequencies (1 in 1000) of spontaneous recombination has previously been used to incorporate artificial DNA sequences at specific genome target sites (189-192). ssDNA damage to the pCH-9/3091 plasmid may occur naturally and a single stranded DNA break (SSB) in the path of a replication fork can be converted to a DSB and result in replication fork collapse. dsDNA damage to pCH-9/3091 is the result of these stalled replication forks and transfection stress, and can be repaired by NHEJ, microhomology-mediated end joining (MMEJ) and HDR. DSB repair by these repair mechanisms may result in spontaneous recombination and insertion of

the three stop codons (163, 193). This integration of the stop codons disrupts the target sites and effect HBsAg knockdown. The little knockdown observed by the Core donor template strands are consistent with the Core TALEN results and confirm that disruption of the *core* target site does not result in a significant decrease in HBsAg expression ($p=0.1857$).

Both Core and Surface donor template strands that contain the pri-miR-31/5/8/9 insert resulted in significant reduction in HBsAg expression ($p<0.0001$ in both cases) when TALENs were absent (Figure 3.11 and 3.12). As discussed in the previous paragraph, the decreased HBsAg expression may be a result of spontaneous incorporation of pri-miR-31/5/8/9 at DNA repair sites. Once the pri-miR cassette is inserted, pri-miR expression is driven by an HBV promoter (Core promoter at the *core* site and S2 promoter at the *surface* site). Pri-miR is cleaved by Drosha to form pre-miR, which is exported to the cytoplasm. The pre-miR is cleaved by Dicer and the resultant miRNA guides the RISC complex to the *HBx* site, where it prevents gene expression (Figure 1.5). HBx is important for HBV replication, therefore, silencing *HBx* will disrupt HBV replication and should result in decreased HBsAg expression. The Core donor template strands with the pri-miR insert reduced HBsAg expression by 32-42%, while the Surface donor template strands with the pri-miR insert resulted in 55-60% HBsAg knockdown (Figure 3.11 and 3.12). The HBsAg reduction by the Core donor template strands with the pri-miR insert is significantly improved when compared to C TALEN mediated knockdown ($p<0.0001$), which resulted in no significant HBsAg knockdown. This decrease in HBsAg expression could be the result of pri-miR expression by the inserted pri-miR-31/5/8/9 cassette. The increased HBsAg reduction by the Core donor template strands with the pri-miR insert compared to the Core donor template strands without the pri-miR insert ($p<0.0001$) also supports the conclusion that pri-miR expressed by the inserted pri-miR-31/5/8/9 cassette results in gene silencing and subsequent HBsAg knockdown (Figure 1.9 and 1.11). HBsAg knockdown by the Surface

donor template strands with the pri-miR insert was also significantly improved when compared to Surface donor template strands without the pri-miR insert, and was slightly less effective than the S TALENs (p=0.0276) (Figure 1.10 and 1.12). This increase in HBsAg reduction was also a possible result of pri-miR expression, suggesting that pri-miR expression by the integrated pri-miR cassette is as efficient as S TALENs in decreasing HBsAg expression. Cells were transfected with the pri-miR expressing pCI-pri-miR-31/5/8/9 plasmid as a positive control and the resultant decrease in HBsAg expression (≈85%) was a result of pri-miR expression and was consistent with the findings reported by Ely *et al*. (169) (Figure 3.9 and 3.10). As a negative control, cells were transfected with a promoter-less linear pri-miR-31/5/8/9 sequence (see Table 2.1) that was not inserted into a plasmid (Figure 3.10). No reduction in HBsAg expression occurred, confirming that the pri-miR-31/5/8/9 sequence cannot express pri-miR on its own and successful integration of the pri-miR-31/5/8/9 cassette is required for HBV promoter mediated pri-miR expression.

3.2.3 Co-transfected donor template strands and TALEN pairs reduce HBsAg expression

Co-transfecting cells with the donor template strands and TALENs should induce HDR and subsequent integration of the donor sequence. TALENs should increase the amount of DSBs (compared to transfection mediated damage) and result in increased donor insertion frequency. The increased insertion frequency will then result in increased target site disruption as well as gene silencing when the donor template strand contains the pri-miR-31/5/8/9 cassette.

No significant reduction in HBsAg expression was observed when co-transfecting cells with the C TALENs and Core donor template strands without the pri-miR insert (p>0.4) (Figure 3.9). In this case HBsAg expression was

significantly higher than that of the mock HBV infection. This may be a result of missense mutations introduced by NHEJ at the *core* target site. The start of the HBV *polymerase* ORF (2307) is overlapped by the *precore/core* region that is targeted by the Core TALENs (2319) (15, 194). HBV polymerase is required for initiation of viral reverse transcription and the assembly of replication-competent viral nucleocapsids, therefore, a missense mutation introduced at this site could result in higher surface antigen expression as a result of overexpression of HBV polymerase(195). This mutation may also change the 4^{th} and 5^{th} amino acid in the terminal protein (TP) of HBV polymerase, which is essential for pgRNA encapsidation and has a protein priming capability (196, 197). Changes in these amino acids could affect the binding of the polymerase to the encapsidation signal and alter the efficiency of TP initiation, resulting in increased viral replication (194, 198). Co-transfection with the S TALENs and Surface donor template strands without the pri-miR insert resulted in significant HBsAg knockdown ($p<0.0001$). The results were a significant improvement over transfection with the Surface donor template strands without the pri-miR insert ($p=0.0015$). However, the HBsAg reduction was slightly less than the S TALEN-mediated HBsAg knockdown ($p=0.0086$). The spacer region between the *Fok*I catalytic unit and the TALE region causes TALENs to express lower specificity for the exact cut site (110, 199). Therefore, it is possible that the S TALENs may target the Surface donor template strands, as the flanking homologous regions are separated by only 20 bp. This would explain the slight decrease in HBsAg reduction, as the amount of TALENs available to cleave the target DNA would decrease.

Co-transfection with C TALENs and Core donor template strands with the pri-miR insert resulted in significant reduction ($p<0.0001$) in HBsAg expression (55-60%) when compared to the mock transfection (Figure 3.11). The combination of the pri-miR-containing Core donor template strand with 50 bp flanking homologous regions and C TALENs was the most effective and

decreased HBsAg expression by 60% ($p<0.0001$). The HBsAg knockdown was also significantly improved compared to the Core donor template strands with the pri-miR insert and no TALENs ($p<0.0001$), indicating that TALEN-mediated DSBs likely result in increased pri-miR-31/5/8/9 integration and expression. Transfection with the negative control pri-miR-linear sequence and S-TALENs reduced HBsAg expression by approximately 75% and was not significantly different from S TALEN-mediated HBsAg knockdown ($p=0.5388$). This supports the previous findings that the pri-miR-31/5/8/9 cassette has to be inserted at the target site to result in HBV promoter driven pri-miR expression and subsequent silencing of *HBx*. The S TALENs and Surface donor template strands with the pri-miR insert resulted in >85% decrease in HBsAg expression (Figure 3.12). The pri-miR-containing donor template strands with 100 bp flanking homologous regions and S TALENs were the most effective and resulted in 93% HBsAg knockdown, a significant improvement over S TALENs without the donor template strands ($p=0.0039$). The HBsAg knockdown was not significantly different from the pCI-pri-miR-31/5/8/9 positive control ($p=0.6555$) (Figure 3.12). However, cells transfected with pCI-pri-miR-31/5/8/9 were saturated with pri-miR, while cells transfected with TALENs and donor template strands possibly resulted in limited pri-miR-31/5/8/9 integration and subsequent lower pri-miR expression. This suggests that pri-miR mediated genome silencing should be effective even at low concentrations and may be improved by increasing integration of the pri-miR-31/5/8/9 cassette and subsequent pri-miR expression. These observations warrant further optimisation of our method.

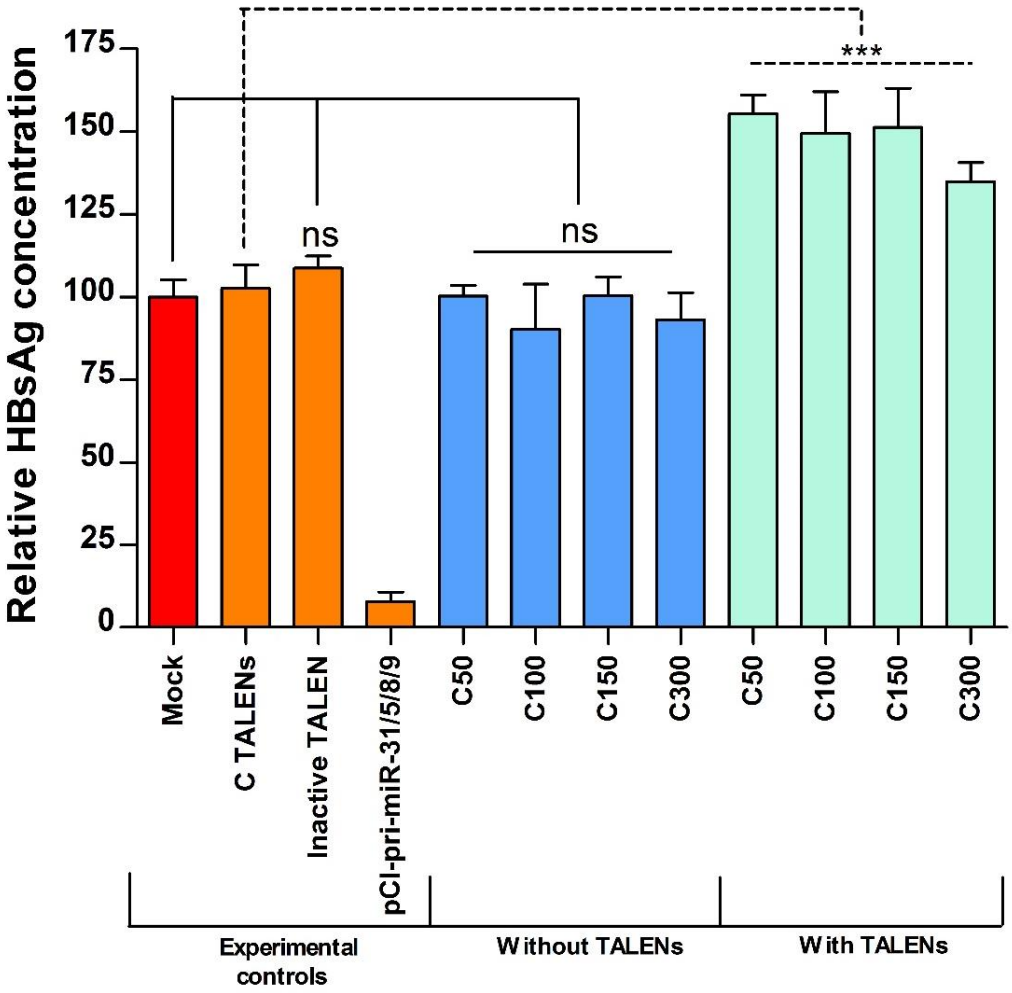

Figure 3.9: C TALEN and Core donor template strand (without pri-miR) mediated knockdown of HBsAg in Huh7 cells. The mock represents baseline HBsAg expression and the C TALEN controls did not significantly affect HBsAg concentration. The inactive TALEN was a control for transfection mediated changes in HBsAg expression and did not result in reduced HBsAg expression. pCI-pri-miR-31/5/8/9 was used as a positive control for pri-miR expression and resulted in significant HBsAg knockdown. Cells were transfected with donor template strands that did not contain the pri-miR cassette. These donor template strands resulted in small changes in HBsAg concentration. Donor template strands were co-transfected with C TALENs to assess their combined effect on HBsAg concentration and resulted in an increase in HBsAg concentration. HBsAg concentrations were measured by HBsAg ELISA. The results were averaged and the values are relative to the mock HBV infection. Means are indicated with SEM. All readings were done in triplicate or more, except pCI-pri-miR-31/5/8/9, which only had two readings. (**: $p<0.01$;***: $p<0.001$; ns: not significant)

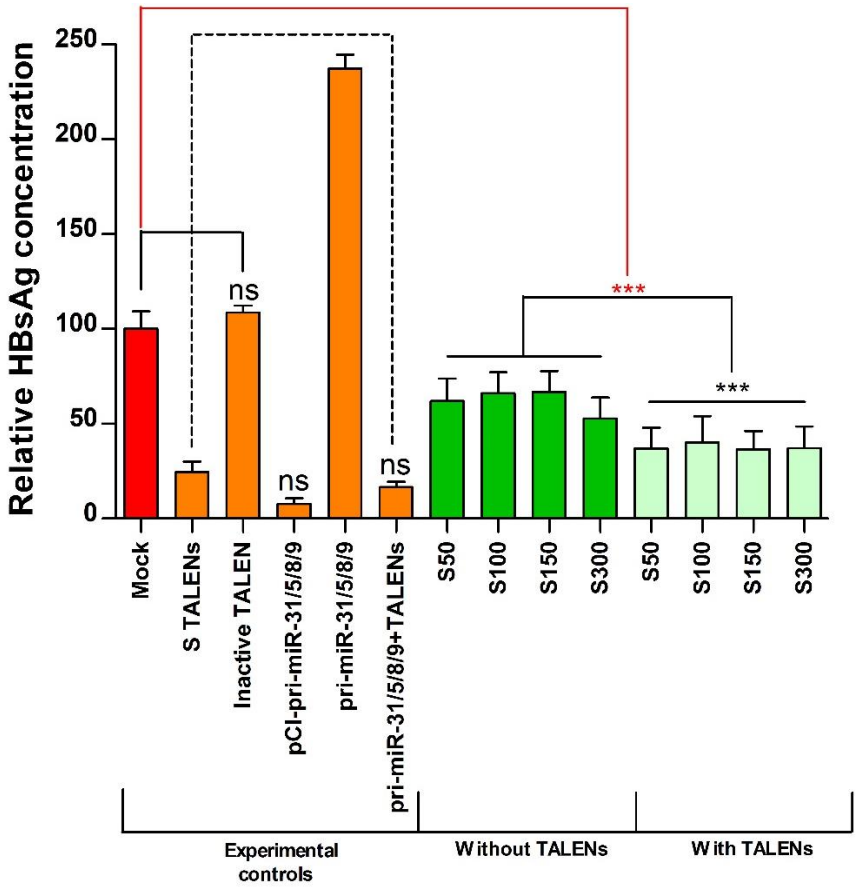

Figure 3.10: S TALEN and Surface donor template (without pri-miR) strand mediated knockdown of HBsAg in Huh7 cells. The mock represents baseline HBsAg expression. The S TALEN controls resulted in significant reduction of HBsAg concentration, while the inactive TALEN did not result in decreased HBsAg expression and acted as a control for transfection mediated changes in HBsAg expression. A linear pri-miR-31/5/8/9 cassette increased HBsAg concentrations while S TALENs and the linear cassette resulted in decreased HBsAg concentrations. pCI-pri-miR-31/5/8/9 was used as a positive control for pri-miR expression and resulted in a significant decrease in HBsAg concentration. All Surface samples (with and without S TALENs) resulted in significant knockdown (red line). HBsAg knockdown for the positive control was not significantly different from that of the linear pri-miR-31/5/8/9 and TALEN combination. Donor template strands that did not contain the pri-miR cassette caused small changes in HBsAg concentration, while co-transfecting donor template strands with S TALENs resulted in an increase in HBsAg concentration. HBsAg concentrations were measured by HBsAg ELISA. The results were averaged and the values are relative to the mock HBV infection. Means are indicated with SEM. All readings were done in triplicate or more, except pCI-pri-miR-31/5/8/9, which only had two readings. (***: $p<0.001$; ns: not significant)

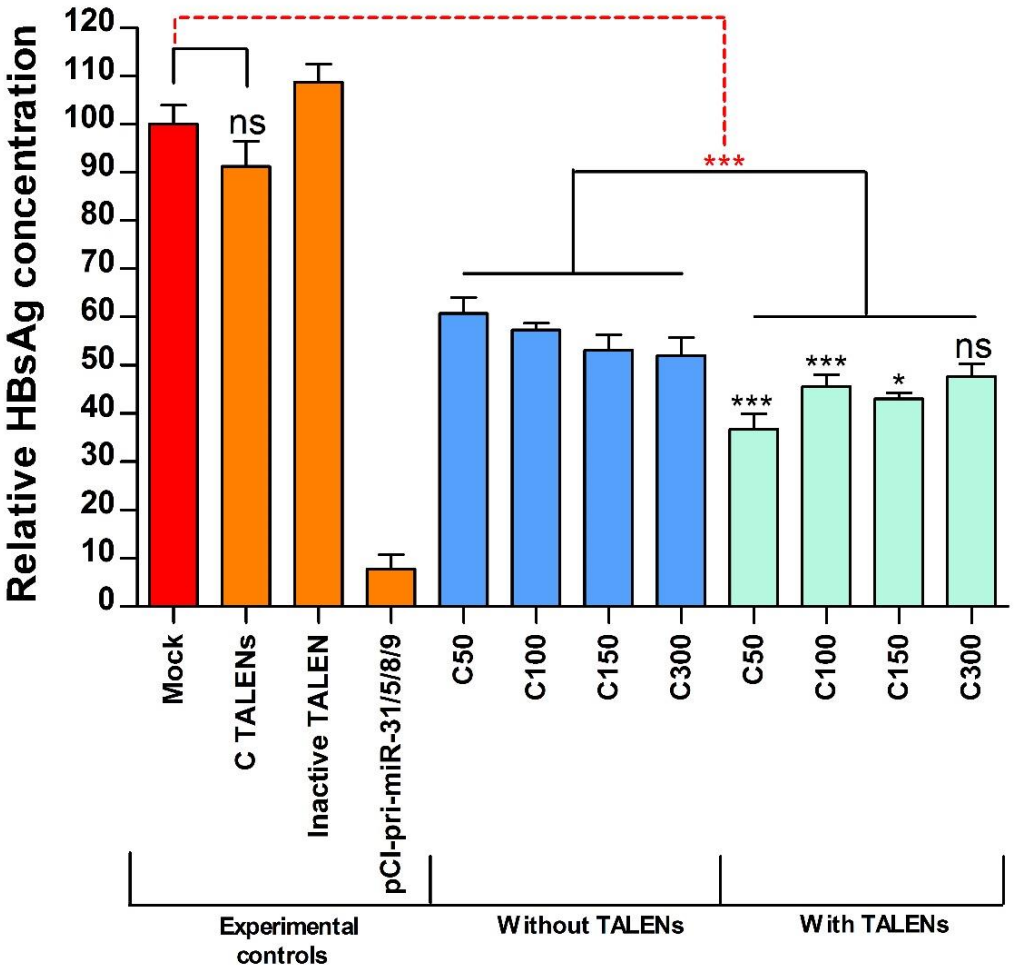

Figure 3.11: C TALEN and Core donor template strand (with pri-miR) mediated knockdown of HBsAg in Huh7 cells. The mock represents baseline HBsAg expression. C TALEN controls did not significantly affect HBsAg concentration and the inactive TALEN did not result in reduced HBsAg expression. pCI-pri-miR-31/5/8/9 was used as a positive control for pri-miR expression and resulted in significant HBsAg knockdown. All Core samples (with and without C TALENs) resulted in significant knockdown (red line). Cells were transfected with donor template strands that contained the pri-miR cassette, which resulted in a significant reduction in HBsAg concentrations when TALENs were absent. Donor template strands co-transfected with C TALENs significantly improved HBsAg knockdown when compared to donor template strands without TALENs. HBsAg concentrations were measured by HBsAg ELISA. The results were averaged and the values are relative to the mock HBV infection. Means are indicated with SEM. All readings were done in triplicate or more, except pCI-pri-miR-31/5/8/9, which only had two readings. (**: p<***: p<0.001; ns: not significant)

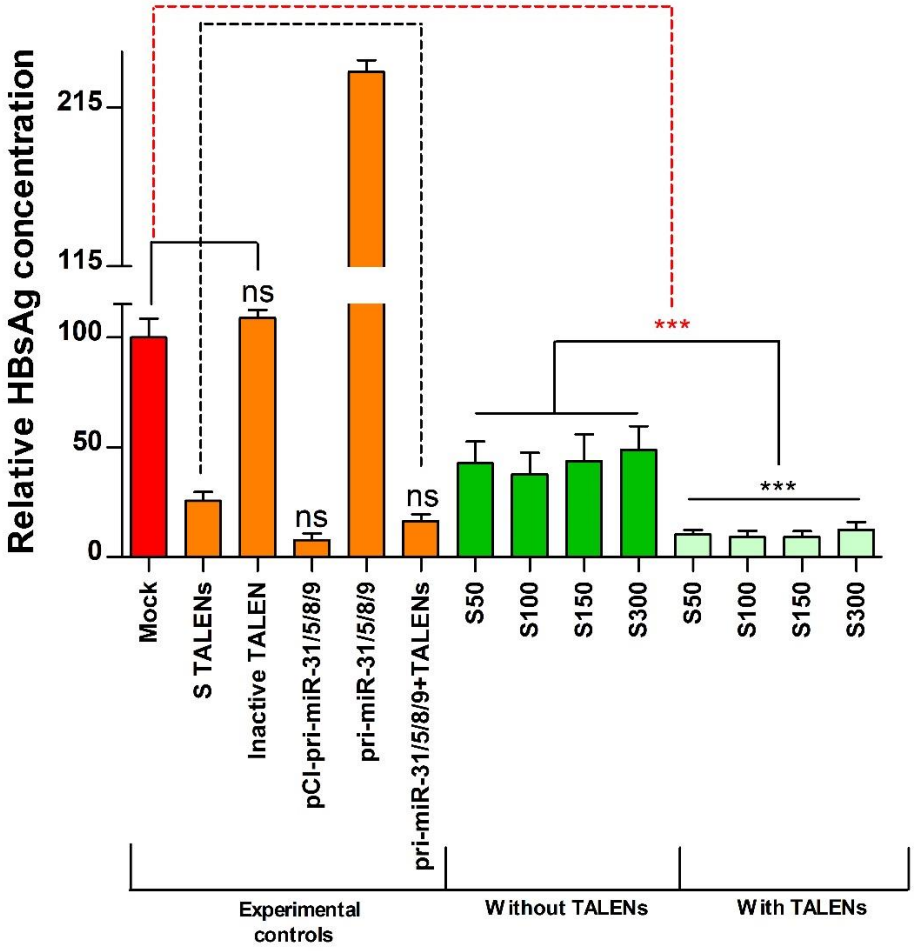

Figure 3.12: S TALEN and Surface donor template strand (with pri-miR) mediated knockdown of HBsAg in Huh7 cells. The mock represents baseline HBsAg expression. S TALEN controls resulted in significant reduction of HBsAg concentration, while the inactive TALEN (TALEN negative control) did not result in a significant decrease in HBsAg expression. A linear pri-miR-31/5/8/9 cassette increased HBsAg concentrations while S TALENs and the linear cassette resulted in decreased HBsAg concentrations that were not significantly different from TALEN-mediated knockdown. pCI-pri-miR-31/5/8/9 was used as a positive control for pri-miR expression and resulted in a significant decrease in HBsAg concentration. All Surface samples (with and without S TALENs) resulted in significant knockdown (red line). The HBsAg knockdown by co-transfected TALENs and donor template strands was a significant improvement compared to the TALEN control and donor templates without TALENs, but was similar to pCI-pri-miR-31/5/8/9 mediated HBsAg knockdown. HBsAg concentrations were measured by HBsAg ELISA. The results were averaged and the values are relative to the mock HBV infection. Means are indicated with SEM. All readings were done in triplicate or more, except pCI-pri-miR-31/5/8/9, which only had two readings. (***: $p<0.001$; ns: not significant)

3.3 pri-miR-31/5/8/9 cassette integration at the pCH-9/3091 *core* and *surface* target sites

Integration of the pri-miR-31/5/8/9 cassette should result in pri-miR expression that is driven by an HBV promoter. Therefore, successful insertion of the pri-miR-31/5/8/9 cassette has to be confirmed to determine if insertion of the pri-miR-31/5/8/9 cassette could result in HBV promoter driven pri-miR expression and subsequent HBsAg knockdown. In this project conventional PCR and DNA sequencing were used to assess insertion of the pri-miR-31/5/8/9 cassette at the *core* and *surface* target sites. To evaluate insertion, primer pairs were designed to amplify the *core* and *surface* insertion sites respectively (Figure 3.13). The forward primer binds to a sequence located within the inserted artificial sequence while the reverse primers bind to a sequence downstream from the right homologous region. These primers were designed to prevent amplification of the donor template strands and should ensure that amplification only occurs when the insert is present at the target sites. Multiple controls were introduced to confirm that these primers do not amplify the donor templates or any of the other co-transfected plasmids.

3.3.1 PCR analysis of pri-miR-31/5/8/9 insertion at the *core* target site

pCH-9/3091 and pri-miR-containing Core donor template strands were used as PCR controls to confirm that the correct donor template strands were used for transfection and that the Core primer pair (Table 2.6) does not amplify pCH-9/3091 or the donor template strands (Figure 3.14). The Core donor template strands with 50 bp flanking homologous regions yielded a 630 bp band (lane 2), while the donor with the 300 bp homologous regions resulted in a ≈1200 bp band (lane 3) on a 1% agarose gel. These donor template strand sizes were consistent with the PCR results in 3.1.3 (Figure 3.3), indicating that the correct

donor template strands were used for transfection. PCR was performed on the pCH-9/3091 plasmids as well as the donor template strands and did not result in DNA bands (lanes 4, 5 and 6), confirming that the Core primer pair does not amplify the pCH-9/3091 plasmids or Core donor template strands. PCR of the pCH-9/3091 plasmids purified from transfected Huh7 cells (Table 2.5) resulted in an 1100 bp band (lanes 7, 8, 9 and 10) and confirms that the pri-miR-31/5/8/9 cassette was successfully incorporated at the *core* target site in all four transfected samples. The 1100 bp bands in lanes 7 and 9 support the hypothesis that DNA is damaged during transfection and that insertion of the pri-miR cassette occur even in the absence of TALENs. A 500 bp band was also present in lane 9 and 10 and may be a result of primers that do not bind exclusively to their designed targets. It is possible that other recombination events occurred as a result of NHEJ and MMEJ. HDR and these recombination events may result in partial insertion of the artificial sequence and yield PCR products with different lengths. Potentially only small sections of the artificial sequence are needed to allow NHEJ, MMEJ and HDR-mediated dsDNA repair. Nakade *et al*. also demonstrated that precise HDR mediated integration occurs, but that not all inserted sequences contain the complete donor sequence (200).

Figure 3.13: Analysis of pri-miR-31/5/8/9 integration at the *core* target sites. A forward primer binds a target sequence within the region containing the three stop codons and a reverse primer binds a downstream target sequence within the pCH-9/3091 plasmid. The primer pair should not amplify the donor template strands and should only yield products if the insert is present in the pCH-9/3091 plasmid.

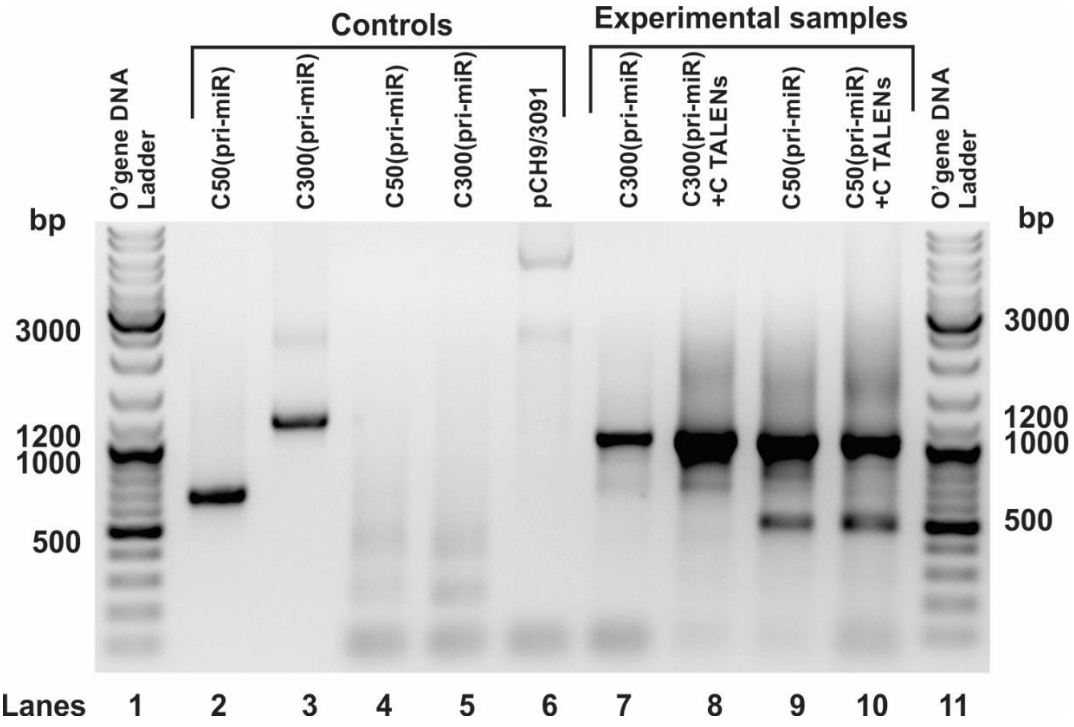

Figure 3.14: PCR analysis of the *core* target site. The control bands in lanes 2 and 3 are consistent with the size of the C50(pri-miR) and C300(pri-miR) donor templates in Figure 3.3 and were used as positive controls to confirm transfection with the correct donor template strands. None of the negative controls resulted in DNA bands (lanes 4, 5 and 6), confirming that the TALEN pair does not amplify pCH-9/3091 or the donor template strands. A ≈1100 bp band in lanes 7, 8, 9 and 10 confirms that the pri-miR-31/5/8/9 cassette was successfully integrated at the *core* target site. The identity of the 500 bp band in lanes 9 and 10 is unknown.

3.3.2 PCR analysis of pri-miR-31/5/8/9 insertion at the s*urface* target site

The negative controls for the Surface primer pair consisted of pCH-9/3091 and pUC118 samples (lanes 3 and 4) (Figure 3.16). These samples were amplified with Surface primer pairs (Table 2.6) and did not yield DNA bands, confirming that the primer pair does not amplify these plasmids (Figure 3.16). PCR of the insert-containing Surface donor template strands (negative control) resulted in an 800 bp band (lanes 5 and 6) when no bands were predicted. The primers and donor template strands were purified to rule out contamination (no DNA band in dH_2O: lane 2), but still resulted in 800 bp PCR products. Thus, these bands indicate that the Surface primers could be binding to off-site sequences. Purified plasmids from cells that were only transfected with pCH-9/3091 plasmids also acted as negative controls and did not yield DNA bands (lanes 8 and 9). Successful insertion of the pri-miR-31/5/8/9 cassette results in a 1200 bp band. Using this criterion, successful insertion was confirmed in cells transfected with Surface donor template strands and S TALENs (lanes 10, 11, 12 and 13). However, the bands were very light, a possible result of a low insertion frequency or poor PCR efficiency. Another unknown 800 bp band was observed in lanes 11 and 13 and support the possibility that the primers are binding to off-site sequences. The multiple bands also support the PCR results in 3.3.1 that yielded multiple bands in the Core samples, and reinforces the hypothesis that alternative or partial recombination events are occurring. These 800 bp bands were sequenced to determine their identity.

Figure 3.15: Analysis of pri-miR-31/5/8/9 integration at the *surface* target sites. A forward primer binds a target sequence within the region containing the three stop codons and a reverse primer binds a downstream target sequence within the pCH-9/3091 plasmid. The primer pair should not amplify the donor template strands and should only yield products if the insert is present in the pCH-9/3091 plasmid.

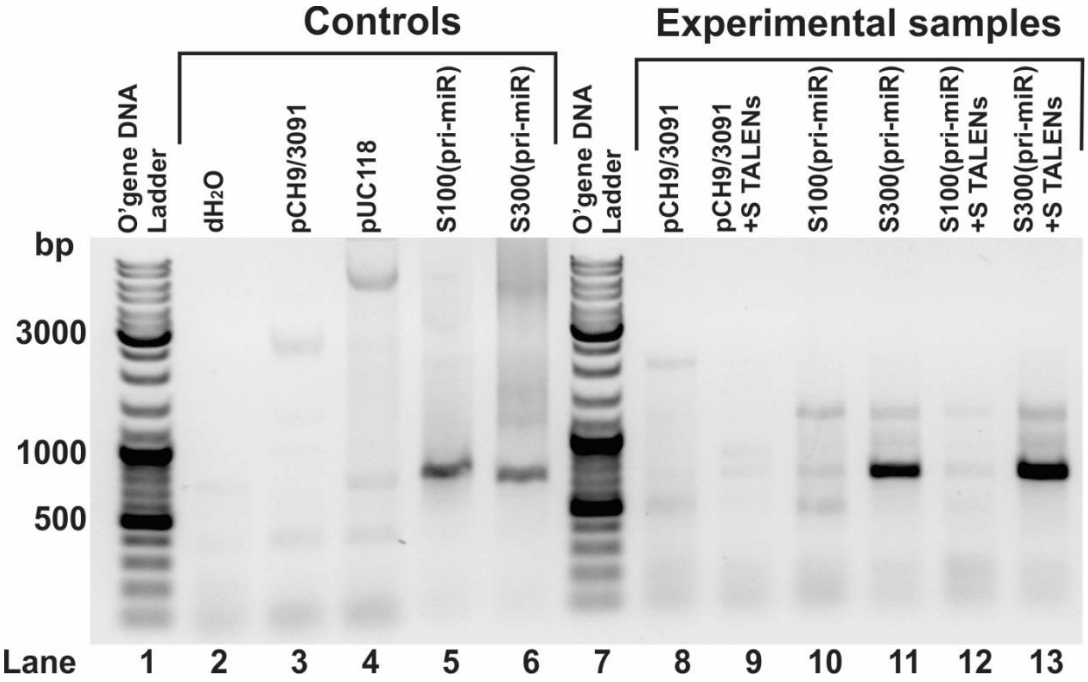

Figure 3.16: PCR analysis of the *surface* target site after transfection. The negative controls in lanes 2, 3 and 4 did not yield DNA bands and confirm that the primer pair does not amplify pCH-9/3091 or pUC118. The control samples in lanes 5 and 6 resulted in an unidentified 800 bp band. No DNA bands were visible in the experimental samples without donor template strands (lanes 8 and 9), also confirming that the primer pair does not amplify pCH-9/3091. Successful insertion of the pri-miR-31/5/8/9 cassette at the *surface* target site resulted in light 1200 bp bands (lanes 10, 11, 12 and 13). An unknown 800 bp band was also present in two of the experimental samples (lanes 11 and 13).

3.3.3 Sequencing of the pri-miR-31/5/8/9 insertion site

PCR results are not sufficient to confirm pri-miR-31/5/8/9 insertion at the target sites and warrants the use of a more precise analysis method such as sequencing. Sequencing provides the exact nucleotide sequence at the insert sites and can be compared to the pCH-9/3091 and pri-miR-31/5/8/9 sequences to confirm insertion of the pri-miR-31/5/8/9 cassette. Therefore, the 1000 bp amplicon from the Core PCR analysis (Figure 3.14: lanes 7, 8, 9 and 10) and the 1200 bp and 800 bp amplicons from the Surface PCR analysis (Figure 3.16: lanes 5, 6, 10, 11, 12 and 13) were extracted from the agarose gels and sequenced by Inqaba Biotech (Pretoria, Gauteng, South Africa). BLAST sequence alignments were performed to compare the sequencing results to the pCH-9/3091 sequence with the pri-miR-31/5/8/9 cassette at the *core* and *surface* sites (187, 188).

The 1000 bp Core amplicon contained the pri-miR-31/5/8/9 cassette

The complete pri-miR-31/5/8/9 cassette, a stop codon and a section of the pCH-9/3091 were present in the sequencing results of the 1000 bp Core sample (Figure 3.17). These results are consistent with the PCR results (Figure 3.14) and confirm that co-transfecting cells with C TALENs and pri-miR-containing Core donor templates with 50 bp and 300 bp flanking homologous regions result in HDR and subsequent integration of the pri-miR-31/5/8/9 cassette at the *core* target site. The results also support the hypothesis that non-specific DSBs caused by transfection and collapsed replication forks are repaired by HDR, which successfully inserts the pri-miR-31/5/8/9 cassette at the *core* target site when the Core donor template strands with the pri-miR insert and no TALENs are introduced.

Sequencing results of the 800 bp Surface amplicon

The sequencing results of the 800 bp PCR product from the Surface PCR analysis (Figure 3.16: lanes 5, 6, 11 and 13) confirmed that the pri-miR-31/5/8/9 cassette and three stop codons were not integrated at the *surface* target site (Figure 3.18).

Sequencing results of the 1200 bp Surface amplicon

The expected size of the amplified insertion site with the pri-miR-31/5/8/9 cassette was 1200 bp. This 1200 bp PCR product from the Surface sample (Figure 3.16: lanes 10, 11, 12 and 13) was sequenced twice. Both results confirmed that the stop codons and pri-miR-31/5/8/9 cassette were not incorporated at the *surface* target site. The short sequence length (540 bp) suggests that sequencing may have been incomplete or the forward PCR primer bound to a sequence further downstream within the right flanking homologous region of the *surface* target site (Figure 3.19). This would support the idea that the forward primer does not bind exclusively to its designed *surface* target.

Partial insertion of the artificial sequence at the *surface* site

The purified plasmids of cells transfected with the Surface donor template strands and S TALENs (Figure 3.16: lanes 10, 11, 12 and 13) were amplified (PCR) and sequenced by Inqaba Biotech (Pretoria, Gauteng, South Africa) to confirm that the absence of the stop codons and pri-miR cassette is not the result of a fault in the PCR protocol. The new results confirmed that two stop codons were successfully integrated at the *surface* target site, but the pri-miR-

31/5/8/9 cassette was absent (Figure 3.20). This reinforces the hypothesis that HDR, NHEJ and MMEJ can repair DSBs by only partially inserting the artificial sequence. This suggests that only small sections of the artificial sequence are needed to allow NHEJ, MMEJ and HDR-mediated dsDNA repair, thus supporting the results reported by Nakade *et al*. (200). However, this surface sample is not a representative of the whole and it is possible that complete integration of our artificial sequence occurs at a very low frequency and is beyond the detection level of the PCR. This problem might be resolved by increasing the number of transfected cells. An increase in cells will allow larger amounts of pCH-9/3091, TALENs and donor template strands to be transfected and may result in an increase in insertion frequency that is detectable by PCR.

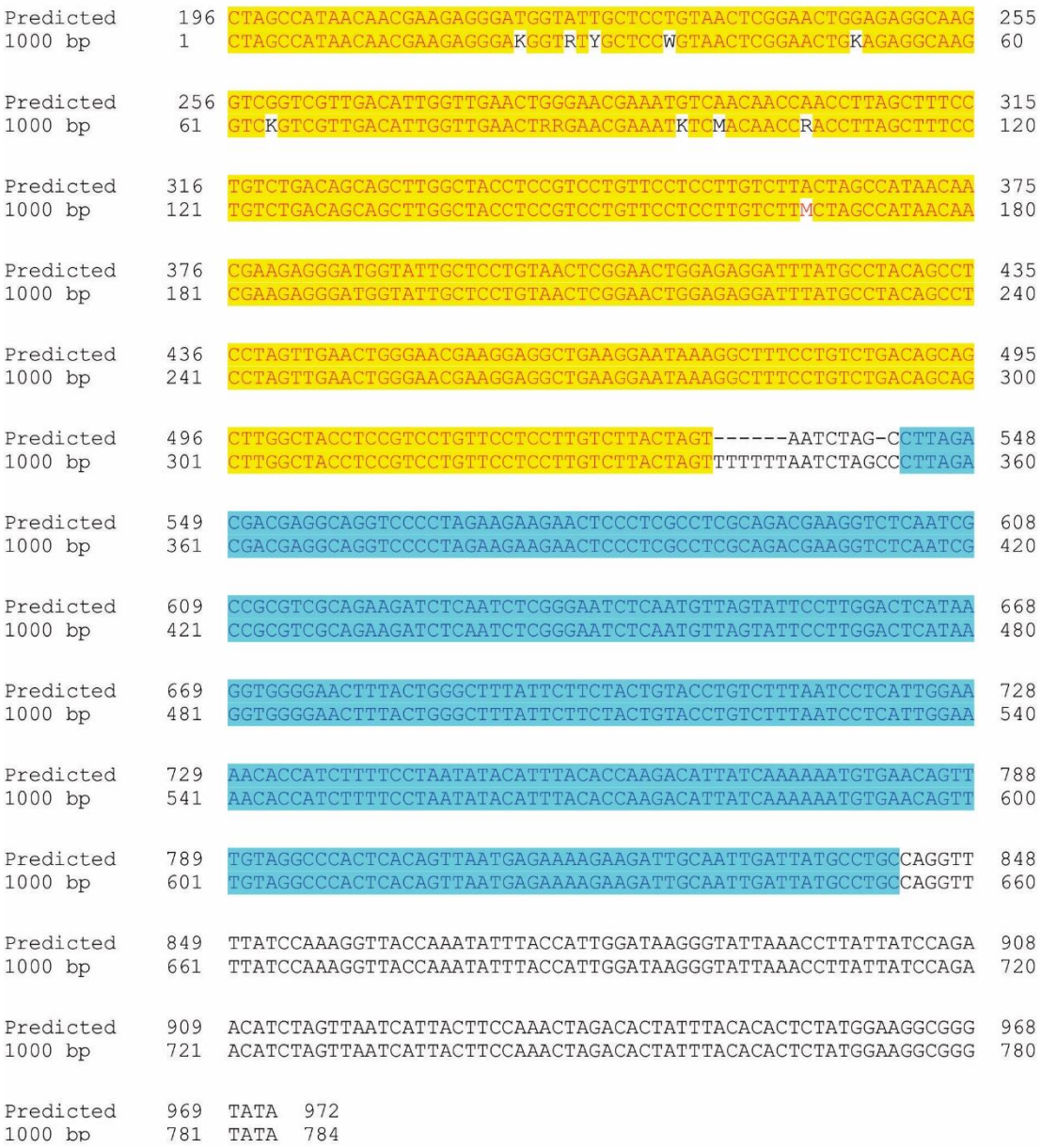

Figure 3.17: Sequence alignment of the 1000 bp Core sample and pri-miR-containing pCH-9/3091. The yellow highlighted area indicates the integrated pri-miR-31/5/8/9 cassette and a stop codon at the *core* target site. The blue highlighted area represents the right homologous region. A partial pCH-9/3091 sequence at the end confirms that the sequencing results are from pCH-9/3091 and not the donor template strands. K: Keto (G or T); R: Purine (A or G); Y: Pyrimidine (C or T); W: Weak (A or T); M: Amino (A or C).

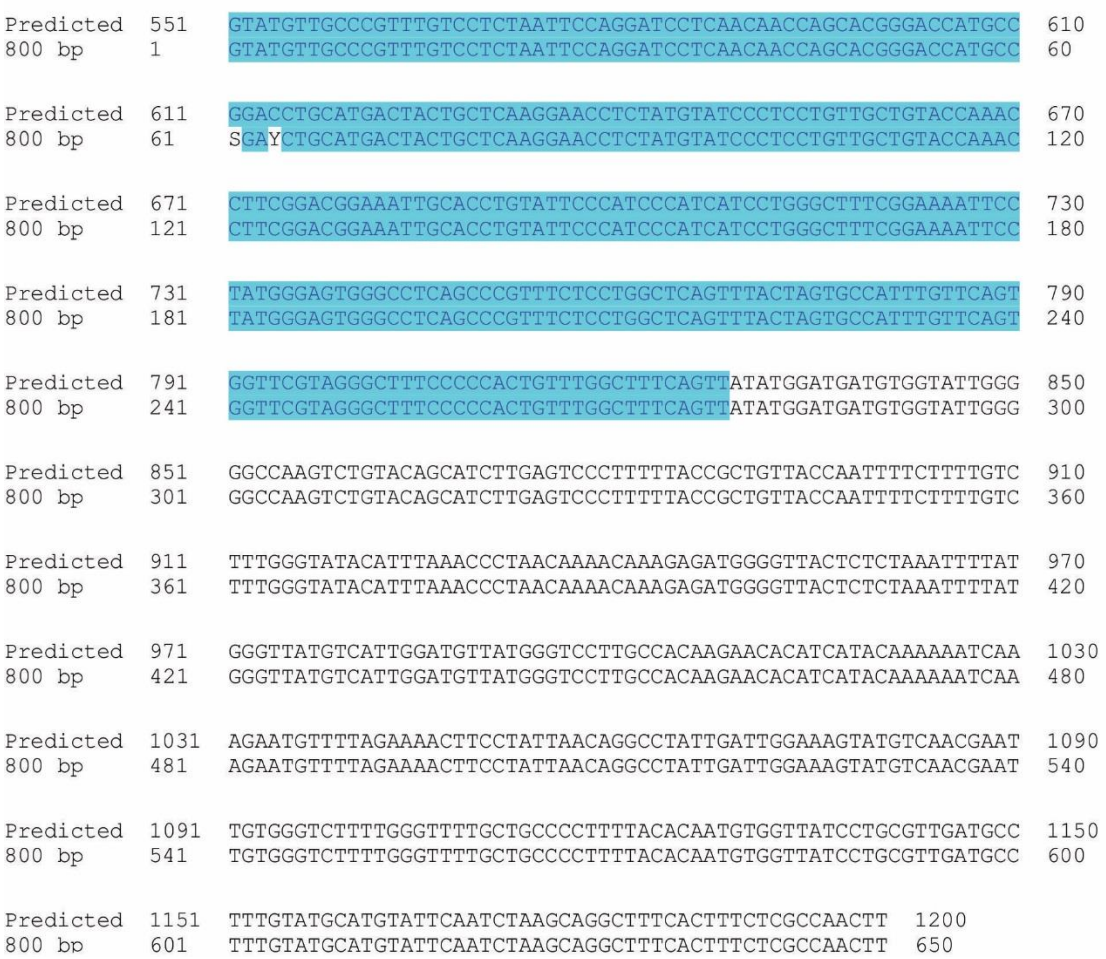

Figure 3.18: Sequence alignment of the 800 bp Surface sample and pri-miR-containing pCH-9/3091. The blue highlighted area indicates the right homologous region. A partial pCH-9/3091 sequence at the end confirms that the sequencing results are from pCH-9/3091 and not the donor template strands. Integration of the pri-miR-31/5/8/9 cassette did not occur. S: Strong (G or C); Y: Pyrimidine (C or T).

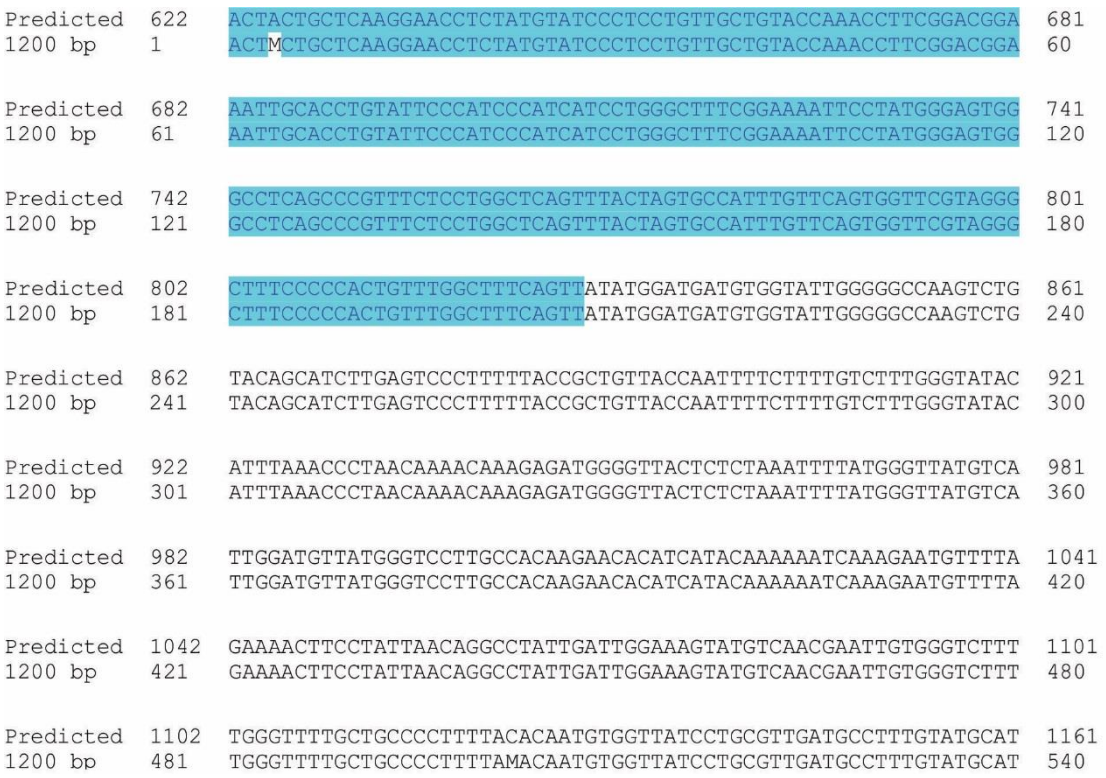

Figure 3.19: Sequence alignment of the 1200 bp Surface sample and pri-miR-containing pCH-9/3091. The sequence length of the 1200 bp is short (540 bp) and the blue highlighted area indicates the right homologous region with a missing upstream section. A partial pCH-9/3091 sequence at the end confirms that the sequencing results are from pCH-9/3091 and not the donor template strands. Integration of the pri-miR-31/5/8/9 cassette did not occur. M: Amino (A or C).

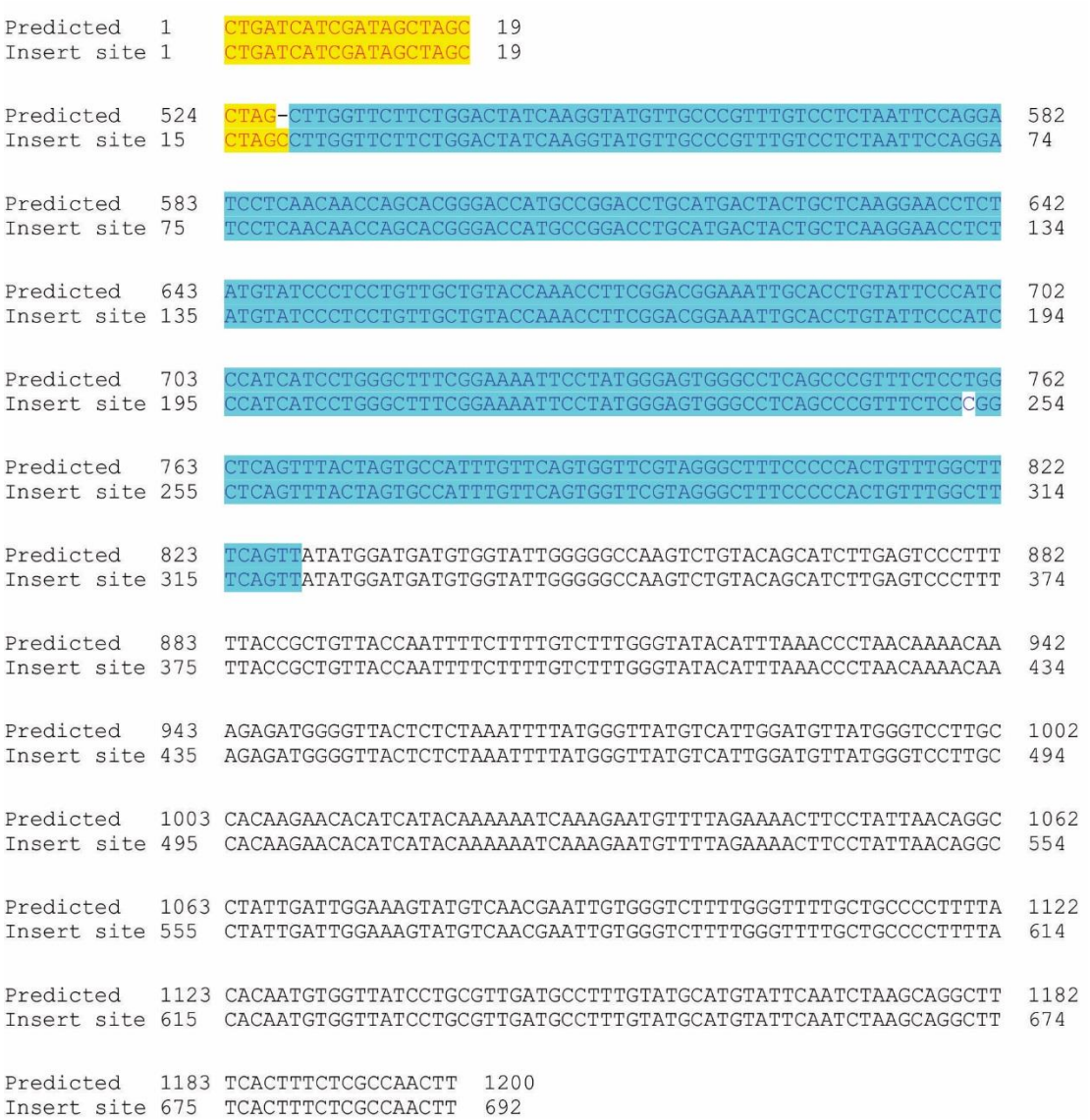

Figure 3.20: Sequence alignment of the pri-miR-31/5/8/9 *surface* insertion site and pri-miR-containing pCH-9/3091. The yellow highlighted section contains two stop codons and the blue highlighted region indicates the right homologous region. The pri-miR-31/5/8/9 cassette was not inserted, confirming that only partial insertion occurred at the *surface* site. A partial pCH-9/3091 sequence at the end confirms that the sequencing results are from pCH-9/3091 and not the donor template strands.

3.4 Pri-miR expression

Ely *et al*., demonstrated that the pri-miR-31/5/8/9 cassette results in efficient HBsAg reduction (169). Therefore, we proposed that inserting the pri-miR cassette at the pCH-9/3091 *core* and *surface* sites should result in pri-miR expression and subsequent HBsAg knockdown. This pri-miR expression by the incorporated pri-miR-31/5/8/9 cassette was assessed by Northern blot, a technique that detects specific RNA or miRNA in a sample.

3.4.1 Cloning donor template strands into pTZ57 R/T

PCR is not sufficient to produce the large quantities of donor template strands required for pri-miRNA detection. Therefore, the donor template strands were cloned into pTZ57 R/T plasmids for large scale plasmid production. The C50(pri-miR) and S100(pri-miR) donor template strands with the pri-miR insert, and the pri-miR-31/5/8/9 cassette were each cloned into pTZ57 R/T plasmids. Positive clones were identified with a *Pvu*II restriction digest (Chapter 2) as the *Pvu*II restriction sites flanked the inserted sequence (Figure 3.21). Successful insertion of the Core donor template strand yielded a 1015 bp band (lane 2), while successful insertion of the Surface template resulted in a 1115 bp band (lane 3) (Figure 3.22). An 898 bp band confirmed successful insertion of the pri-miR-31/5/8/9 cassette (lane 4). These positive clones were maxi prepped and used in transfection experiments.

3.1.1 Northern blot

If the pri-miR-31/5/8/9 cassette is integrated at the target site, the HBV promoter should drive the pri-miR expression. The pri-miR is then processed

to miRNA by the RNA interference pathway. This miRNA can be detected by Northern blot and can be visualised to confirm that pri-miR is being expressed. Northern blot results that are positive for pri-miR expression will support the idea that pri-miR expression is driven by an HBV promoter when the pri-miR-31/5/8/9 cassette is integrated into pCH-9/3091. It will also support the hypothesis that pri-miR expression by the integrated cassette results in HBsAg knockdown. A miR-31/5 guide probe oligonucleotide (169) was used to probe for pri-miR-31/5/8/9, and purified pri-miR-31/5/8/9 was used as a positive control to confirm probe activity. The positive control resulted in a ≈20 bp band and confirmed that the probe was active and that the Northern blot protocol was successful (Figure 3.23). None of the experimental samples resulted in bands. No band was expected for pri-miR-31/5/8/9, pTZ-pri-miR or pTZ-pri-miR with TALENs, as HBsAg ELISA results suggested that the linear pri-miR-31/5/8/9 sequence did not result in pri-miR expression (see Figure 3.9). The absence of bands in the remaining samples may be due to the low insertion frequency of the pri-miR cassette and subsequent low concentrations of RNA. Low concentrations of pri-miR should be enough to cause reduction in HBsAg expression, suggesting that the miRNA concentrations are high enough to effect change in HBsAg expression, but are not sufficient to be detected by Northern blot. This inability to detect the RNA warrants the use of more sensitive RNA detection methods.

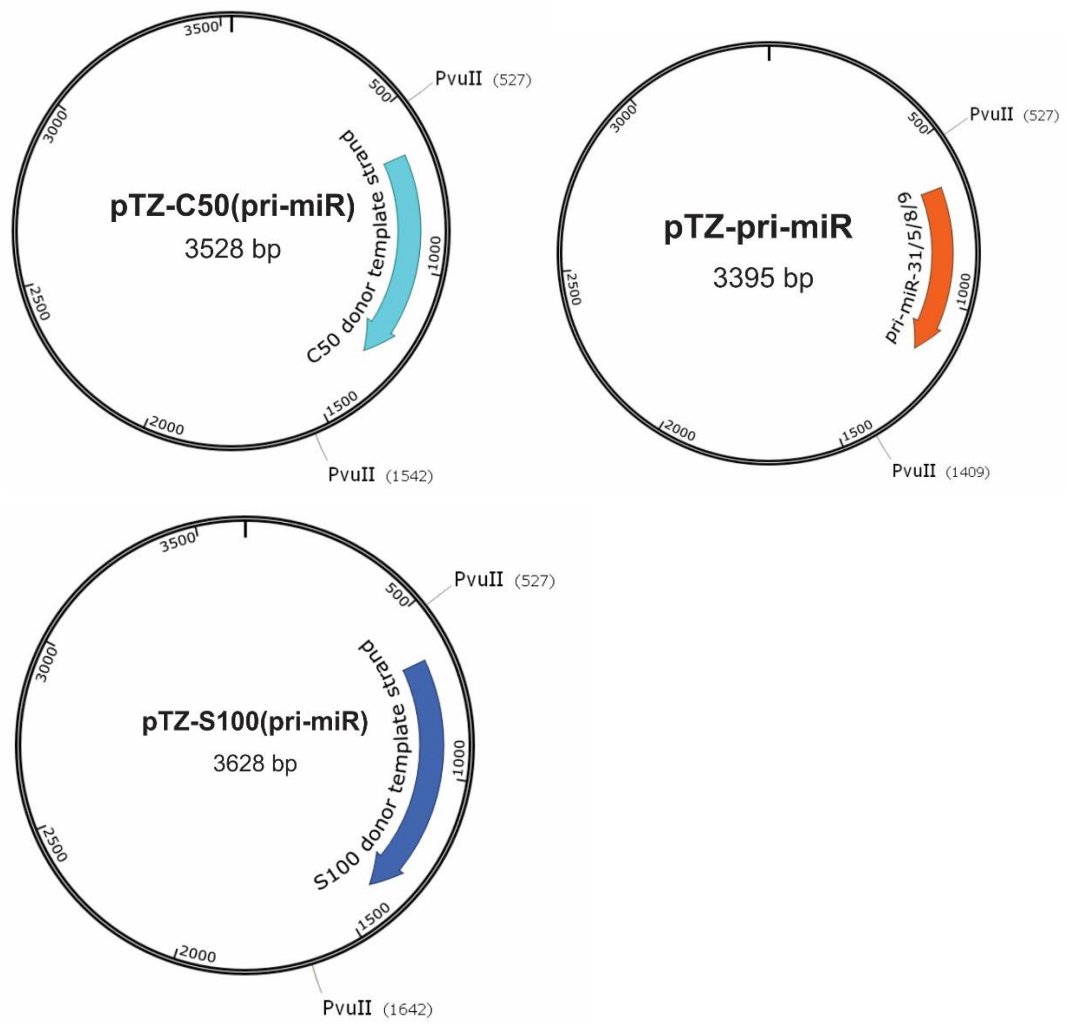

Figure 3.21: pTZ57 R/T plasmids containing the pri-miR-31/5/8/9 cassette and the C50(pri-miR) and S100(pri-miR) donor template strands. C50(pri-miR), S100(pri-miR) and pri-miR-31/5/8/9 were cloned into pTZ57 R/T by TA cloning. Two *Pvu*II restriction sites flank the insertion sites, therefore a *Pvu*II restriction digest was performed to confirm successful integration of C50(pri-miR), S100(pri-miR) and pri-miR-31/5/8/9 into the pTZ57 R/T plasmids.

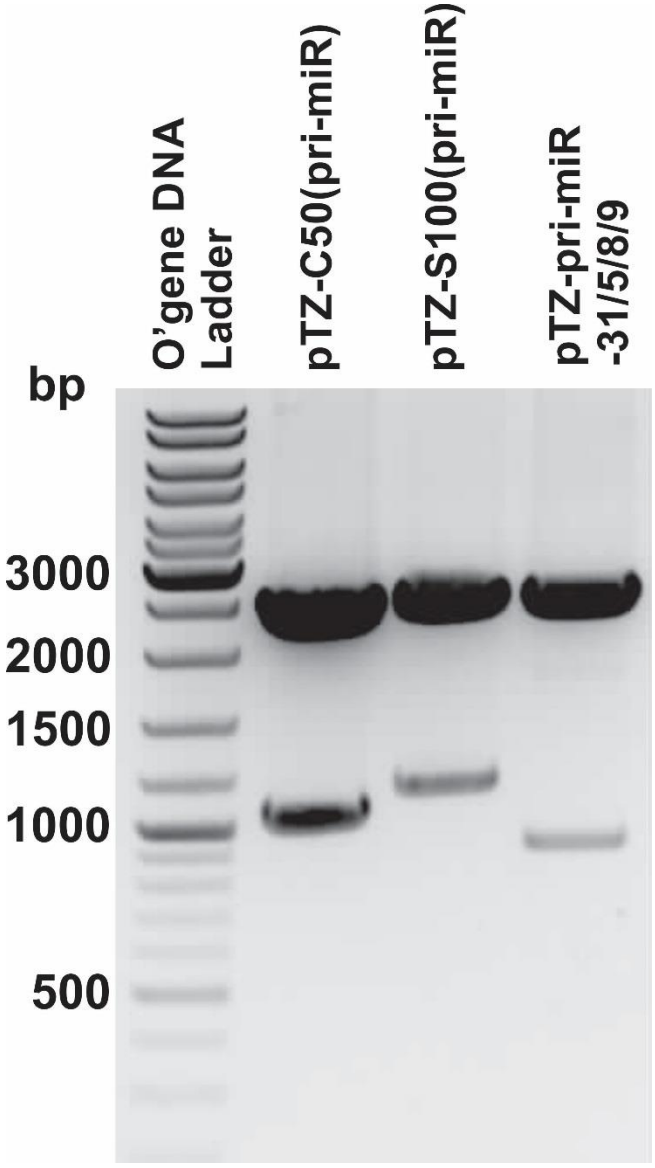

Figure 3.22: C50, S100 and pri-miR31/5/8/9 cloned into pTZ57 R/T. All samples were digested with *Pvu*II and analysed on a 1% agarose gel. Restriction digest with *Pvu*I resulted in 1015 bp, 1115 bp and 898 bp bands for pTZC50, pTZS100 and pTZ-pri-miR-31/5/8/9 clones respectively.

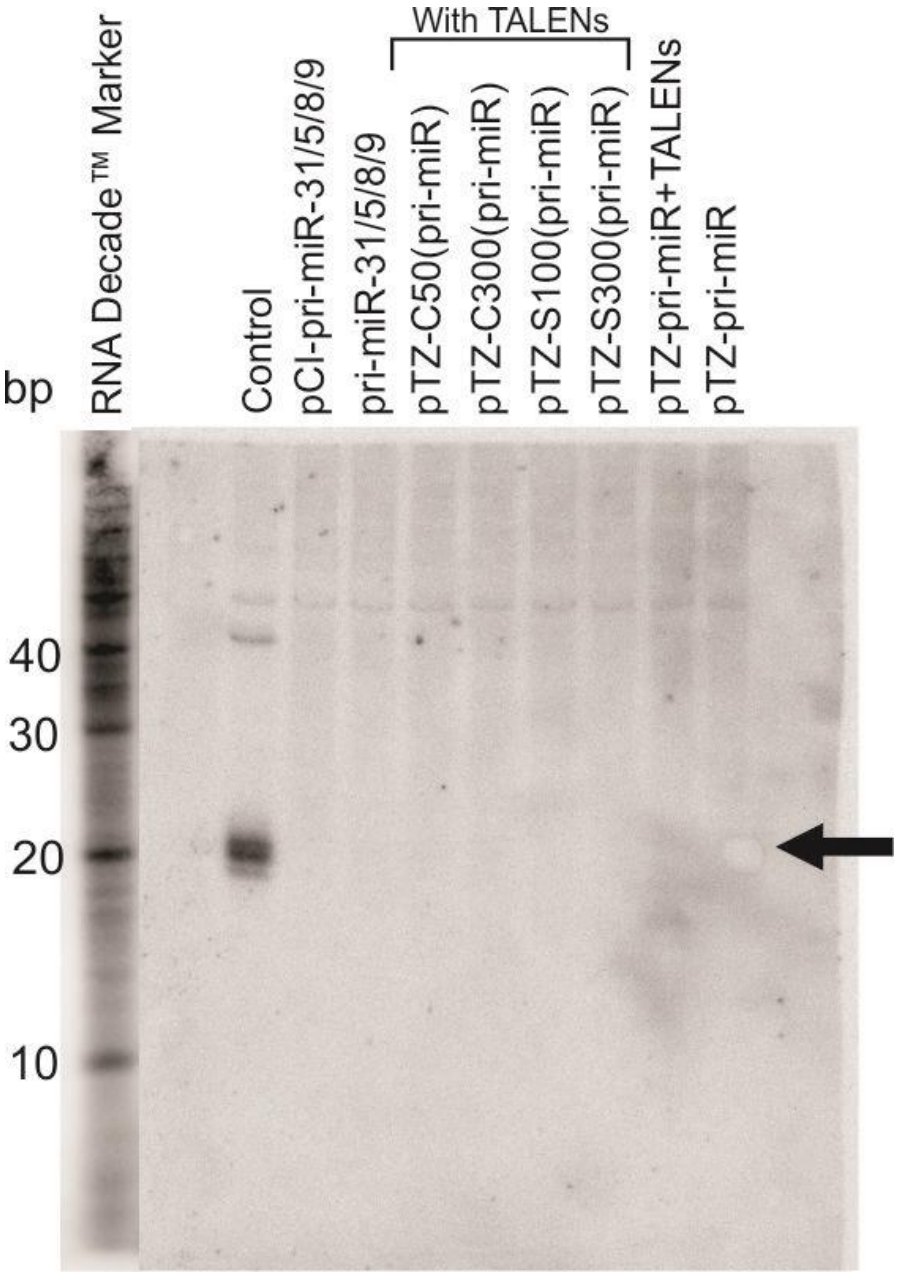

Figure 3.23: Northern blot membrane probed for pri-miR expression. A miR-31/5 guide probe oligonucleotide was used to probe for miRNA expressed by the integrated pri-miR-31/5/8/9 cassette. Samples were analysed on a 15% acrylamide gel. The pri-miR-31/5/8/9 in the control resulted in an ≈20 bp band (black arrow). pCI-pri-miR-31/5/8/9 was a positive control for pri-miR expression, but did not yield a band. No band was expected for pri-miR-31/5/8/9, pTZ-pri-miR or pTZ-pri-miR with TALENs, as these sequences and plasmids should not result in pri-miR expression (see Figure 3.9). The remaining experimental samples did not yield any bands, possibly due to low insertion frequency

4. Discussion

4.1 Disruption of HBV replication through HDR

A novel therapeutic design is required to treat and eliminate chronic hepatitis B virus (HBV) infections. Chronic HBV remains a major challenge for hyper-endemic areas such as Sub-Saharan Africa and Asian countries, therefore, development of affordable and effective treatments remains a top research priority (1). Multiple vaccines are currently available and effectively prevent HBV infection. However, these vaccines do not treat existing HBV infections (25). There are currently various treatments available that successfully manage HBV infections. However, these treatments target viral post transcriptional mechanisms to inhibit HBV and, as a result of persistent cccDNA, do not clear the virus, necessitating continuous treatment (13, 50, 51, 63, 64). Viral cccDNA avoids treatment as well as the host immune response and results in latent or occult infection. Therefore, a novel treatment that targets viral cccDNA is required to eradicate the viral reservoirs and successfully clear HBV. Manipulation of viral DNA and RNA by designer nucleases allows targeting of the pre- and post-transcriptional events in the viral life cycle and shows promise as anti-viral agents against HBV (63, 76-78). It follows then that designer nucleases, such as TALENs and ZFNs, may be used to target the viral cccDNA reservoirs.

Both TALENs and ZFNs have recently been used to manipulate genomes of various organisms and cell lines (79, 103, 108, 125, 129-131). Designer TALENs can target a wide range of targets and are able to discriminate between highly similar sequences, making it a very precise genome editing tool (85, 132). Preliminary studies also indicated that little or no off-target

mutagenesis occurs and concluded that incidence of off-target effects is not a significant concern for disease modelling and genome-editing applications (135-137). Thus, TALENs provide highly specific and efficient genome-editing abilities. The *Fok*I domains of a TALEN pair dimerise and cleave a target DNA sequence, resulting in a DSB that is repaired by HDR, NHEJ or microhomology-mediated end joining (MMEJ). These repair pathways may introduce mutations and result in disruption of the target site. Researchers recently demonstrated that introduction of a homologous donor template strand induces the HDR pathway and results in integration of an artificial sequence at the DSB, confirming that these repair pathways can be exploited for precise genome engineering (163-167).

It is difficult to target the viral cccDNA, as precise targeting of the genome is required to prevent off-target cleavage that may harm the host. Recently researchers reported success in targeting HBV cccDNA with ZFNs and TALENs (15, 177). They managed to significantly reduce viral protein expression and genome replication both *in vitro* and *in vivo*, but were unable to eliminate the viral cccDNA pool. This might be a result of viral mutagenesis, epigenetic regulation or NHEJ repair of the TALEN-mediated DSBs. NHEJ is error prone and results in mutagenesis at the target site, but can also successfully repair DSBs, allowing cccDNA to persist and cause latent infection once treatment is suspended. Alternative gene therapies, such as RNA interference, also demonstrated significant anti-HBV activity (169, 201-206). Ely *et al*. designed a pri-miR expression cassette that expressed anti-HBV pri-miRs and successfully disrupted HBV replication (169). Therefore, we proposed combining TALENs and these pri-miR cassettes to target both the cccDNA reservoirs and HBV replication. TALENs would create DSBs and the introduction of donor template strands containing a promoter-less pri-miR cassette will induce HDR and facilitate HDR-mediated integration of the pri-

miR cassette at the genome target site. Successful integration disrupts the target site and results in HBV-promoter driven pri-miR expression. The resultant silencing of *HBx* by processed pri-miRs should inhibit HBV replication and prevent formation of new cccDNA pools, allowing TALENs to target and eliminate the existing cccDNA genomes (Figure 4.1).

4.2 Combining TALENs and donor template strands significantly affect viral protein expression

TALENs and donor template strands can be co-introduced to facilitate integration of the pri-miR-31/5/8/9 cassette into the HBV genome. TALENs should create DSBs at the HBV *core* and *surface* cccDNA targets and result in NHEJ, MMEJ and HDR. Our TALEN results were consistent with the results reported by Bloom *et al*., confirming that NHEJ is upregulated when DSBs are introduced (15). The presence of the donor template strands should increase or favour HDR and result in increased integration of the pri-miR cassette.

The combination of TALENs and pri-miR-containing donor template strands improved viral disruption significantly. The increased insertion frequency of the pri-miR-31/5/8/9 cassettes at the TALEN-mediated DSBs results in increased pri-miR expression and subsequent gene silencing. This TALEN-donor template strand combination improves both pri-miR and TALEN-mediated virus disruption. Successful integration of the pri-miR cassette disrupts the target genome sequence and allows TALENs to target the remaining cccDNA genomes. Pri-miR expression by the integrated cassette will also inhibit viral replication by silencing *HBx*, which will prevent production of new cccDNA genomes. Therefore, the combination of TALENs and pri-miR should gradually decrease the amount of cccDNA until the latent cccDNA reservoir is depleted.

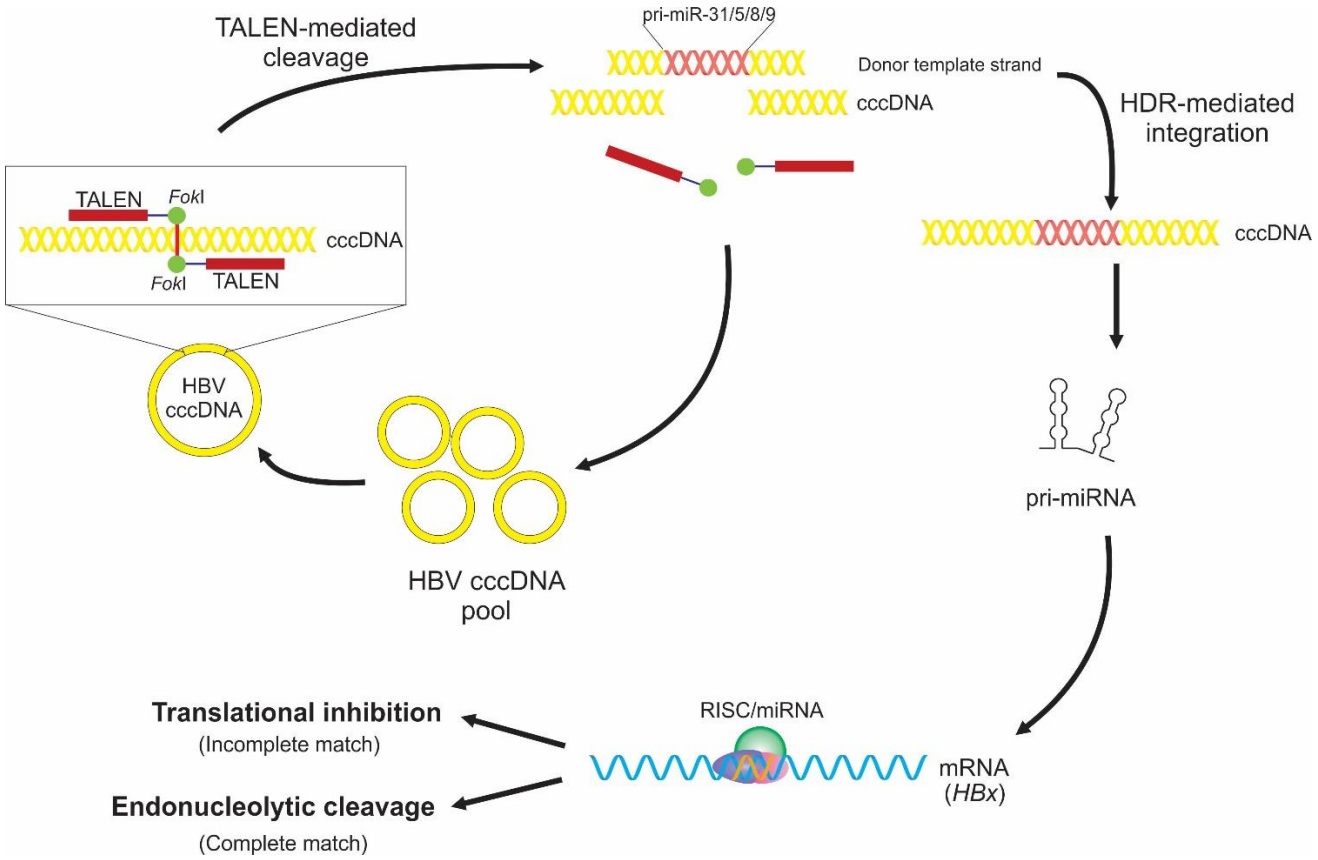

Figure 4.1: Disrupting the HBV genome using TALENs and RNAi. TALENs cleave the HBV cccDNA and create a DSB. A donor template strand containing a pri-miR-31/5/8/9 cassette is introduced and TALENs are free to bind to remaining cccDNA genomes in the cccDNA pool. HDR then utilises the donor template strand to facilitate integration of the pri-miR-31/5/8/9 cassette at the target site. The integrated cassette transcribes pri-miRNA, which is processed to form a RISC/miRNA duplex which facilitates translational inhibition or endonucleolytic cleavage of the HBx mRNA.

4.2.1 The lengths of the flanking homologous regions affect HDR efficiency

Researchers demonstrated that donor templates with longer flanking homologous sequences (400-800 bp) result in increased target efficiency and HDR frequency (167). However, some studies suggest that shorter homologous flanking sequence may also result in optimal HDR in some cell types (127, 179). Our results confirmed that shorter homologous sequences are more effective in Huh7 cells. This effectiveness may indicate that integration of the donor sequence is mediated by both HDR and MMEJ. A shorter homologous sequence should result in less homology search in HDR and may also result in preference for MMEJ. However, micro-homology regions are usually 9-20 bp in length, suggesting that MMEJ may recognise and use templates with longer homologous sequences for DNA damage repair (193).

4.2.2 Upregulation of viral protein expression

Error-prone NHEJ and MMEJ mediated DNA damage repair may introduce mutations or partially integrate the donor template strand. These genome modifications may result in harmful changes in protein expression. We found that upregulation of viral protein expression occurred when the pri-miR-31/5/8/9 cassettes were integrated at the *core* site. This may also be a result of missense mutations introduced by NHEJ. The *precore/core* region that is targeted by the C TALENs (2319) overlaps with the start of the HBV *polymerase* ORF, which encode HBV polymerase (2307) (15, 194). A missense mutation at this site could affect HBsAg expression as HBV polymerase is essential for initiation of viral reverse transcription and the assembly of replication-competent viral nucleocapsids. A missense mutation introduced at this site could result in overexpression of HBV polymerase and

subsequent increased HBsAg expression (195). This mutation may also change the 4th and 5th amino acid in the terminal protein (TP) of HBV polymerase (196, 197). The TP is essential for pgRNA encapsidation and changes in these amino acids could affect the binding of the polymerase to the encapsidation signal and alter the efficiency of TP initiation (194, 196-198). This could result in increased viral replication and subsequent upregulation of HBsAg expression. These results indicate that adverse effects may occur, even when precise nuclease activity and HDR integration are utilised. These adverse effects may be harmful to the host, therefore, further investigation is required to optimise our method and to ensure that no adverse events occur.

4.3 Donor template strand mediated knockdown of viral protein expression and replication

We found that donor template strands without TALENs resulted in disruption of viral activity. HDR occurred without TALENs and integrated the anti-viral sequence at the genome target site, which resulted in pri-miR expression and subsequent silencing of *HBx*. This is consistent with previous methods that induced HDR to insert an artificial DNA sequence at a target site (189-192). It is possible that the HBV equivalent was damaged during transfection. This damage was repaired by NHEJ, MMEJ and HDR, which may have resulted in spontaneous recombination (163, 193). The presence of the donor template strands stimulates HDR and subsequent integration of the artificial sequence at the DNA break site. The DSBs can also be repaired by NHEJ, which repairs breaks at an equal or higher frequency than HDR (163). Gabriel *et al*. demonstrated that NHEJ can also insert donor sequences at DSBs and causes off-target insertion within close proximity of the homologous regions of the TALEN target sites. NHEJ insertion may also occur at unidentified locations as a result of non-TALEN mediated DNA damage (207). Nakade *et al*. also

demonstrated that DSB overhangs that are complementary to linear DNA fragments or donor template strands facilitate integration by NHEJ in zebrafish and cultured cells (200). Recently MMEJ has been described to insert donor sequences at a target site (193, 199, 200). MMEJ is an error-prone minor repair pathway that comprises 10-20% of cellular repair activity and shares the DSB end resection step with HDR (193, 199). The repair mechanism actively repairs DSBs at collapsed replication forks and enables integration of large DNA fragments in cells with low HDR activity (200). In contrast to HDR, MMEJ undergoes short end resection (14-18 bp) on either side of the DSBs to reveal microhomology regions (9-20 bp) and joins the DSB ends by pairing bases at these microhomology regions (193). Therefore, it is possible that the donor sequence can be inserted through multiple pathways. Insertion by this method likely occurs at very low frequencies, suggesting that pri-miR gene silencing significantly disrupts HBV replication even when the pri-miR-31/5/8/9 integration frequency is low (189-192). These pathways do not necessarily result in complete integration of the artificial sequence, but even partial insertion should be enough to disrupt HBV replication. Merrihew *et al.* demonstrated that HDR can also result in off-target integration (189). This finding suggests that the use of these error prone pathways may have significant therapeutic implications, and may result in harmful mutagenesis in untargeted regions of the host genome. It is thus important for the findings of this study to be tested in more biologically relevant models allowing for more complete characterisation of its safety profile.

4.4 Pri-miR expression by the integrated pri-miR-31/5/8/9 cassette

Ely *et al*. demonstrated that a pri-miR-31/5/8/9 expression cassette results in efficient disruption of HBV replication (169). Our donor template strands contained the pri-miR-31/5/8/9 cassette, but lacked a promoter. We

hypothesised that pri-miR expression from the integrated pri-miR-31/5/8/9 cassette should be driven by an HBV promoter. Our results suggested that pri-miR mediated gene silencing occurred, but we were unable to visualise the expressed pri-miR using Northern blot hybridisation. This may be a result of low pri-miR-31/5/8/9 integration frequency and subsequent low pri-miR expression, suggesting that pri-miR expression was sufficient to affect HBV replication, but below the detection threshold for Northern blot. This warrants further investigation using more sensitive detection methods. Increasing the volume of cells and amount of TALENs and donor template strands should increase the amount of expressed pri-miR to a level that is detectable by Northern blot. However, if this does not succeed, alternative methods can be explored. The Northern blot detection sensitivity can be improved by using probe sequences that contain locked nucleic acids (LNAs). Válóczi *et al*. demonstrated that oliginucleotide probes with LNAs have improved hybridisation properties and mismatch discrimination, making them well suited for accurate miRNA detection (208). These probes are easy to synthesise and can be used in a Northern blot analysis that uses standard end-labelling methods and hybridisation conditions. The probe is highly specific and its sensitivity is increased tenfold compared to standard Northern blot, making them an improved and practical alternative (208). qRT-PCR has also been used to detect low amounts (25 pg) of mature miRNA. Chen *et al*. developed a method that uses stem loop reverse transcription (RT) primers to hybridise to miRNA during the RT step in qRT-PCR (209). The RT products can then be quantified using conventional TaqMan PCR. The stem loop primers are more specific and efficient than standard primers and are not affected by genomic DNA contamination. Stem loop qRT-PCR is also much less time consuming than Northern blot. These qualities make qRT-PCR with stem loops an attractive alternative to Northern blot. In contrast to Northern blot, qRT- PCR does not determine the size of the miRNA. However, the size of our target miRNA has already been determined (169), therefore, quantification with qRT-

PCR should be sufficient to confirm pri-miR expression by the integrated pri-miR cassette.

5. Conclusion

We confirmed the findings by Bloom *et al*., that TALENs can be used to achieve targeted disruption of the HBV genome (15). These TALENs can be coupled with HDR by introducing a homologous DNA template strand. Donor template strands can be designed to facilitate integration of a pri-miR-31/5/8/9 cassette into the HBV genome. Introduction and integration of the pri-miR cassette result in miRNA processing that is sufficient for significant and additive HBV knockdown. The synergistic activity of TALENs and pri-miRNA is of significant value for the therapeutic field. Co-introducing TALENs and donor template strands inhibits viral replication, thus preventing formation of more cccDNA in new hepatic cells and allowing more time for TALEN-mediated inactivation of the pre-existing cccDNA pool. This combination could possibly replace lifelong HBV treatments by clearing viral cccDNA and preventing latent infection. The decrease in required treatment could also reduce cost on health systems of developing countries where chronic HBV is prevalent. TALENs and donor template strands could also prevent adverse symptoms caused by current HBV treatments, thus improving the general health of HBV patients. However, we demonstrated that the pri-miR cassette is also integrated by spontaneous recombination, raising the possibility that off-target insertion may occur. This concern warrants further investigation and optimisation of the method, as off-target insertion may result in adverse effects. However, this proof of concept study paves the way for expanded studies in *in vivo* and more advanced *in vitro* models for the development of targeted anti-HBV gene therapies.

6. References

1. **Kew MC.** 2010. Epidemiology of chronic hepatitis B virus infection, hepatocellular carcinoma, and hepatitis B virus-induced hepatocellular carcinoma. Pathologie-biologie **58:**273-277.
2. **Xie Y, Zhai J, Deng Q, Tiollais P, Wang Y, Zhao M.** 2010. Entry of hepatitis B virus: mechanism and new therapeutic target. Pathologie-biologie **58:**301-307.
3. **Chisari FV, Ferrari C.** 1995. Hepatitis B virus immunopathogenesis. Annual Review of Immunology **13:**29-60.
4. **Hwang EW, Cheung R.** 2011. Global epidemiology of hepatitis B virus (HBV) infection. North American Journal of Medicine and Science **4:**7-13.
5. **Kiire CF.** 1996. The epidemiology and prophylaxis of hepatitis B in sub-Saharan Africa: a view from tropical and subtropical Africa. Gut **38 Suppl 2:**S5-12.
6. **McMahon BJ, Alward WL, Hall DB, Heyward WL, Bender TR, Francis DP, Maynard JE.** 1985. Acute hepatitis B virus infection: relation of age to the clinical expression of disease and subsequent development of the carrier state. Journal of Infectious Diseases **151:**599-603.
7. **Ott JJ, Stevens Ga, Groeger J, Wiersma ST.** 2012. Global epidemiology of hepatitis B virus infection: new estimates of age-specific HBsAg seroprevalence and endemicity. Vaccine **30:**2212-2219.
8. **Parkin DM, Pisani P, Ferlay J.** 1999. Global cancer statistics. CA: A Cancer Journal for Clinicians **49:**33-64.
9. **Davidson M, Krugman S.** 1986. Recombinant yeast hepatitis B vaccine compared with plasma-derived vaccine: immunogenicity and effect of a booster dose. Journal of Infection **13 Suppl A:**31-38.
10. **McAleer WJ, Buynak EB, Maigetter RZ, Wampler DE, Miller WJ, Hilleman MR.** 1984. Human hepatitis B vaccine from recombinant yeast. Nature **307:**178-180.
11. **Prince AM.** 1982. Hepatitis B virus vaccine: a current appraisal of human plasma-derived vaccines. Annals of Clinical Research **14:**225-235.
12. **Stephenne J.** 1990. Development and production aspects of a recombinant yeast-derived hepatitis B vaccine. Vaccine **8 Suppl:**S69-73; discussion S79-80.
13. **Ayoub WS, Keeffe EB.** 2011. Review article: current antiviral therapy of chronic hepatitis B. Alimentary Pharmacology & Therapeutics **34:**1145-1158.
14. **Beck J, Nassal M.** 2007. Hepatitis B virus replication. World Journal of Gastroenterology **13:**48-64.
15. **Bloom K, Ely A, Mussolino C, Cathomen T, Arbuthnot P.** 2013. Inactivation of hepatitis B virus replication in cultured cells and in vivo with engineered transcription activator-like effector nucleases. Molecular Therapy **21:**1889-1897.
16. **San Filippo J, Sung P, Klein H.** 2008. Mechanism of eukaryotic homologous recombination. Annual Review of Biochemistry **77:**229-257.
17. **Blum HE, Gerok W, Vyas GN.** 1989. The molecular biology of hepatitis B virus. Trends in Genetics **5:**154-158.
18. **Baumert TF, Meredith L, Ni Y, Felmlee DJ, McKeating JA, Urban S.** 2014. Entry of hepatitis B and C viruses - recent progress and future impact. Current Opinion in Virology **4:**58-65.
19. **Taylor JM.** 2013. Virus entry mediated by hepatitis B virus envelope proteins. World Journal of Gastroenterology **19:**6730-6734.

20. **Schulze A, Gripon P, Urban S.** 2007. Hepatitis B virus infection initiates with a large surface protein-dependent binding to heparan sulfate proteoglycans. Hepatology **46:**1759-1768.
21. **Tuttleman JS, Pourcel C, Summers J.** 1986. Formation of the pool of covalently closed circular viral DNA in hepadnavirus-infected cells. Cell **47:**451-460.
22. **Yan H, Zhong G, Xu G, He W, Jing Z, Gao Z, Huang Y, Qi Y, Peng B, Wang H, Fu L, Song M, Chen P, Gao W, Ren B, Sun Y, Cai T, Feng X, Sui J, Li W.** 2012. Sodium taurocholate cotransporting polypeptide is a functional receptor for human hepatitis B and D virus. eLife **1:**e00049-e00049.
23. **Kann M, Schmitz A, Rabe B.** 2007. Intracellular transport of hepatitis B virus. World Journal of Gastroenterology **13:**39-47.
24. **Lutgehetmann M, Volz T, Köpke A, Broja T, Tigges E, Lohse AW, Fuchs E, Murray JM, Petersen J, Dandri M.** 2010. *In vivo* proliferation of hepadnavirus-infected hepatocytes induces loss of covalently closed circular DNA in mice. Hepatology **52:**16-24.
25. **Seeger C, Mason WS.** 2000. Hepatitis B virus biology. Microbiology and Molecular Biology Reviews **64:**51-68.
26. **Levrero M, Pollicino T, Petersen J, Belloni L, Raimondo G, Dandri M.** 2009. Control of cccDNA function in hepatitis B virus infection. Journal of Hepatology **51:**581-592.
27. **Pollicino T, Belloni L, Raffa G, Pediconi N, Squadrito G, Raimondo G, Levrero M.** 2006. Hepatitis B virus replication is regulated by the acetylation status of hepatitis B virus cccDNA-bound H3 and H4 histones. Gastroenterology **130:**823-837.
28. **Hu K-Q.** 2002. Occult hepatitis B virus infection and its clinical implications. Journal of Viral Hepatitis **9:**243-257.
29. **Mulrooney-Cousins PM, Michalak TI.** 2007. Persistent occult hepatitis B virus infection: experimental findings and clinical implications. World Journal of Gastroenterology **13:**5682-5686.
30. **Raimondo G, Pollicino T, Cacciola I, Squadrito G.** 2007. Occult hepatitis B virus infection. Journal of Hepatology **46:**160-170.
31. **Moolla N, Kew M, Arbuthnot P.** 2002. Regulatory elements of hepatitis B virus transcription. Journal of Viral Hepatitis **9:**323-331.
32. **Nassal M.** 2008. Hepatitis B viruses: reverse transcription a different way. Virus Research **134:**235-249.
33. **Karimi K, Blois SM, Arck PC.** 2008. The upside of natural killers. Nature Medicine **14:**1184-1185.
34. **Martín-Fontecha A, Thomsen LL, Brett S, Gerard C, Lipp M, Lanzavecchia A, Sallusto F.** 2004. Induced recruitment of NK cells to lymph nodes provides IFN-gamma for T(H)1 priming. Nature Immunology **5:**1260-1265.
35. **Jegaskanda S, Ahn SH, Skinner N, Thompson AJ, Ngyuen T, Holmes J, De Rose R, Navis M, Winnall WR, Kramski M, Bernardi G, Bayliss J, Colledge D, Sozzi V, Visvanathan K, Locarnini SA, Kent SJ, Revill PA.** 2014. Downregulation of interleukin-18-mediated cell signaling and interferon gamma expression by the hepatitis B virus e antigen. Journal of Virology **88:**10412-10420.
36. **Oliviero B, Varchetta S, Paudice E, Michelone G, Zaramella M, Mavilio D, De Filippi F, Bruno S, Mondelli MU.** 2009. Natural killer cell functional dichotomy in chronic hepatitis B and chronic hepatitis C virus infections. Gastroenterology **137:**1151-1160.

37. **Summers J, Mason WS.** 1982. Replication of the genome of a hepatitis B--like virus by reverse transcription of an RNA intermediate. Cell **29:**403-415.
38. **Will H, Cattaneo R, Koch H-G, Darai G, Schaller H, Schellekens Hu, van Eerd PMCA, Deinhardt F.** 1982. Cloned HBV DNA causes hepatitis in chimpanzees. Nature **299:**740-742.
39. **Hirschman S, Vernace S, Schaffner F.** 1971. DNA polymerase in preparations containing Australia antigen. Lancet **297:**1099-1103.
40. **Robinson WS, Clayton DA, Greenman RL.** 1974. DNA of a human hepatitis B virus candidate. Journal of Virology **14:**384-391.
41. **Feitelson MA, Duan LX.** 1997. Hepatitis B virus X antigen in the pathogenesis of chronic infections and the development of hepatocellular carcinoma. American Journal of Pathology **150:**1141-1157.
42. **Lian Z, Liu J, Li L, Li X, Satiroglu Tutan NL, Clayton M, Wu M-C, Wang H-Y, Arbuthnot P, Kew M, Feitelson MA.** 2003. Upregulated expression of a unique gene by hepatitis B X antigen promotes hepatocellular growth and tumorigenesis. Neoplasia **5:**229-244.
43. **Lucifora J, Arzberger S, Durantel D, Belloni L, Strubin M, Levrero M, Zoulim F, Hantz O, Protzer U.** 2011. Hepatitis B virus X protein is essential to initiate and maintain virus replication after infection. Journal of Hepatology **55:**996-1003.
44. **Gong D-Y, Chen E-Q, Huang F-J, Leng X-H, Cheng X, Tang H.** 2013. Role and functional domain of hepatitis B virus X protein in regulating HBV transcription and replication *in vitro* and *in vivo*. Viruses **5:**1261-1271.
45. **Chu C-J, Lok ASF.** 2002. Clinical significance of hepatitis B virus genotypes. Hepatology **35:**1274-1276.
46. **Schaefer S.** 2007. Hepatitis B virus taxonomy and hepatitis B virus genotypes. World Journal of Gastroenterology **13:**14-21.
47. **Tatematsu K, Tanaka Y, Kurbanov F, Sugauchi F, Mano S, Maeshiro T, Nakayoshi T, Wakuta M, Miyakawa Y, Mizokami M.** 2009. A genetic variant of hepatitis B virus divergent from known human and ape genotypes isolated from a Japanese patient and provisionally assigned to new genotype J. Journal of Virology **83:**10538-10547.
48. **Yu H, Yuan Q, Ge S-X, Wang H-Y, Zhang Y-L, Chen Q-R, Zhang J, Chen P-J, Xia N-S.** 2010. Molecular and phylogenetic analyses suggest an additional hepatitis B virus genotype "I". PloS ONE **5:**e9297-e9297.
49. **Lin C-L, Kao J-H.** 2011. The clinical implications of hepatitis B virus genotype: Recent advances. Journal of Gastroenterology and Hepatology **26 Suppl 1:**123-130.
50. **Krastev Z-A.** 2006. The "return" of hepatitis B. World Journal of Gastroenterology **12:**7081-7086.
51. **Lavanchy D.** 2004. Hepatitis B virus epidemiology, disease burden, treatment, and current and emerging prevention and control measures. Journal of Viral Hepatitis **11:**97-107.
52. **Lewin S, Walters T, Locarnini S.** 2002. Hepatitis B treatment: rational combination chemotherapy based on viral kinetic and animal model studies. Antiviral Research **55:**381-396.
53. **Malik AH, Lee WM.** 2000. Chronic hepatitis B virus infection: treatment strategies for the next millennium. Annals of Internal Medicine **132:**723-723.
54. **Pawlotsky J-M.** EASL Clinical Practice Guidelines: management of chronic hepatitis B. Journal of Hepatology **50(2):** 227-242.

55. **Hui C-K, Lau GKK.** 2005. Immune system and hepatitis B virus infection. Journal of Clinical Virology **34 Suppl 1:**S44-48.
56. **Karayiannis P.** 2003. Hepatitis B virus: old, new and future approaches to antiviral treatment. Journal of Antimicrobial Chemotherapy **51:**761-785.
57. **Chisari FV.** 1997. Cytotoxic T cells and viral hepatitis. Journal of Clinical Investigation **99:**1472-1477.
58. **Maini MK, Casorati G, Dellabona P, Wack A, Beverley PCL.** 1999. T-cell clonality in immune responses. Immunology Today **20:**262-266.
59. **Ganem D, Prince AM.** 2004. Hepatitis B virus infection - natural history and clinical consequences. New England Journal of Medicine **350:**1118-1129.
60. **Spearman CWN, Sonderup MW, Botha JF, van der Merwe SW, Song E, Kassianides C, Newton KA, Hairwadzi HN.** South African guideline for the management of chronic hepatitis B: 2013. South African Medical Journal **103:**335-349.
61. **Guidotti LG, Ishikawa T, Hobbs MV, Matzke B, Schreiber R, Chisari FV.** 1996. Intracellular inactivation of the hepatitis B virus by cytotoxic T lymphocytes. Immunity **4:**25-36.
62. **Webster GJ, Reignat S, Maini MK, Whalley SA, Ogg GS, King A, Brown D, Amlot PL, Williams R, Vergani D, Dusheiko GM, Bertoletti A.** 2000. Incubation phase of acute hepatitis B in man: dynamic of cellular immune mechanisms. Hepatology **32:**1117-1124.
63. **Hilleman MR.** 2003. Critical overview and outlook: pathogenesis, prevention, and treatment of hepatitis and hepatocarcinoma caused by hepatitis B virus. Vaccine **21:**4626-4649.
64. **Lai CL, Ratziu V, Yuen M-F, Poynard T.** 2003. Viral hepatitis B. Lancet **362:**2089-2094.
65. **Wong DK, Cheung AM, O'Rourke K, Naylor CD, Detsky AS, Heathcote J.** 1993. Effect of alpha-interferon treatment in patients with hepatitis B e antigen-positive chronic hepatitis B. A meta-analysis. Annals of Internal Medicine **119:**312-323.
66. **Carreño V, Marcellin P, Hadziyannis S, Salmerón J, Diago M, Kitis GE, Vafiadis I, Schalm SW, Zahm F, Manzarbeitia F, Jiménez FJ, Quiroga JA.** 1999. Retreatment of chronic hepatitis B e antigen-positive patients with recombinant interferon alfa-2a. The European Concerted Action on Viral Hepatitis (EUROHEP). Hepatology (Baltimore, Md.) **30:**277-282.
67. **van Zonneveld M, Honkoop P, Hansen BE, Niesters HGM, Darwish Murad S, de Man RA, Schalm SW, Janssen HLA.** 2004. Long-term follow-up of alpha-interferon treatment of patients with chronic hepatitis B. Hepatology **39:**804-810.
68. **Brunetto MR, Oliveri F, Coco B, Leandro G, Colombatto P, Gorin JM, Bonino F.** 2002. Outcome of anti-HBe positive chronic hepatitis B in alpha-interferon treated and untreated patients: a long term cohort study. Journal of Hepatology **36:**263-270.
69. **Papatheodoridis GV, Manesis E, Hadziyannis SJ.** 2001. The long-term outcome of interferon-alpha treated and untreated patients with HBeAg-negative chronic hepatitis B. Journal of Hepatology **34:**306-313.
70. **Lau GKK, Piratvisuth T, Luo KX, Marcellin P, Thongsawat S, Cooksley G, Gane E, Fried MW, Chow WC, Paik SW, Chang WY, Berg T, Flisiak R, McCloud P, Pluck N.** 2005. Peginterferon Alfa-2a, lamivudine, and the combination for HBeAg-positive chronic hepatitis B. New England Journal of Medicine **352:**2682-2695.

71. **Dienstag JL, Schiff ER, Wright TL, Perrillo RP, Hann HW, Goodman Z, Crowther L, Condreay LD, Woessner M, Rubin M, Brown NA.** 1999. Lamivudine as initial treatment for chronic hepatitis B in the United States. New England Journal of Medicine **341:**1256-1263.
72. **Yuen M-F, Seto W-K, Chow DH-F, Tsui K, Wong DK-H, Ngai VW-S, Wong BC-Y, Fung J, Yuen JC-H, Lai C-L.** 2007. Long-term lamivudine therapy reduces the risk of long-term complications of chronic hepatitis B infection even in patients without advanced disease. Antiviral Therapy **12:**1295-1303.
73. **Fischer KP, Gutfreund KS, Tyrrell DL.** 2001. Lamivudine resistance in hepatitis B: mechanisms and clinical implications. Drug resistance updates : reviews and commentaries in antimicrobial and anticancer chemotherapy **4:**118-128.
74. **Lee JM, Kim HJ, Park JY, Lee CK, Kim DY, Kim JK, Lee HW, Paik YH, Lee KS, Han KH, Chon CY, Hong SP, Nguyen T, Ahn SH.** 2009. Rescue monotherapy in lamivudine-resistant hepatitis B e antigen-positive chronic hepatitis B: Adefovir versus entecavir. Antiviral Therapy **14:**705-712.
75. **Low E, Cox A, Atkins M, Nelson M.** 2009. Telbivudine has activity against HIV-1. AIDS **23:**546-547.
76. **Arbuthnot P, Carmona S, Ely A.** 2005. Exploiting the RNA interference pathway to counter hepatitis B virus replication. Liver International **25:**9-15.
77. **Schiffer JT, Aubert M, Weber ND, Mintzer E, Stone D, Jerome KR.** 2012. Targeted DNA mutagenesis for the cure of chronic viral infections. Journal of Virology **86:**8920-8936.
78. **Urnov FD, Rebar EJ, Holmes MC, Zhang HS, Gregory PD.** 2010. Genome editing with engineered zinc finger nucleases. Nature Reviews: Genetics **11:**636-646.
79. **Gaj T, Gersbach CA, Barbas CF.** 2013. ZFN, TALEN, and CRISPR/Cas-based methods for genome engineering. Trends in Biotechnology **31:**397-405.
80. **Nimjee SM, Rusconi CP, Sullenger BA.** 2005. Aptamers: an emerging class of therapeutics. Annual Review of Medicine **56:**555-583.
81. **Sarver N, Cantin E, Chang P, Zaia J, Ladne P, Stephens D, Rossi J.** 1990. Ribozymes as potential anti-HIV-1 therapeutic agents. Science **247:**1222-1225.
82. **Schreier H.** 1994. The new frontier: gene and oligonucleotide therapy. Pharmaceutica Acta Helvetiae **68:**145-159.
83. **Uprichard SL.** 2005. The therapeutic potential of RNA interference. FEBS letters **579:**5996-6007.
84. **Wagner RW, Flanagan WM.** 1997. Antisense technology and prospects for therapy of viral infections and cancer. Molecular Medicine Today **3:**31-38.
85. **Mussolino C, Morbitzer R, Lütge F, Dannemann N, Lahaye T, Cathomen T.** 2011. A novel TALE nuclease scaffold enables high genome editing activity in combination with low toxicity. Nucleic Acids Research **39:**9283-9293.
86. **Morbitzer R, Elsaesser J, Hausner J, Lahaye T.** 2011. Assembly of custom TALE-type DNA binding domains by modular cloning. Nucleic Acids Research **39:**5790-5799.
87. **Sander JD, Joung JK.** 2014. CRISPR-Cas systems for editing, regulating and targeting genomes. Nature Biotechnology **32:**347-355.
88. **Jacquier A, Dujon B.** 1985. An intron-encoded protein is active in a gene conversion process that spreads an intron into a mitochondrial gene. Cell **41:**383-394.
89. **Thierry A, Dujon B.** 1992. Nested chromosomal fragmentation in yeast using the meganuclease I- Sce I: a new method for physical mapping of eukaryotic genomes. Nucleic Acids Research **20:**5625-5631.

90. **Chevalier BS, Kortemme T, Chadsey MS, Baker D, Monnat RJ, Stoddard BL.** 2002. Design, activity, and structure of a highly specific artificial endonuclease. Molecular Cell **10:**895-905.
91. **Grizot S, Epinat J-C, Thomas S, Duclert A, Rolland S, Pâques F, Duchateau P.** 2010. Generation of redesigned homing endonucleases comprising DNA-binding domains derived from two different scaffolds. Nucleic Acids Research **38:**2006-2018.
92. **Rosen LE, Morrison HA, Masri S, Brown MJ, Springstubb B, Sussman D, Stoddard BL, Seligman LM.** 2006. Homing endonuclease I-CreI derivatives with novel DNA target specificities. Nucleic Acids Research **34:**4791-4800.
93. **Silva G, Poirot L, Galetto R, Smith J, Montoya G, Duchateau P, Pâques F.** 2011. Meganucleases and other tools for targeted genome engineering: perspectives and challenges for gene therapy. Current Gene Therapy **11:**11-27.
94. **Ran FA, Hsu PD, Lin C-Y, Gootenberg JS, Konermann S, Trevino AE, Scott DA, Inoue A, Matoba S, Zhang Y, Zhang F.** 2013. Double nicking by RNA-guided CRISPR Cas9 for enhanced genome editing specificity. Cell **154:**1380-1389.
95. **Wiedenheft B, Sternberg SH, Doudna JA.** 2012. RNA-guided genetic silencing systems in bacteria and archaea. Nature **482:**331-338.
96. **Cho SW, Kim S, Kim JM, Kim J-S.** 2013. Targeted genome engineering in human cells with the Cas9 RNA-guided endonuclease. Nature Biotechnology **31:**230-232.
97. **Jinek M, East A, Cheng A, Lin S, Ma E, Doudna J.** 2013. RNA-programmed genome editing in human cells. eLife **2:**e00471-e00471.
98. **Qi LS, Larson MH, Gilbert LA, Doudna JA, Weissman JS, Arkin AP, Lim WA.** 2013. Repurposing CRISPR as an RNA-guided platform for sequence-specific control of gene expression. Cell **152:**1173-1183.
99. **Wei C, Liu J, Yu Z, Zhang B, Gao G, Jiao R.** 2013. TALEN or Cas9 - rapid, efficient and specific choices for genome modifications. Journal of Genetics and Genomics **40:**281-289.
100. **Moore FE, Reyon D, Sander JD, Martinez Sa, Blackburn JS, Khayter C, Ramirez CL, Joung JK, Langenau DM.** 2012. Improved somatic mutagenesis in Zebrafish using transcription activator-like effector nucleases (TALENs). PLoS ONE **7:**1-9.
101. **Schierling B, Dannemann N, Gabsalilow L, Wende W, Cathomen T, Pingoud A.** 2012. A novel zinc-finger nuclease platform with a sequence-specific cleavage module. Nucleic Acids Research **40:**2623-2638.
102. **Anguela XM, Sharma R, Doyon Y, Miller JC, Li H, Haurigot V, Rohde ME, Wong SY, Davidson RJ, Zhou S, Gregory PD, Holmes MC, High KA.** 2013. Robust ZFN-mediated genome editing in adult hemophilic mice. Blood **122:**3283-3287.
103. **Beane JD, Lee GK, Zheng Z, Gandhi N, Abate-Daga D, Bharathan M, Black M, Mendel M, Yu Z, Kassim SH, Chandran S, Giedlin M, Ando D, Rebar E, Reik A, Holmes M, Gregory PD, Restifo NP, Rosenberg SA, Morgan RA, Feldman SA.** 2014. Clinical scale zinc finger nuclease (ZFN)-driven gene-editing of PD-1 in tumor infiltrating lymphocytes (TIL) for the potential treatment of metastatic melanoma. Journal for ImmunoTherapy of Cancer **2:**P2-P2.
104. **Foley JE, Yeh J-RJ, Maeder ML, Reyon D, Sander JD, Peterson RT, Joung JK.** 2009. Rapid mutation of endogenous zebrafish genes using zinc finger nucleases made by Oligomerized Pool ENgineering (OPEN). PloS ONE **4:**e4348-e4348.
105. **Scholze H, Boch J.** 2011. TAL effectors are remote controls for gene activation. Current Opinion in Microbiology **14:**47-53.

106. **Sealover NR, Davis AM, Brooks JK, George HJ, Kayser KJ, Lin N.** 2013. Engineering Chinese hamster ovary (CHO) cells for producing recombinant proteins with simple glycoforms by zinc-finger nuclease (ZFN)-mediated gene knockout of mannosyl (alpha-1,3-)-glycoprotein beta-1,2-N-acetylglucosaminyltransferase (Mgat1). Journal of Biotechnology **167:**24-32.
107. **Torikai H, Reik A, Liu P-Q, Zhou Y, Zhang L, Maiti S, Huls H, Miller JC, Kebriaei P, Rabinovitch B, Lee DA, Champlin RE, Bonini C, Naldini L, Rebar EJ, Gregory PD, Holmes MC, Cooper LJN.** 2012. A foundation for universal T-cell based immunotherapy: T cells engineered to express a CD19-specific chimeric-antigen-receptor and eliminate expression of endogenous TCR. Blood **119:**5697-5705.
108. **Yi G, Choi JG, Bharaj P, Abraham S, Dang Y, Kafri T, Alozie O, Manjunath MN, Shankar P.** 2014. CCR5 Gene Editing of Resting CD4(+) T Cells by Transient ZFN Expression From HIV Envelope Pseudotyped Nonintegrating Lentivirus Confers HIV-1 Resistance in Humanized Mice. Molecular therapy. Nucleic Acids **3:**e198-e198.
109. **Zhu C, Smith T, McNulty J, Rayla AL, Lakshmanan A, Siekmann AF, Buffardi M, Meng X, Shin J, Padmanabhan A, Cifuentes D, Giraldez AJ, Look AT, Epstein JA, Lawson ND, Wolfe SA.** 2011. Evaluation and application of modularly assembled zinc-finger nucleases in zebrafish. Development **138:**4555-4564.
110. **Bogdanove aJ, Voytas DF.** 2011. TAL Effectors: customizable proteins for DNA targeting. Science **333:**1843-1846.
111. **Joung JK, Sander JD.** 2013. TALENs: a widely applicable technology for targeted genome editing. Nature Reviews: Molecular Cell Biology **14:**49-55.
112. **Ramirez CL, Foley JE, Wright DA, Müller-Lerch F, Rahman SH, Cornu TI, Winfrey RJ, Sander JD, Fu F, Townsend JA, Cathomen T, Voytas DF, Joung JK.** 2008. Unexpected failure rates for modular assembly of engineered zinc fingers. Nature Methods **5:**374-375.
113. **Sander JD, Cade L, Khayter C, Reyon D, Peterson RT, Joung JK, Yeh J-RJ.** 2011. Targeted gene disruption in somatic zebrafish cells using engineered TALENs. Nature Biotechnology **29:**697-698.
114. **Wolfe SA, Nekludova L, Pabo CO.** 2000. DNA recognition by Cys2His2 zinc finger proteins. Annual Review of Biophysics and Biomolecular Structure **29:**183-212.
115. **Boch J, Scholze H, Schornack S, Landgraf A, Hahn S, Kay S, Lahaye T, Nickstadt A, Bonas U.** 2009. Breaking the code of DNA binding specificity of TAL-type III effectors. Science **326:**1509-1512.
116. **Moscou MJ, Bogdanove AJ.** 2009. A simple cipher governs DNA recognition by TAL effectors. Science **326:**1501-1501.
117. **Bogdanove AJ, Schornack S, Lahaye T.** 2010. TAL effectors: finding plant genes for disease and defense. Current Opinion in Plant Biology **13:**394-401.
118. **Kay S, Hahn S, Marois E, Hause G, Bonas U.** 2007. A bacterial effector acts as a plant transcription factor and induces a cell size regulator. Science **318:**648-651.
119. **Boch J, Bonas U.** 2010. Xanthomonas AvrBs3 family-type III effectors: discovery and function. Annual Review of Phytopathology **48:**419-436.
120. **Christian ML, Demorest ZL, Starker CG, Osborn MJ, Nyquist MD, Zhang Y, Carlson DF, Bradley P, Bogdanove AJ, Voytas DF.** 2012. Targeting G with TAL effectors: a comparison of activities of TALENs constructed with NN and NK repeat variable di-residues. PloS ONE **7:**e45383-e45383.
121. **Bultmann S, Morbitzer R, Schmidt CS, Thanisch K, Spada F, Elsaesser J, Lahaye T, Leonhardt H.** 2012. Targeted transcriptional activation of silent *oct4*

pluripotency gene by combining designer TALEs and inhibition of epigenetic modifiers. Nucleic Acids Research **40:**5368-5377.

122. **Valton J, Dupuy A, Daboussi F, Thomas S, Maréchal A, Macmaster R, Melliand K, Juillerat A, Duchateau P.** 2012. Overcoming transcription activator-like effector (TALE) DNA binding domain sensitivity to cytosine methylation. Journal of Biological Chemistry **287:**38427-38432.
123. **Streubel J, Blücher C, Landgraf A, Boch J.** 2012. TAL effector RVD specificities and efficiencies. Nature Biotechnology **30:**593-595.
124. **Miller JC, Tan S, Qiao G, Barlow KA, Wang J, Xia DF, Meng X, Paschon DE, Leung E, Hinkley SJ, Dulay GP, Hua KL, Ankoudinova I, Cost GJ, Urnov FD, Zhang HS, Holmes MC, Zhang L, Gregory PD, Rebar EJ.** 2011. A TALE nuclease architecture for efficient genome editing. Nature Biotechnology **29:**143-148.
125. **Zhang F, Cong L, Lodato S, Kosuri S, Church GM, Arlotta P.** 2011. Efficient construction of sequence-specific TAL effectors for modulating mammalian transcription. Nature Biotechnology **29:**149-153.
126. **Schmid-Burgk JL, Schmidt T, Kaiser V, Höning K, Hornung V.** 2013. A ligation-independent cloning technique for high-throughput assembly of transcription activator–like effector genes. Nature Biotechnology **31:**76-81.
127. **Li T, Huang S, Jiang WZ, Wright D, Spalding MH, Weeks DP, Yang B.** 2011. TAL nucleases (TALNs): hybrid proteins composed of TAL effectors and FokI DNA-cleavage domain. Nucleic Acids Research **39:**359-372.
128. **Hockemeyer D, Wang H, Kiani S, Lai CS, Gao Q, Cassady JP, Cost GJ, Zhang L, Santiago Y, Miller JC, Zeitler B, Cherone JM, Meng X, Hinkley SJ, Rebar EJ, Gregory PD, Urnov FD, Jaenisch R.** 2011. Genetic engineering of human pluripotent cells using TALE nucleases. Nature Biotechnology **29:**731-734.
129. **Ma N, Liao B, Zhang H, Wang L, Shan Y, Xue Y, Huang K, Chen S, Zhou X, Chen Y, Pei D, Pan G.** 2013. Transcription activator-like effector nuclease (TALEN)-mediated gene correction in integration-free β-thalassemia induced pluripotent stem cells. Journal of Biological Chemistry **288:**34671-34679.
130. **Ménoret S, Tesson L, Rémy S, Usal C, Thépenier V, Thinard R, Ouisse L-H, De Cian A, Giovannangeli C, Concordet J-P, Anegon I.** 2014. Gene targeting in rats using transcription activator-like effector nucleases. Methods **69:**102-107.
131. **Sommer D, Peters A, Wirtz T, Mai M, Ackermann J, Thabet Y, Schmidt J, Weighardt H, Wunderlich FT, Degen J, Schultze JL, Beyer M.** 2014. Efficient genome engineering by targeted homologous recombination in mouse embryos using transcription activator-like effector nucleases. Nature Communications **5:**3045-3045.
132. **Reyon D, Tsai SQ, Khayter C, Foden JA, Sander JD, Joung JK.** 2012. FLASH assembly of TALENs for high-throughput genome editing. Nature Biotechnology **30:**460-465.
133. **Huang P, Xiao A, Zhou M, Zhu Z, Lin S, Zhang B.** 2011. Heritable gene targeting in zebrafish using customized TALENs. Nature Biotechnology **29:**699-700.
134. **Ramalingam S, Annaluru N, Kandavelou K, Chandrasegaran S.** 2014. TALEN-mediated generation and genetic correction of disease-specific human induced pluripotent stem cells. Current Gene Therapy **14(6):**461-472.
135. **Smith C, Gore A, Yan W, Abalde-Atristain L, Li Z, He C, Wang Y, Brodsky RA, Zhang K, Cheng L, Ye Z.** 2014. Whole-genome sequencing analysis reveals high specificity of CRISPR/Cas9 and TALEN-based genome editing in human iPSCs. Cell Stem Cell **15:**12-13.

136. **Suzuki K, Yu C, Qu J, Li M, Yao X, Yuan T, Goebl A, Tang S, Ren R, Aizawa E, Zhang F, Xu X, Soligalla RD, Chen F, Kim J, Kim NY, Liao H-K, Benner C, Esteban CR, Jin Y, Liu G-H, Li Y, Izpisua Belmonte JC.** 2014. Targeted gene correction minimally impacts whole-genome mutational load in human-disease-specific induced pluripotent stem cell clones. Cell Stem Cell **15:**31-36.
137. **Veres A, Gosis BS, Ding Q, Collins R, Ragavendran A, Brand H, Erdin S, Talkowski ME, Musunuru K.** 2014. Low incidence of off-target mutations in individual CRISPR-Cas9 and TALEN targeted human stem cell clones detected by whole-genome sequencing. Cell Stem Cell **15:**27-30.
138. **Bee L, Fabris S, Cherubini R, Mognato M, Celotti L.** 2013. The efficiency of homologous recombination and non-homologous end joining systems in repairing double-strand breaks during cell cycle progression. PloS ONE **8:**e69061-e69061.
139. **Haber JE.** 2000. Partners and pathways: repairing a double-strand break. Trends in Genetics **16:**259-264.
140. **Sonoda E, Hochegger H, Saberi A, Taniguchi Y, Takeda S.** 2006. Differential usage of non-homologous end-joining and homologous recombination in double strand break repair. DNA Repair **5:**1021-1029.
141. **Handel E-M, Cathomen T.** 2011. Zinc-Finger Nuclease based genome surgery: it's all about specificity. Current Gene Therapy **11:**28-37.
142. **Bajinskis A, Natarajan AT, Erixon K, Harms-Ringdahl M.** 2013. DNA double strand breaks induced by the indirect effect of radiation are more efficiently repaired by non-homologous end joining compared to homologous recombination repair. Mutation Research **756:**21-29.
143. **Helleday T.** 2003. Pathways for mitotic homologous recombination in mammalian cells. Mutation Research/Fundamental and Molecular Mechanisms of Mutagenesis **532:**103-115.
144. **Paques F, Haber JE.** 1999. Multiple Pathways of Recombination Induced by Double-Strand Breaks in Saccharomyces cerevisiae. Microbiology and Molecular Biology Reviews **63:**349-404.
145. **Roth DB, Wilson JH.** 1986. Nonhomologous recombination in mammalian cells: role for short sequence homologies in the joining reaction. Molecular and Cellular Biology **6:**4295-4304.
146. **Takata M, Sasaki MS, Sonoda E, Morrison C, Hashimoto M, Utsumi H, Yamaguchi-Iwai Y, Shinohara A, Takeda S.** 1998. Homologous recombination and non-homologous end-joining pathways of DNA double-strand break repair have overlapping roles in the maintenance of chromosomal integrity in vertebrate cells. EMBO journal **17:**5497-5508.
147. **Lieber MR.** 2008. The mechanism of human nonhomologous DNA end joining. Journal of Biological Chemistry **283:**1-5.
148. **Nalbantoglu J, Miles C, Meuth M.** 1988. Insertion of unique and repetitive DNA fragments into the aprt locus of hamster cells. Journal of Molecular Biology **200:**449-459.
149. **Frankenberg-schwager M, Gebauer A, Koppe C, Wolf H, Pralle E, Frankenberg D.** 2009. Single-strand annealing, conservative homologous recombination, nonhomologous DNA end joining , and the cell cycle-dependent repair of DNA double-strand breaks induced by sparsely or densely ionizing radiation. Radiation Research **171:**265-273.

150. **Porteus M.** 2007. Using homologous recombination to manipulate the genome of human somatic cells. Biotechnology and Genetic Engineering Reviews **24:**195-212.
151. **Shrivastav M, De Haro LP, Nickoloff JA.** 2008. Regulation of DNA double-strand break repair pathway choice. Cell Research **18:**134-147.
152. **Fishman-Lobell J, Rudin N, Haber JE.** 1992. Two alternative pathways of double-strand break repair that are kinetically separable and independently modulated. Molecular and Cellular Biology **12:**1292-1303.
153. **Maryon E, Carroll D.** 1991. Characterization of recombination intermediates from DNA injected into Xenopus laevis oocytes: evidence for a nonconservative mechanism of homologous recombination. Molecular and Cellular Biology **11:**3278-3287.
154. **Hackett JA, Greider CW.** 2003. End resection initiates genomic instability in the absence of telomerase. Molecular and Cellular Biology **23:**8450-8461.
155. **McEachern MJ, Haber JE.** 2006. Break-induced replication and recombinational telomere elongation in yeast. Annual Review of Biochemistry **75:**111-135.
156. **Heyer W-D, Ehmsen KT, Liu J.** 2010. Regulation of homologous recombination in eukaryotes. Annual Review of Genetics **44:**113-139.
157. **Bianco PR, Tracy RB, Kowalczykowski SC.** 1998. DNA strand exchange proteins: a biochemical and physical comparison. Frontiers in Bioscience **3:**D570-603.
158. **Sung P, Klein H.** 2006. Mechanism of homologous recombination: mediators and helicases take on regulatory functions. Nature Reviews: Molecular Cell Biology **7:**739-750.
159. **Szostak JW, Orr-Weaver TL, Rothstein RJ, Stahl FW.** 1983. The double-strand-break repair model for recombination. Cell **33:**25-35.
160. **Shinohara A, Ogawa T.** 1995. Homologous recombination and the roles of double-strand breaks. Trends in Biochemical Sciences **20(10):**387-391.
161. **Ferguson DO, Holloman WK.** 1996. Recombinational repair of gaps in DNA is asymmetric in Ustilago maydis and can be explained by a migrating D-loop model. Proceedings of the National Academy of Sciences **93:**5419-5424.
162. **Wu L, Hickson ID.** 2003. The Bloom's syndrome helicase suppresses crossing over during homologous recombination. Nature **426:**870-874.
163. **Ramirez CL, Certo MT, Mussolino C, Goodwin MJ, Cradick TJ, McCaffrey AP, Cathomen T, Scharenberg AM, Joung JK.** 2012. Engineered zinc finger nickases induce homology-directed repair with reduced mutagenic effects. Nucleic Acids Research **40:**5560-5568.
164. **Wang J, Friedman G, Doyon Y, Wang NS, Li CJ, Miller JC, Hua KL, Yan JJ, Babiarz JE, Gregory PD, Holmes MC.** 2012. Targeted gene addition to a predetermined site in the human genome using a ZFN-based nicking enzyme. Genome Research **22:**1316-1326.
165. **Bedell VM, Wang Y, Campbell JM, Poshusta TL, Starker CG, Krug Ii RG, Tan W, Penheiter SG, Ma AC, Leung AYH, Fahrenkrug SC, Carlson DF, Voytas DF, Clark KJ, Essner JJ, Ekker SC.** 2012. *In vivo* genome editing using a high-efficiency TALEN system. Nature **491:**114-118.
166. **Osborn MJ, Starker CG, McElroy AN, Webber BR, Riddle MJ, Xia L, DeFeo AP, Gabriel R, Schmidt M, von Kalle C, Carlson DF, Maeder ML, Joung JK, Wagner JE, Voytas DF, Blazar BR, Tolar J.** 2013. TALEN-based gene correction for epidermolysis bullosa. Molecular Therapy **21:**1151-1159.
167. **Wang H, Hu Y-C, Markoulaki S, Welstead GG, Cheng AW, Shivalila CS, Pyntikova T, Dadon DB, Voytas DF, Bogdanove AJ, Page DC, Jaenisch R.** 2013.

TALEN-mediated editing of the mouse Y chromosome. Nature Biotechnology **31:**530-532.

168. **Arbuthnot P, Ely A, Weinberg MS.** 2009. Hepatic delivery of RNA interference activators for therapeutic application. Current Gene Therapy **9:**91-103.
169. **Ely A, Naidoo T, Arbuthnot P.** 2009. Efficient silencing of gene expression with modular trimeric Pol II expression cassettes comprising microRNA shuttles. Nucleic Acids Research **37(13):**e91.
170. **Hammond SM, Caudy Aa, Hannon GJ.** 2001. Post-transcriptional gene silencing by double- stranded RNA. Genetics **2:**110-119.
171. **Morlando M, Ballarino M, Gromak N, Pagano F, Bozzoni I, Proudfoot NJ.** 2008. Primary microRNA transcripts are processed co-transcriptionally. Nature Structural and Molecular Biology **15:**902-909.
172. **Yi R, Qin Y, Macara IG, Cullen BR.** 2003. Exportin-5 mediates the nuclear export of pre-microRNAs and short hairpin RNAs. Genes and Development **17:**3011-3016.
173. **Filipowicz W.** 2005. RNAi: The nuts and bolts of the RISC machine. Cell **122:**17-20.
174. **Chattopadhyay S, Ely A, Bloom K, Weinberg MS, Arbuthnot P.** 2009. Inhibition of hepatitis B virus replication with linear DNA sequences expressing antiviral micro-RNA shuttles. Biochemical and Biophysical Research Communications **389:**484-489.
175. **Ely A, Naidoo T, Mufamadi S, Crowther C, Arbuthnot P.** 2008. Expressed anti-HBV primary microRNA shuttles inhibit viral replication efficiently *in vitro* and *in vivo*. Molecular Therapy **16:**1105-1112.
176. **Zimmerman KA, Fischer KP, Joyce MA, Tyrrell DLJ.** 2008. Zinc finger proteins designed to specifically target duck hepatitis B virus covalently closed circular DNA inhibit viral transcription in tissue culture. Journal of Virology **82:**8013-8021.
177. **Chen J, Zhang W, Lin J, Wang F, Wu M, Chen C, Zheng Y, Peng X, Li J, Yuan Z.** 2014. An efficient antiviral strategy for targeting hepatitis B virus genome using transcription activator-like effector nucleases. Molecular Therapy **22:**303-311.
178. **Orlando SJ, Santiago Y, DeKelver RC, Freyvert Y, Boydston EA, Moehle EA, Choi VM, Gopalan SM, Lou JF, Li J, Miller JC, Holmes MC, Gregory PD, Urnov FD, Cost GJ.** 2010. Zinc-finger nuclease-driven targeted integration into mammalian genomes using donors with limited chromosomal homology. Nucleic Acids Research **38:**e152-e152.
179. **Hendel A, Kildebeck EJ, Fine EJ, Clark JT, Punjya N, Sebastiano V, Bao G, Porteus MH.** 2014. Quantifying genome-editing outcomes at endogenous loci with SMRT sequencing. Cell Reports **7:**293-305.
180. **Nassal M, Junker-Niepmann M, Schaller H.** 1990. Translational inactivation of RNA function: Discrimination against a subset of genomic transcripts during HBV nucleocapsid assembly. Cell **63:**1357-1363.
181. **Passman M, Weinberg M, Kew M, Arbuthnot P.** 2000. *In situ* demonstration of inhibitory effects of hammerhead ribozymes that are targeted to the hepatitis B X sequence in cultured cells. Biochemical and Biophysical Research Communications **268:**728-733.
182. **Vieira J, Messing J.** 1987. Recombinant DNA Part D. Elsevier **153:**3-11
183. **Sun D, Nassal M.** 2006. Stable HepG2- and Huh7-based human hepatoma cell lines for efficient regulated expression of infectious hepatitis B virus. Journal of Hepatology **45:**636-645.

184. **Vecchi C, Montosi G, Pietrangelo A.** 2010. Huh-7: A human "hemochromatotic" cell line. Hepatology **51:**654-659.
185. **Akinc A, Thomas M, Klibanov AM, Langer R.** 2005. Exploring polyethylenimine-mediated DNA transfection and the proton sponge hypothesis. Journal of Gene Medicine **7:**657-663.
186. **Boussif O, Lezoualc'h F, Zanta MA, Mergny MD, Scherman D, Demeneix B, Behr JP.** 1995. A versatile vector for gene and oligonucleotide transfer into cells in culture and in vivo: polyethylenimine. Proceedings of the National Academy of Sciences **92:**7297-7301.
187. **Altschul SF, Gish W, Miller W, Myers EW, Lipman DJ.** 1990. Basic local alignment search tool. Journal of Molecular Biology **215:**403-410.
188. **Ye J, McGinnis S, Madden TL.** 2006. BLAST: improvements for better sequence analysis. Nucleic Acids Research **34:**W6-W9.
189. **Merrihew RV, Marburger K, Pennington SL, Roth DB, Wilson JH.** 1996. High-frequency illegitimate integration of transfected DNA at preintegrated target sites in a mammalian genome. Molecular and Cellular Biology **16:**10-18.
190. **Smithies O, Gregg RG, Boggs SS, Koralewski MA, Kucherlapati RS.** 1985. Insertion of DNA sequences into the human chromosomal β-globin locus by homologous recombination. Nature **317:**230-234.
191. **Thomas KR, Capecchi MR.** 1987. Site-directed mutagenesis by gene targeting in mouse embryo-derived stem cells. Cell **51:**503-512.
192. **Thomas KR, Folger KR, Capecchi MR.** 1986. High frequency targeting of genes to specific sites in the mammalian genome. Cell **44:**419-428.
193. **Truong LN, Li Y, Shi LZ, Hwang PY-H, He J, Wang H, Razavian N, Berns MW, Wu X.** 2013. Microhomology-mediated End Joining and Homologous Recombination share the initial end resection step to repair DNA double-strand breaks in mammalian cells. Proceedings of the National Academy of Sciences **110:**7720-7725.
194. **Cento V, Mirabelli C, Dimonte S, Salpini R, Han Y, Trimoulet P, Bertoli A, Micheli V, Gubertini G, Cappiello G.** 2013. Overlapping structure of hepatitis B virus (HBV) genome and immune selection pressure are critical forces modulating HBV evolution. Journal of General Virology **94:**143-149.
195. **Jones SA, Clark DN, Cao F, Tavis JE, Hu J.** 2014. Comparative Analysis of Hepatitis B Virus Polymerase Sequences Required for Viral RNA Binding, RNA Packaging, and Protein Priming. Journal of Virology **88:**1564-1572.
196. **Boregowda RK, Adams C, Hu J.** 2012. TP-RT Domain Interactions of Duck Hepatitis B Virus Reverse Transcriptase in cis and in trans during Protein-Primed Initiation of DNA Synthesis In Vitro. Journal of Virology **86:**6522-6536.
197. **Shin Y-C, Park S, Ryu W-S.** 2011. A conserved arginine residue in the terminal protein domain of hepatitis B virus polymerase is critical for RNA pre-genome encapsidation. Journal of General Virology **92:**1809-1816.
198. **Cao F, Jones S, Li W, Cheng X, Hu Y, Hu J, Tavis JE.** 2014. Sequences in the terminal protein and reverse transcriptase domains of the hepatitis B virus polymerase contribute to RNA binding and encapsidation. Journal of Viral Hepatitis **21:**882-893.
199. **Thomas HR, Percival SM, Yoder BK, Parant JM.** 2014. High-throughput genome editing and phenotyping facilitated by high resolution melting curve analysis. PLoS ONE **9:**e114632.
200. **Nakade S, Tsubota T, Sakane Y, Kume S, Sakamoto N, Obara M, Daimon T, Sezutsu H, Yamamoto T, Sakuma T, Suzuki K-iT.** 2014. Microhomology-

mediated end-joining-dependent integration of donor DNA in cells and animals using TALENs and CRISPR/Cas9. Nature Communications **5**:1-8.

201. **Ahmed M, Wang F, Levin A, Le C, Eltayebi Y, Houghton M, Tyrrell L, Barakat K.** Targeting the Achilles heel of the hepatitis B virus: a review of current treatments against covalently closed circular DNA. Drug Discovery Today.
202. **Ivacik D, Ely A, Ferry N, Arbuthnot P.** 2015. Sustained inhibition of hepatitis B virus replication in vivo using RNAi-activating lentiviruses. Gene Therapy **22:**163-171.
203. **Li G, Jiang G, Lu J, Chen S, Cui L, Jiao J, Wang Y.** 2014. Inhibition of hepatitis B virus cccDNA by siRNA in transgenic mice. Cell Biochemistry and Biophysics **69:**649-654.
204. **Li X, Hong Y, Wang Q, Liu S, Wei H, Cheng J.** 2013. Short hairpin RNAs with a 2- or 3-base mismatch inhibit HBV expression and replication in HepG2 cells. Hepatology International **7:**127-133.
205. **McCaffrey AP, Nakai H, Pandey K, Huang Z, Salazar FH, Xu H, Wieland SF, Marion PL, Kay MA.** 2003. Inhibition of hepatitis B virus in mice by RNA interference. Nature Biotechnology **21:**639-644.
206. **Ying C, De Clercq E, Neyts J.** 2003. Selective inhibition of hepatitis B virus replication by RNA interference. Biochemical and Biophysical Research Communications **309:**482-484.
207. **Gabriel R, Lombardo A, Arens A, Miller JC, Genovese P, Kaeppel C, Nowrouzi A, Bartholomae CC, Wang J, Friedman G, Holmes MC, Gregory PD, Glimm H, Schmidt M, Naldini L, von Kalle C.** 2011. An unbiased genome-wide analysis of zinc-finger nuclease specificity. Nature Biotechnology **29:**816-823.
208. **Válóczi A, Hornyik C, Varga N, Burgyán J, Kauppinen S, Havelda Z.** 2004. Sensitive and specific detection of microRNAs by northern blot analysis using LNA-modified oligonucleotide probes. Nucleic Acids Research **32:**e175-e175.
209. **Chen C, Ridzon DA, Broomer AJ, Zhou Z, Lee DH, Nguyen JT, Barbisin M, Xu NL, Mahuvakar VR, Andersen MR, Lao KQ, Livak KJ, Guegler KJ.** 2005. Real-time quantification of microRNAs by stem–loop RT–PCR. Nucleic Acids Research **33:**e179-e179.